

Quantifying and Modelling the Responses of Leaf Gas Exchange to Drought

By

Shuangxi Zhou (BSc., MSc.)

Supervised By

Colin Prentice

Belinda Medlyn

A thesis submitted to Macquarie University for the degree of

Doctor of Philosophy

Department of Biological Sciences



October 2014

To my mother, Xiaojiao Du, and all families

List of Contents

Abstract	xiii
Statement of Candidate	xv
Acknowledgements	xvii
Chapter 1	
Introduction	1
1.1 General introduction.....	1
1.1.1 The importance of plant drought responses	2
1.1.2 Mechanisms underlying drought-induced plant mortality	3
1.1.3 The importance of quantifying and modelling plant drought responses	4
1.2 Drought responses of plant gas exchange	5
1.2.1 Stomatal limitation	5
1.2.2 Non-stomatal limitation	6
1.3 Differential drought sensitivity of plant species from contrasting climates	8
1.4 Differential drought acclimation in plant species from contrasting climates	10
1.5 Improving representation of photosynthesis in vegetation modelling	12
1.6 Philosophy and approach in this thesis	14
1.7 Collaboration and candidate's role	17
1.8 Reference.....	19
Chapter 2	
How should we model plant responses to drought? An analysis of stomatal and non-stomatal responses to water stress	29
2.1 Abstract	30
2.2 Introduction	30
2.3 Materials and methods	32
2.3.1 Sources of data	32
2.3.2 Analytical models.....	32
2.3.2.1 Stomatal limitation	32
2.3.2.2 Non-stomatal limitation	33
2.3.3 Multivariate analysis	34
2.4 Results	34
2.4.1 Response of g_1 to water stress	34
2.4.2 Response of V_{cmax} to water stress	36
2.4.3 Water relation strategies.....	37
2.5 Discussion	38

2.6 References.....	39
2S1 Supplementary Information	40

Chapter 3

Short-term water stress impacts on stomatal, mesophyll, and biochemical limitations to photosynthesis differ consistently among tree species from contrasting climates	49
--	----

3.1 Abstract.....	50
3.2 Introduction.....	50
3.3 Materials and methods	52
3.3.1 Choice of species and range of hydroclimates.....	52
3.3.2 Plant material, growth condition and drought treatments.....	53
3.3.3 Pre-dawn leaf water potential measurement.....	53
3.3.4 Photosynthetic parameters based on CO ₂ response curves.....	53
3.3.5 Chlorophyll fluorescence measurement.....	54
3.3.6 Mesophyll conductance and the 'true' values of V_{cmax} and J_{max}	54
3.3.7 Analytical model for stomatal limitation	54
3.3.8 Analytical model for non-stomatal limitation.....	55
3.3.9 Statistical analyses	55
3.4 Results.....	56
3.4.1 Response of g_1 to water stress.....	56
3.4.2 Response of g_m to water stress.....	57
3.4.3 Response of V_{cmax} to water stress	57
3.4.4 Response of V_{cmax} to water stress.....	58
3.4.5 Response of J_{max} , J_{max} , and maximum J_{ETR} to water stress.....	58
3.4.6 Water relation strategies	58
3.5 Discussion.....	58
3.5.1 Concurrent limitation on g_1 , g_m , V_{cmax} and J_{max}	59
3.5.2 Variation of responses between species of contrasting hydroclimatic origins	59
3.5.3 Implications for ecosystem models.....	59
3.6 References.....	60
3S1 Supplementary Information	62

CHAPTER 4

Long-term water stress leads to acclimation of drought sensitivity of photosynthetic capacity in xeric but not riparian <i>Eucalyptus</i> species.....	83
--	----

4.1 Abstract.....	84
4.2 Introduction.....	85
4.3 Materials and methods	87
4.3.1 Choice of plant taxa	87
4.3.2 Plant material, growth conditions, and experimental design	87
4.3.3 Pre-dawn leaf water potential	88
4.3.4 Leaf gas exchange, carbon response curve, chlorophyll fluorescence, and mesophyll conductance	89

4.3.5 Estimation of V_{cmax}' , J_{max}' , V_{cmax} and J_{max}	90
4.3.6 Conduit anatomy, HV , sapwood-specific and leaf-specific hydraulic conductivity	90
4.3.7 LMA, intrinsic water use efficiency, leaf nitrogen content, height and basal diameter	91
4.3.8 Stomatal sensitivity to water stress	91
4.3.9 Analytical model for the function of stomatal, mesophyll, and biochemical responses during the drying-down process	92
4.3.10 Statistical analyses	93
4.4 Results	94
4.4.1 Effect of partial drought on A_{sat} , g_s , g_1 , V_{cmax}' and J_{max}' after two and four months	94
4.4.2 Effect of partial drought on $\delta^{13}\text{C}$, K_L , K_S , HV , height, basal diameter, LMA, and N_{area} after four months	96
4.4.3 Response of g_1 , g_m , V_{cmax}' and J_{max}' in the drying-down process after four months	98
4.4.4 Water relation strategies	100
4.5 Discussion	103
4.5.1 Differential acclimation of photosynthetic responses in contrasting Eucalyptus taxa to long-term water stress	104
4.5.2 Hydraulic adjustments after the longer-term water stress	106
4.6 References	107
4S1 Supplementary Information	112
Chapter 5	
Representing observed plant responses to drought in a land surface model	115
5.1 Abstract	116
5.2 Introduction	117
5.3 Methods	118
5.3.1 Model description	118
5.3.2 Implementation of the “optimal” stomatal model	119
5.3.3 Implementation of analytical models for the drought responses of g_1 and V_{cmax}	121
5.3.4 Site data and model simulations	123
5.4 Results	124
5.4.1 CABLE-Standard and CABLE-No Drought <i>versus</i> observations	124
5.4.2 Standard <i>versus</i> modified parameters	129
5.4.3 Parameter sensitivity analysis	129
5.4.4 Comparison among soil moisture stress factors	130
5.5 Discussion	132
5.6 References	134
Chapter 6	
Conclusion	139
6.1 Reference	144

List of Figures

- Figure 2-1 A (filled squares) and g_s (open squares) responses to Ψ_{pd} , from two data sets representative for each of three PFTs. Herbs: (10) *Helianthus annuus*, and (13) *Mediterranean Herbs*; Malacophyll angiosperm tree: (2) *Broussonetia papyrifera* (Linnaeus), and (16) *Platycarya longipes* Wu; Sclerophyll angiosperm tree: (20) *Quercus ilex*, and (21) *Quercus suber*31
- Figure 2-2 Framework for the analysis of stomatal and non-stomatal limitations to photosynthesis. The non-stomatal limitation is represented by the solid lines, which shows the response of A to C_i . This curve depends on the apparent V_{cmax} . The stomatal limitation is represented by the dashed lines, which depend on g_1 . Blue lines represent well-watered conditions and red lines represent drought conditions. Under drought, a reduction in g_1 (stomatal limitation only) leads to a trajectory of A from Aa to Ab; a reduction in apparent V_{cmax} (non-stomatal limitation only) leads to a trajectory from Aa to Ac; and reduction in both parameters leads to a trajectory from Aa to Ad32
- Figure 2-3 Variability of g_1 responses to Ψ_{pd} from two data sets representative for each of three PFTs. Herbs: (10) *Helianthus annuus*, and (13) *Mediterranean Herbs*; Malacophyll angiosperm tree: (2) *Broussonetia papyrifera* (Linnaeus), and (16) *Platycarya longipes* Wu; Sclerophyll angiosperm tree: (20) *Quercus ilex*, and (21) *Quercus suber*34
- Figure 2-4 g_1 responses to Ψ_{pd} from 22 data sets, grouped by PFT (herb, shrub and liana, sclerophyll angiosperm tree, malacophyll angiosperm tree, gymnosperm).....35
- Figure 2-5 Relative effect of Ψ_{pd} on V_{cmax} from two data sets representative for each of three PFTs. Herbs: (10) *Helianthus annuus*, and (13) *Mediterranean Herbs*; Malacophyll angiosperm tree: (2) *Broussonetia papyrifera* (Linnaeus), and (16) *Platycarya longipes* Wu; Sclerophyll angiosperm tree: (20) *Quercus ilex*, and (21) *Quercus suber*35
- Figure 2-6 V_{cmax} responses to Ψ_{pd} from 21 data sets, grouped by PFT (herb, shrub and liana, sclerophyll angiosperm tree, malacophyll angiosperm tree, gymnosperm).....35
- Figure 2-7 Estimated responses of mesophyll conductance (g_m) to Ψ_{pd} under the assumption that true V_{cmax} is constant, for two data sets representative of each of three PFTs. These curves were estimated from data by assuming that true V_{cmax} is constant and equal to its observed value at $\Psi_{pd} = 0$, and calculating the reduction in g_m that would be needed to explain the observed reduction in apparent V_{cmax} 36
- Figure 2-8 Estimated responses of true V_{cmax} to Ψ_{pd} under the assumption that mesophyll conductance is constant, for two data sets representative of each of three PFTs. These curves were estimated from data by assuming that g_m is constant and equal to $0.15 \text{ mol m}^{-2} \text{ s}^{-1}$, and calculating the reduction in true V_{cmax} that would be needed to explain the observed reduction in apparent V_{cmax} 37
- Figure 2-9 Principal components analysis of the five traits, S_f , Ψ_f , b , g_1 (g_1 estimated at $\Psi_{pd} = -0.5 \text{ MPa}$) and V_{cmax} (apparent V_{cmax} estimated at $\Psi_{pd} = 0$). The first principal component (PC1) explained 35.2% of total variance, and the second principal component (PC2) explained 23.5% of total variance. The two principal components together accounted for 58.7% of the total variation in these five parameters.38
- Figure 3-1 Responses of A (filled squares) and g_s (open squares) to Ψ_{pd} in the experiment on three contrasting *Quercus* species and also two mesic species in Europe (plot 1 to plot 5), and in the experiment on four contrasting *Eucalyptus* species in Australia (plot 6 to plot 9).52
- Figure 3-2 Response of g_1 to Ψ_{pd} in the first experiment on four contrasting *Eucalyptus* species in Australia (solid lines), and in the second experiment on three contrasting *Quercus* species and two other species in Europe (dashed lines). The exponential function of g_1 decline with decreasing Ψ_{pd}

- was fitted to observations of each species with equation (5). The fitted b_1 and g_1^* values are shown in Table 2..... 56
- Figure 3-3 Responses of V_{cmax}' to Ψ_{pd} in the first experiment on four contrasting *Eucalyptus* species in Australia (solid lines), and in the second experiment on three contrasting *Quercus* species and two other species in Europe (dash lines). The logistic function of V_{cmax}' decline with decreasing Ψ_{pd} was fitted to observations of each species with equation (7). The fitted values of V_{cmax}' , S_{fv}' , and Ψ_{fv}' were shown in Table 2..... 56
- Figure 3-4 Responses of g_m to Ψ_{pd} in the first experiment on three contrasting *Eucalyptus* species in Australia (solid lines), and in the second experiment on three contrasting *Quercus* species and two other species in Europe (dashed lines). There was no fluorometer measurement on *E. striatocalyx* to estimate g_m . The exponential function of g_m decline with decreasing Ψ_{pd} was fitted to observations of each species with equation (6). The fitted b_2 and g_m^* values are shown in Table 2 56
- Figure 3-5 Responses of V_{cmax} to Ψ_{pd} in the first experiment on four contrasting *Eucalyptus* species in Australia (solid lines), and in the second experiment on three contrasting *Quercus* species and two other species in Europe (dashed lines). The logistic function of V_{cmax} decline with decreasing Ψ_{pd} was fitted to observations of each species with equation (7). The fitted values of V_{cmax} , S_{fv} , and Ψ_{fv} are shown in Table 2. There was no fluorometer measurement on *E. striatocalyx* to estimate g_m and V_{cmax} . *Alnus glutinosa* L. and *Fraxinus excelsior* L., with limited number of V_{cmax} data points for parameter estimation, showed large variance for S_{fv} . *Fraxinus excelsior* L. also showed large variance for V_{cmax} 57
- Figure 3-6 Responses of J_{max}' to Ψ_{pd} in the first experiment on four contrasting *Eucalyptus* species in Australia (solid lines), and in the second experiment on three contrasting *Quercus* species and two other species in Europe (dashed lines). The logistic function of J_{max}' decline with decreasing Ψ_{pd} was fitted to observations of each species with equation (7). The fitted values of J_{max}' , S_{fj}' , and Ψ_{fj}' are shown in Table 2. 57
- Figure 3-7 Principal components analysis of nine drought-response traits, Ψ_0 (the Ψ_{pd} threshold for gas exchange measurement), b_1 (sensitivity of g_1), g_1^* (g_1 estimated at $\Psi_{pd} = -0.3$ MPa), V_{cmax}^* (V_{cmax}' estimated at $\Psi_{pd} = 0$), S_{fv}' , Ψ_{fv}' , J_{max}^* (J_{max}' estimated at $\Psi_{pd} = 0$), S_{fj}' , and Ψ_{fj}' . Species fall roughly into three groups through a continuum along the first principal component (PC1), which explained 58.5% of the total variation in these traits. Species scores are shown in Table 2. 58
- Figure 4-1 (a) Leaf net photosynthesis at saturating light (A_{sat}) and (b) stomatal conductance (g_s) of three *Eucalyptus* taxa exposed to watering treatments of 100% and 70% field capacity (FC), measured after 2 months and 4 months of treatment. Values are means \pm SE (n = 3). 95
- Figure 4-2 Components of leaf gas exchange in three *Eucalyptus* taxa exposed to watering treatments of 100% and 70% FC, after 2 months and 4 months of treatment. (a) Stomatal sensitivity parameter g_1 ; (b) Apparent Rubisco activity V_{cmax}' ; (c) Apparent maximum electron transport rate J_{max}' ; (d) Ratio of J_{max}' to V_{cmax}' . Values are means \pm SE (n = 3)..... 96
- Figure 4-3 Hydraulic traits, growth status, and leaf nitrogen content of three *Eucalyptus* taxa exposed to watering treatments of 100% and 70% field capacity (FC), measured after 2 months and 4 months of treatment. (a) Carbon-isotope composition $\delta^{13}C$; (b) leaf-specific conductivity; (c) sapwood-specific conductivity; (d) Huber value (sapwood area per unit leaf area); (e) height; (f) basal diameter; (g) leaf mass per area; (h) leaf nitrogen content on an area basis. Values are means \pm SE (n = 3)..... 97
- Figure 4-4 (a) Light-saturated CO_2 assimilation rate (A_{sat}) and (b) stomatal conductance as a function of pre-dawn leaf water potential during a drying cycle following 4 months of treatment at 100% FC (solid squares) or 70% FC (open squares). Dark green: *E. camaldulensis* subsp.

camaldulensis; Light green: *E. camaldulensis* subsp. *subcinerea*; Red: *E. occidentalis*.....99

Figure 4-5 Components of leaf gas exchange as a function of pre-dawn leaf water potential during a drying cycle following 4 months of treatment at 100% FC (solid squares for raw data; solid lines for fitted curves) or 70% FC (open squares for raw data; solid lines for fitted curves). (a) Stomatal sensitivity parameter g_1 ; (b) Mesophyll conductance g_m ; (c) Apparent Rubisco activity V_{cmax}' ; (d) Apparent maximum electron transport rate J_{max}' . Dark green: *E. camaldulensis* subsp. *camaldulensis*; Light green: *E. camaldulensis* subsp. *subcinerea*; Red: *E. occidentalis*..... 100

Figure 4-6 Principal components analysis of ten drought-response traits, b_1 (sensitivity of g_1), g_1^* (g_1 estimated at $\Psi_{pd} = -0.3$ MPa), b_2 (sensitivity of g_m), g_m^* (g_m estimated at $\Psi_{pd} = -0.3$ MPa), $V_{cmax}'^*$ (V_{cmax}' estimated at $\Psi_{pd} = 0$), S_{fv}' , Ψ_{fv}' , $J_{max}'^*$ (J_{max}' estimated at $\Psi_{pd} = 0$), S_{ff}' , and Ψ_{ff}' . The first principal component (PC1) showed a continuum of species from more mesic to more xeric species, which explained 49.2% of total variation. The second principal component (PC2) showed a continuum of plants from 70% FC to 100% FC treatment, which explained 24.1% of total variation. Value of traits are shown in Table 2 103

Figure 5-1 Meteorological data of six sites during the growing season of 2003: (a) day sum of rainfall (Rainf); (b) day mean of air temperature (Tair); (3) day mean of photosynthetically active radiation (PAR, calculated as a product of 2.3 and downward shortwave)..... 125

Figure 5-2 CABLE simulations of (a) net ecosystem exchange (NEE; $g\ C\ m^{-2}\ d^{-1}$), (b) gross primary production (GPP; $g\ C\ m^{-2}\ d^{-1}$), (c) transpiration (E; $mm\ d^{-1}$) and (d) latent heat flux (LE; $W\ m^{-2}$) at two flux sites (Hesse and Roccarespampani) from deciduous broadleaf forest in 2003, compared to observations of NEE and LE. Blue ribbons: simulations with modified parameters whose values were increased and decreased by 30% of their reference value. The grey bar marks the heatwave period between June 1st and August 31st 2003..... 126

Figure 5-3 CABLE simulations of (a) net ecosystem exchange (NEE; $g\ C\ m^{-2}\ d^{-1}$), (b) gross primary production (GPP; $g\ C\ m^{-2}\ d^{-1}$), (c) transpiration (E; $mm\ d^{-1}$) and (d) latent heat flux (LE; $W\ m^{-2}$) at two flux sites (Castelporziano and Espirra) from evergreen broadleaf forest in 2003, compared to observations of NEE and LE. Blue ribbons: simulations with modified parameters whose values were increased and decreased by 30% of their reference value. The grey bar marks the heatwave period between June 1st and August 31st 2003..... 127

Figure 5-4 CABLE simulations of (a) net ecosystem exchange (NEE; $g\ C\ m^{-2}\ d^{-1}$), (b) gross primary production (GPP; $g\ C\ m^{-2}\ d^{-1}$), (c) transpiration (E; $mm\ d^{-1}$) and (d) latent heat flux (LE; $W\ m^{-2}$) at two flux sites (El Saler and Tharandt) from evergreen needleleaf forest in 2003, compared to observations of NEE and LE. Blue ribbons: simulations with modified parameters whose values were increased and decreased by 30% of their reference value. The grey bar marks the heatwave period between June 1st and August 31st 2003 128

Figure 5-5 Assimilation rate (A) as a function of volumetric soil moisture content (θ) caused by the reduction of β (Black), β_{g1} (Blue), $\beta_{V_{cmax}}$ (Green), or both β_{g1} and $\beta_{V_{cmax}}$ (Red) during drought, respectively for three PFTs: deciduous broadleaf forest (DBF), evergreen broadleaf forest (EBF), evergreen needleleaf forest (ENF); and seven soil types 130

List of Tables

Table 2-1 Parameter values across 22 species and 5 PFTs	33
Table 3-1 The value of Moisture Index of the habitat in which the species occur, and the duration of drying-down process in number of days	53
Table 3-2 Values of 14 traits defining drought-responses of stomatal and non-stomatal components across 9 species. The 14 traits are: Ψ_0 (the Ψ_{pd} threshold for gas exchange measurement), b_1 (sensitivity of g_1), g_1^* (g_1 estimated at $\Psi_{pd} = -0.3$ MPa), b_2 (sensitivity of g_m), g_m^* (g_m estimated at $\Psi_{pd} = -0.3$ MPa), $V_{cmax}'^*$ (V_{cmax}' estimated at $\Psi_{pd} = 0$), S_{fV}' (sensitivity of V_{cmax}'), Ψ_{fV}' , V_{cmax}^* (V_{cmax} estimated at $\Psi_{pd} = 0$), S_{fV} (sensitivity of V_{cmax}), Ψ_{fV} , $J_{max}'^*$ (J_{max}' estimated at $\Psi_{pd} = 0$), S_{fJ}' (sensitivity of J_{max}'), Ψ_{fJ}' . NA means the value is not applicable.....	55
Table 4-1 Description of the seed origin for the three taxa.....	87
Table 4-2 Table 2 Values of 13 traits defining the drought-responses of stomatal and non-stomatal components of three <i>Eucalyptus</i> taxa during the drying down process after 4 months of treatment. The 13 traits are: g_1^* (g_1 estimated at $\Psi_{pd} = -0.3$ MPa), b_1 (sensitivity of g_1), g_m^* (g_m estimated at $\Psi_{pd} = -0.3$ MPa), b_2 (sensitivity of g_m), $V_{cmax}'^*$ (V_{cmax}' estimated at $\Psi_{pd} = 0$), S_{fV}' (sensitivity of V_{cmax}'), Ψ_{fV}' , V_{cmax}^* (V_{cmax} estimated at $\Psi_{pd} = 0$), S_{fV} (sensitivity of V_{cmax}), Ψ_{fV} , $J_{max}'^*$ (J_{max}' estimated at $\Psi_{pd} = 0$), S_{fJ}' (sensitivity of J_{max}'), Ψ_{fJ}'	102
Table 5-1 Values of soil parameters used in CABLE	121
Table 5-2 Baseline values of g_1 and V_{cmax} , and values of b_1 , S_f , and Ψ_f applied to three PFTs	123
Table 5-3 A summary of model simulations.....	123
Table 5-4 The flux tower sites	124

Abstract

Global climate change is expected to increase drought duration and intensity in certain regions while increasing rainfall in others. The quantitative consequences of increased drought for ecosystems are not easy to predict. Process-based models must be informed by experiments to determine the resilience of plants and ecosystems from different climates. The thesis provides quantitative information aimed at improving land surface models (LSMs). It includes four papers. (1) Responses of leaf-atmosphere gas exchange to short-term drought were analysed, across plant functional types and climates, based on a synthesis of previous experiments. Explicit and consistent definitions of stomatal *versus* non-stomatal responses were adopted. Both types of response were shown to be important, and plants adapted to arid climates responded very differently from others. (2) Parallel responses of stomatal conductance, mesophyll conductance, and photosynthetic capacity were found in two glasshouse experiments with tree species from Australia and Europe, revealing a common, coordinated pattern of increasing tolerance in plants from drier environments. (3) Xeric and riparian species of *Eucalyptus* were subjected to short- and long-term drought. The species were found to differ not only in their tolerance for short-term drought, but also in the extent to which they could acclimate to long-term drought. (4) Experimentally based drought responses were used to define new, plant type-dependent relationships of stomatal sensitivity and photosynthetic capacity to soil water potential in the Community Atmosphere Biosphere Land Exchange (CABLE) LSM. Comparison with CO₂ and latent heat flux measurements from eddy covariance flux measurement sites in Europe during the ‘heatwave’ year of 2003 showed that discrepancies between model results and observations were not substantially improved by the inclusion of the more realistic functions, due to a persistent positive bias in

the model's simulation of evapotranspiration which overshadowed the differences between different representations of drought response functions.

Statement of Candidate

I certify that the work presented in this thesis entitled “Quantifying and Modelling the Responses of Leaf Gas Exchange to Drought” has not been previously submitted for a degree, nor has it been submitted as part of requirements for a degree to any other university of institution other than Macquarie University. I also certify that this thesis is an original piece of research and it has been written by me. Any help and assistance that I have received in my research work and the preparation of the thesis itself have been appropriately acknowledged. In addition, I certify that all information sources and literature used are indicated in the thesis. The research presented in this thesis did not require approval from Macquarie University Ethics Committee.

Shuangxi Zhou

October 2014

Acknowledgements

I hope to thank Macquarie University for the precious education and research opportunities on plant eco-physiology and modeling for the past 3.5 years with the Macquarie University International Research Scholarship (iMQRES), including glasshouse experiments in Macquarie University and University of Barcelona, Spain; field work in Yunnan, China; field training in west Australia; isotope training in the University of Sydney; attendance to field training and conferences. I thank the Faculty of Science, for all help from HDR team, and the Macquarie University Postgraduate Research Fund (PGRF) award for my attendance at the American Geographical Union Conference in San Francisco at the December 2013 to present my research and discuss with world-wide ecologists and modellers. I thank the Department of Biological Sciences for its important supports and strong research building-ups in this area to make the above happen.

In the past 3.5 years at Macquarie University I have been very lucky to have the opportunity to work with the world-leading scientists in the field. My main supervisor Colin Prentice and second supervisor Belinda Medlyn have been very supportive during my studies and research. Their research passion, vision, and capacities on biology, modeling, and the bridging, have guided me to sense the beauty of science and re-evaluate the Chinese old saying on “inheriting the knowledge from previous saints”. Essentially, Colin and Belinda have cultured me to structure my PhD research bridging ecophysiological processes and large-scale modeling, including the whole process from the use of experimental observations, theory to explain the observations, quantitative parameterizations to describe the theory, to model simulations for model evaluation and improvement. In this integrative process I also have

accumulated substantial important experiences on writing for publishing high-level papers, relative to my first poorly written paper manuscript.

In addition, Colin and Belinda performed as a great model to network and collaborate for achieving high-standard research. All my national and international experiments were completed by closely liaising and collaborating with research groups of different disciplinary backgrounds: Professor Brian Atwell and Dr Srikanta Kaidala-ganesha in Macquarie University, the plant ecology group led by professor Santiago Sabaté in University of Barcelona, and the environmental geochemistry group led by Professor Jian Ni in Chinese Academy of Sciences. The glasshouse experiments in University of Barcelona cannot be achieved without the collaboration with the research group led by Professor Santiago Sabaté in Barcelona in August 2013. Professor Santiago also took care of me during the experiments. Professor Ni's group assists the fieldwork on four vegetation types and two water-limited woodlands in Yunnan, China. Meanwhile, I also have extensive chances to learn from and work with other colleagues in Macquarie University (particularly with Dr Sean Gleason and Dr Martin De Kauwe) and University of Western Sydney (Dr Remko Duursma). I thank Dr Remko Duursma and Dr Drew Allen with whom I have been accumulating skills on R. Dr Martin De Kauwe plays an essential role on exposing me to Fortran and Python and modeling with the CABLE land surface model. Meanwhile, by interacting with the comparative ecology group led by Professor Mark Westoby (especially with Dr Sean Gleason and Dr Kasia Zieminska, the visiting Mark Olson) I mastered the skills to quantify the vessel and stoma traits (thanks to the help of Debra Birch and Nicole Vella), leaf traits (specific leaf area, leaf thickness), leaf nitrogen, Huber value, and branch hydraulics (hydraulically weighted vessel diameter, sapwood and leaf-specific conductance). I also would like to thank Dr Ian Wright, Dr Allyson Eller, and Dr Tanja Lenz for their research suggestions. Dr Sofia Baig firstly showed me how to use the Licor in 2011. In addition, I have opened my research vision greatly through the magnificent Genes to Geoscience Research Enrichment Program. I hereby

thank these (and the associated) colleagues, and again my University and Faculty and Department which offer these platforms, and also my colleagues in two groups – the biosphere and climate dynamics group led by Colin Prentice, and the climate and forest ecosystem modelling group led by Belinda Medlyn, for all their help, care, and encouragement which are important for me to achieve my PhD research. I also hope to thank Alison Downing and her husband Kevin, Graeme Armstrong and Lynda, for their supports and encouragements during my study in Macquarie University.

I also hope to thank the EU pro-iBiosphere committee fund me to attend and present my research at the pro-iBiosphere meeting in Berlin in May 2013, which entitles me to visit the two research groups led by professor Santiago Sabaté in Barcelona and establish the collaboration on experiments. I thank the NSW Adaptation Research Hub to fund me to attend and present my research at the NCCARF 2014 Climate Adaptation conference. I thank the University of Sydney for the scholarship to attend the “Stable Isotopes in Biosphere Systems” course in the in February 2013, during which I met Graham Farquhar, Jonn Evans, and Susanne Caemmerer. Thanks to Dennis Baldocchi and Lawren Sack for their research suggestions during my visiting to their groups in December 2013.

Above all, I wish to thank my mother, Xiaojiao Du, my father, Zhikuan Zhou, my grandparents, my wife Yu Zhang and her families, my sister Huijuan Zhou and her husband, Yanwen Chen, and my nephew Changhao Chen. Nothing can be achieved without their selfless supports, while nothing is worth their sacrifice.

Chapter 1

Introduction

1.1 General introduction

1.1.1 The importance of plant drought responses

Climate change projections foresee increased temperatures in all continents, and increased drought duration and intensity in many regions – particularly in Mediterranean and subtropical ecosystems (Giorgi et al., 2004; Giorgi, 2006; Beniston et al., 2007; Allison et al., 2009; IPCC, 2014). Climate change may also lead to increased inter-annual and seasonal variability in precipitation, thus episodically reducing soil water availability for plants (Christensen et al., 2007; Smith, 2011; IPCC, 2014). Increased drought duration and intensity, accompanied by high temperatures, are likely to have negative impacts on plant photosynthesis, respiration, and whole-plant reserves of non-structural carbohydrates (NSC) (Duan et al., 2013) which buffer plant function against episodes of reduced carbohydrate supply. Such effects on plants would be expected to cascade upwards to the ecosystem scale by limiting plant growth and productivity (Nemani et al., 2003), causing mortality and species replacement, and modifying the geographic distributions of species and communities (Engelbrecht et al., 2007) – potentially with major consequences for ecosystems and their services (Tezara et al., 1999). Soil water deficit is already the main environmental driver that limits Aboveground Net Primary Production (ANPP) in land vegetation (Webb et al., 1983; Zeppel et al. 2014), and vegetation mortality induced by drought has been documented on all

six vegetated continents and for most biomes across the globe (Potts 2003; Allen et al., 2010; Phillips et al., 2010; Anderegg et al., 2012; Choat et al., 2012; Williams, et al., 2013).

Understanding the drought responses of trees is especially important because forests play an essential role in the carbon and water cycles. Covering nearly a third of the global land surface and accounting for nearly three-quarters of the net primary production (NPP) of terrestrial ecosystems, forests have a strong influence on climate through the hydrological cycle, soil biogeochemistry and land-surface exchanges (Bonan, 2008; Adams et al., 2011). Terrestrial ecosystems absorb on average about a quarter of annual anthropogenic CO₂ emissions (Le Quéré et al., 2013) and much of this uptake occurs in forests. Forest ecosystems are thus a major CO₂ sink, with an estimated gross uptake of 4.0 ± 0.5 Pg C year⁻¹ and net uptake of 1.1 ± 0.8 Pg C year⁻¹ between 1990 and 2007 (Pan et al., 2011). But this exceptionally important global function of forests could be at risk, due to effects of the climate changes consequent on continuing emissions of CO₂. Many plant communities have been predicted to exceed mortality thresholds in the near future, due to climate change (Breshears et al., 2005; Allison et al., 2009; Malhi et al., 2009; Choat et al., 2012). By eliciting physiological (e.g. canopy conductance), structural (e.g. leaf area, root length) and biogeographic (e.g. forest composition and species distribution) responses at the plant and community levels, extreme drought is expected to cause regional losses of biodiversity and biomass (Allison et al., 2009; Phillips et al., 2009) with impacts on ecosystem function and the terrestrial carbon sink (Pitman, 2003; Bonan, 2008; Phillips et al., 2010). Yet these processes are not well quantified. We do not know the likely extent of drought-induced changes in the function of forest ecosystems for different levels of climate change. Current state-of-the-art Earth System models (ESMs), which include dynamic global vegetation models (DGVMs) (Prentice and Cowling, 2013) coupled to physical representations of land-atmosphere exchanges of energy, water vapour and CO₂ (Land Surface Models, LSMs), make

widely divergent predictions of these effects (Ciais et al., 2013; Prentice et al., 2014b). This divergence is due in part to the lack of an established, empirically supported method for the representation of drought effects on plants (Egea et al., 2011).

Relative to the large volume of published studies on physiological processes at the leaf and plant scale (e.g. photosynthesis, transpiration) (e.g. Flexas and Medrano 2002; Lawlor and Cornic 2002), studies on the drought effects at ecosystem scale are far fewer. This is partly because drought duration and intensity in humid and temperate environments are unpredictable (Baldocchi, 2008). The weather conditions to be expected during a multi-year field experiment are not known in advance. Studies at the ecosystem scale have been carried out in semi-arid ecosystems that reliably experience seasonal drought (Reichstein et al. 2002a; 2002b; Rambal et al. 2003; Williams and Albertson 2005; Xu and Baldocchi 2004; Pereira et al. 2007). Such climates also typically show large year-to-year variation in rainfall and therefore in the duration and intensity of drought. Specific studies have also been focused on the large-scale droughts which occurred across North America in 1995 (Baldocchi 1997), across the boreal zone of western Canada between 2001 and 2003 (Kljun et al. 2006), and across Europe in 2003 (Ciais et al., 2005; Fischer et al., 2007; Granier et al., 2007; Reichstein et al., 2007).

1.1.2 Mechanisms underlying drought-induced plant mortality

A drier and warmer climate is likely to accelerate drought-induced vegetation mortality by amplifying several mechanisms that underlie drought-induced mortality. The principal mechanisms are: failure of hydraulic function due to xylem embolism; carbon starvation due to stomatal closure and therefore reduced photosynthetic carbon fixation; inhibition of the transport and use of stored NSC; and opportunistic pathogen and insect attacks. These mechanisms do not act in isolation (Sala et al., 2010; McDowell et al., 2011; Sala et al., 2012; Hartmann et al., 2013; O'Brien et al., 2014; Sevanto et al., 2014) but rather are

interdependent, so for example xylem embolism causes further stomatal closure and increases the risk of carbon starvation.

Hydraulic failure and carbon starvation are the two most studied mechanisms underlying drought-induced tree mortality (McDowell et al., 2011). Uninterrupted transport of water through the xylem is essential for plant growth and survival, because it replaces water lost by transpiration, and allows stomata to remain open for photosynthesis. Water moves through the xylem under negative pressure. The rate of water flow is limited by the need to avoid cavitation – a sudden change from liquid to vapor phase within normally water-filled xylem conduits (Pockman and Sperry, 2000). Soil water deficit can cause insufficient water availability for the plants to replace the lost water through stomata, such that the tension in the plant xylem increases. Increased xylem tension in turn increases the risk of hydraulic failure, leading to death (Choat et al., 2012). To minimize the hydraulic risk, plants have to prevent water loss by closing the stomata, but this also prevent CO₂ intake and slows or stops photosynthesis. Carbon starvation can thus occur due to a negative carbon balance (the difference between assimilation and utilization of carbohydrates) due to stomatal closure. When photosynthesis is scaled down or stopped during drought, plants rely on the storage of NSC compounds which help mitigate drought effects (O'Brien et al., 2014); but NSC stores are limited and mortality may ultimately occur when the NSC reserve is used up. NSC accumulation or hydraulic failure cannot be predicted without realistic prediction of photosynthesis and stomatal conductance under drought.

1.1.3 The importance of quantifying and modelling plant drought responses

Modelling the quantitative consequences of increased drought for forest ecosystems is challenging (McDowell et al., 2011), and requires unraveling the interaction between drought and plant gas exchange at different time scales, and in ecosystems with different degrees of adaptation to drought. Reliable prediction of drought effects must be based on the analysis

of observations to identify key traits that promote plant resistance to drought, and process-based modelling including realistic representation of the ecophysiological mechanisms relating plant gas exchange to water availability and transport.

Thousands of experiments have been done on the drought responses of plants; yet the fundamental mechanisms underpinning such responses of plants remain rather poorly understood in the quantitative sense required for modelling. Data sets containing enough quantitative information for the improvement of model representations are limited. Moreover, work is needed (a) to directly determine how different aspects of plant function respond to experimentally imposed drought and (b) to analyse experimental results in a theoretical framework, suitable for inclusion in LSMs and DGVMs.

1.2 Drought responses of plant gas exchange

1.2.1 Stomatal limitation

Quantifying the drought stress effects on plant gas exchange – the exchanges of CO₂ and water vapour between leaves and the atmosphere – is fundamentally important for the prediction of drought effects on vegetation (Ciais et al., 2005). Accurate model prediction of drought impacts on the global carbon and water cycles requires realistic representation of these processes at the leaf level. CO₂ and water vapour exchange are strongly coupled through stomata, because stomatal conductance (g_s) regulates both the CO₂ uptake for photosynthesis, and the loss of water vapour by transpiration (Egea et al., 2011).

The leaf carbon assimilation rate (A) is mainly driven by light, temperature and intercellular CO₂, as represented in the almost universally used leaf photosynthesis model for C₃ plants introduced by Farquhar *et al.* (1980). Intercellular CO₂, in turn, is co-determined by g_s (diffusional limitation) and A . The sensitivity of stomata to multiple environmental influences reflects the fact that plants have to trade off CO₂ uptake and water loss. Reduction of g_s is one

of the foremost, short-term, leaf-scale physiological responses both to atmospheric vapour pressure deficit (the driving force of transpiration) and soil water deficit.

Stomatal behaviour is expected to be related to the marginal (carbon) cost of water loss (Berninger and Hari, 1993). Cowan and Farquhar postulated that for any given amount of total water available for transpiration in a period of time, the leaf can achieve the maximum CO₂ uptake if it adjusts leaf scale conductance in the way that the derivative of E with respect to A ($\partial A/\partial E$) is maintained constant throughout the period (Cowan 1977; Cowan & Farquhar 1977). This criterion amounts to saying that a plant with a given water availability regulates stomata to ensure maximal carbon gain per unit water loss in a finite period of time. Therefore, the constancy of $\partial A/\partial E$ has long been viewed as an optimality hypothesis (Cowan, 1977; Cowan & Farquhar, 1977). It has also been suggested that the rate at which water stress is imposed might influence the response of $\partial A/\partial E$ to water stress (Hall and Schulze, 1980). Medlyn et al. (2011) and Prentice et al. (2014a) have proposed re-interpretations of widely used empirical models of stomatal conductance, in terms of optimization theory. Medlyn et al. (2011) derived a simple expression that is a good approximate solution of the Cowan-Farquhar optimization problem; and demonstrated its predictive power for a range of species. Prentice et al. (2014a) introduced a different derivation of the same expression, with further empirical support, based on the alternative hypothesis that plants minimize the sum of the unit costs (carbon expended per unit assimilation) of CO₂ uptake and water loss. The theoretical analysis of Mäkelä et al. (1996) further predicted that the marginal carbon cost of water should decline exponentially with decreased soil moisture, and that the rate of decline should increase according to the probability of rain.

1.2.2 Non-stomatal limitation

Besides the stomatal resistance on CO₂ diffusion from the atmosphere to the intercellular air spaces of the leaves, there is now known to be a considerable mesophyll resistance to CO₂

diffusion from the substomatal cavity to the carboxylation sites in the mesophyll. In other words there is a mesophyll conductance, which is not infinite and can significantly limit the assimilation rate. Mesophyll conductance has been shown to play an important role in determining photosynthetic responses to environmental drivers such as temperature and CO₂ (e.g. Niinemets et al., 2011; Evans & von Caemmerer, 2013). Photosynthesis is reported to be limited by decreased mesophyll conductance (g_m) – together with g_s – in the initial stages of drought (Bota et al., 2004; Flexas *et al.*, 2004; 2007; 2008; 2012; Grassi & Magnani, 2005; Egea et al., 2011). There has been controversy on the magnitude of the g_m effect on photosynthesis under mild to moderate drought conditions, largely due to the methodological issues on estimation of the intercellular or the chloroplastic CO₂ concentration (Pinheiro and Chaves 2011). In addition, there is controversy on whether, and how, to include g_m in models (Rogers et al., 2014). Some recent studies suggested that the decrease of g_m with increasing soil water deficit could contribute as much as the decrease of g_s to the reduction of A under drought (see e.g. Flexas et al., 2012). However, far less is known about the environmental regulation and interspecific differences in g_m compared with g_s .

As plant water status worsens, there is a further possibility that drought impedes enzyme activity and hence, photosynthetic capacity. In other words, there can be directly drought-induced biochemical limitations on the activity of Rubisco (ribulose-1,5-bisphosphate carboxylase/oxygenase) and the regeneration capacity of RuBP (ribulose-1,5-bisphosphate) (Kanechi et al., 1996; Tezara et al., 1999; 2002; Thimmanaik et al., 2002; Castrillo et al., 2001; Parry et al., 2002; Grassi & Magnani 2005). Drought-induced decrease of Rubisco activity is associated with down-regulation of the activation state of the enzyme (e.g., by de-carbamylation and/or binding of inhibitory sugar phosphates). The maximum carboxylation rate (V_{cmax}) and the maximum rate of electron transport (J_{max}) are the two key parameters limiting photosynthetic capacity in the Farquhar, von Caemmerer and Berry model (Farquhar

et al., 1980). Varying among leaves within a plant, with leaf age, between plants, among species and seasonally (e.g. Wilson, Baldocchi & Hanson 2000; Xu & Baldocchi 2003), V_{cmax} plays an important role in linking the carbon fluxes between the leaves and the atmosphere and thus in governing plant productivity and resource use efficiency (Long *et al.*, 2006) and determining large-scale fluxes of CO₂ between vegetation and the atmosphere (Bonan *et al.*, 2011; 2012). The trigger for decreased Rubisco activity depends on the severity and/or the duration of the stress imposed (Flexas *et al.*, 2006; Galmés *et al.*, 2011). The value of V_{cmax} is largely variable within individual PFTs among ecosystem models (Kattge *et al.*, 2009; Bonan *et al.*, 2011; 2012; Groenendijk *et al.*, 2011). Recent studies have suggested that it is necessary to represent the effect of climate change on V_{cmax} in models to predict NPP (e.g. Bernacchi *et al.*, 2013; Galmés *et al.*, 2013).

It is generally thought that with the increase of drought intensity and/or duration, biochemical limitations on photosynthesis should eventually come to dominate over diffusional (stomatal and mesophyll) limitations (for a review see Lawlor & Tezara 2009). However, there has been a good deal of debate about the relative importance of photosynthetic limitations of diffusive and biochemical origin, in the context of drought (e.g. Grassi & Magnani 2005). Reasons for controversy include the use of different measures of drought; the imposition of drought at different rates in experiments; different applied intensities and duration of drought; and different experimental designs, growth conditions, and (importantly) species – with different physiological and structural adaptations.

1.3 Differential drought sensitivity of plant species from contrasting climates

The drought responses of different species are likely to depend not only on drought duration and intensity, but also on the species-specific degree of adaptation to the soil water conditions in their native habitat. It is well documented that plants from dry climates can operate better than plants from wet climates down to severe soil water deficits. However, recent studies

have highlighted that mesic and xeric forest ecosystems are equally vulnerable to drought-induced mortality, based on their functional hydraulic limits (Choat et al. 2012). Differential drought adaptations among species are presumed to underpin their different levels of sensitivity, resistance, and resilience to soil water deficits (Chaves et al., 2003; McDowell et al., 2008), and differential effectiveness of physiological mechanisms of drought tolerance in the face of decreasing water potential (Engelbrecht et al., 2007). The wide variation of drought adaptations among species is likely to be fundamentally important in determining their different degrees of vulnerability to biomass loss and mortality (Ciais et al., 2005; Adams et al., 2009; Allen et al., 2010).

The theoretical analysis of Mäkelä et al. (1996) predicted that species that experience higher probability of rain in their natural habitats will show rates of increase in the marginal carbon cost of water with decreasing soil water content, relative to species that experience lower probability of rain in their natural habitats. This response could be quantified with the help of the sensitivity parameter (g_1) of the Medlyn stomatal optimality model. This parameter is directly related to the marginal carbon cost of water (Medlyn et al., 2011). Both the value of this parameter and its response to soil water deficit is expected *a priori* to differ among plant functional types and species of different geographical origins (Medlyn et al., 2011; Hérault et al., 2013). On the other hand, V_{cmax} tends to be higher in plant species from drier climates (Prentice et al., 2014a), in compensation for reduced stomatal conductance. There is also significant variability in the Rubisco specificity factor among closely related C3 higher plants, which is associated mainly with temperature and drought (Galmés et al., 2005).

Under a hotter and drier climate, the intra- and inter-specific variation in plant traits may provide an important contribution to plants' resistance to drought, with responses characteristic of plants from dry environments promoting persistence and adaptation, reducing mortality and improving survival (Yachi and Loreau, 1999; Clark et al., 2012). Understanding

how these effects vary among species from contrasting climates is key to predicting the large-scale consequences of drought on different communities and ecosystems. Few published experiments have systematically tested how the various components of plant drought response vary across species from contrasting hydro-climates.

In addition, we need to understand how drought impacts vary among ecosystems. The drought impacts on different ecosystems depends on the drought duration, magnitude, and spatial extent, the vegetation type-specific responses to drought at different characteristic time-scales, and the mechanisms affecting the drought resistance and resilience of the vegetation types (Pasho et al., 2011; Vicente-Serrano et al., 2013). Different terrestrial ecosystems are reported to differ in their sensitivity to drought (Knapp et al., 2001; Zeppel et al., 2014). For example, the conifer forests were found to withstand drought impacts better than the broadleaf forests in Canada (Kljun et al. 2006) and in Europe (during the extremely dry year of 2003) (Granier et al. 2007).

1.4 Differential drought acclimation in plant species from contrasting climates

Plants subjected to short-term experimental drought are well documented to experience a decline in photosynthetic capacity. However, plants in the field may be able to acclimate to drought to some extent, for example through morphological adaptations such as changes in allocation to leaves *versus* roots, provided the drought is imposed slowly enough for such changes to take effect. In general, therefore, it is to be expected that the mechanisms underlying plant responses to water stress vary according to time scale (Maseda and Fernandez, 2006; Limousin et al., 2010a, b; Martin StPaul et al., 2012, 2013). Maseda and Fernandez (2006) proposed that plants acclimate to drought at the whole-organism level through physiological, anatomical, and morphological adjustments that are adaptive over a time scale of months.

Under long-term drought, leaves developed during the drought can acclimate by increasing partitioning to total soluble proteins, allowing higher Rubisco activity per unit leaf area (Pankovic et al., 1999). The Rubisco content could increase in leaves under prolonged drought, and the increase could be significantly higher in leaves of the drought-tolerant plant taxa than other taxa, conferring the drought-tolerant taxa with better acclimation and higher drought tolerance (Pankovic et al., 1999).

In addition, plant functional traits that mediate the vegetation responses to environmental drivers are strongly coordinated within and among species along the leaf economics spectrum (Wright et al., 2004; Prentice et al., 2014a; Reich 2014). As leaf function critically depends on the transport of water and nutrients *via* the stem, leaf and stem functional traits are expected to be closely correlated (Reich, 2014). For example, hydraulic adjustments can occur together with the photosynthetic acclimation in long-lived plants such as trees during long-term drought, rendering the xylem less vulnerable to cavitation while maintaining gas exchange at a high level. Stomatal conductance is thus strongly and necessarily linked to plant hydraulic architecture (Mencuccini, 2003; Choat et al., 2012). Under short-term drought, maximizing gas exchange while avoiding hydraulic failure would lead to dysfunction (Sperry, 2004). Hydraulic failure occurs when insufficient control of water loss during severe drought leads to the formation of embolisms, xylem damage and desiccation. Alternatively, when plants maintain leaf and xylem water potentials by stomatal closure, photosynthesis is inhibited, risking mortality from carbon starvation (Sala et al., 2012; Adams et al., 2013). Under long-term drought, hydraulic adjustment is expected to proceed in parallel with photosynthetic acclimation, in order to reduce water loss while maintaining photosynthesis.

Ignoring potentially important acclimation processes in the field could lead to overestimation of the long-term consequences of drought. Reliable prediction of drought effects on contrasting species and forest ecosystems under field conditions requires long-term

experiments on the drought-induced diffusional and biochemical limitations, and their potential acclimation to the drought. The number of such studies in the literature however is surprisingly small, with most published manipulative experiments focusing exclusively on short-term responses to drought (Cano et al., 2014).

1.5 Improving representation of photosynthesis in vegetation modelling

There is an increasing motivation to improve the representation of photosynthetic responses to environmental drivers in large-scale vegetation modelling (e.g. Medlyn et al., 2011; Bonan et al., 2014; Prentice et al., 2014a). Photosynthesis is well described in the Farquhar, von Caemmerer and Berry model (Farquhar et al., 1980). Coupling of a variant of this photosynthesis model to the empirical Ball–Berry stomatal conductance model (Ball et al., 1987; Collatz et al., 1991) was introduced into the land component of climate models in the mid-1990s, in order to estimate gross primary production (GPP) on a mechanistic basis (Bonan, 1995; Sellers et al., 1996; Cox et al., 1998). This or similar formulations are used widely in state-of-the-art ESMs. Research efforts have also been devoted specifically to the implementation of different modelling approaches for stomatal conductance (e.g. Bonan et al., 2014).

However, the present generation of DGVMs and LSMs embody a simplistic representation of plant ecophysiological properties and processes (Prentice & Cowling, 2013). Although photosynthesis accounts for the largest CO₂ flux from the atmosphere into ecosystems and is the driving process for terrestrial ecosystem function (Bernacchi et al., 2013), the fundamental component processes of plant gas exchange are still incompletely represented in global models, notably in the area of drought responses, and photosynthetic and morphological acclimation generally (including acclimation to drought) (Prentice & Cowling, 2013). There has been a scientific debate on how to represent stomatal closure as soil moisture declines (Bonan et al., 2014). Powell et al. (2013) reported unrealistic drought responses from

five terrestrial biosphere models, using different water-stress functions – loosely constrained by data – to down-regulate g_s . Another specific issue is that the V_{cmax} parameter has usually been attributed to a PFT as a single value, or as a single-valued function of environmental drivers (Haxeltine & Prentice, 1996). Emerging evidence points to the importance of representing both stomatal and non-stomatal responses to drought in models (Egea et al., 2011).

Currently there are large discrepancies in the way ecosystem models represent the drought responses of plant gas exchange (De Kauwe et al., 2013). Present ecosystem models treat all PFTs as experiencing similar stomatal limitation during drought (via soil texture and assumed rooting depths), and few considered non-stomatal limitation, such that the modelling approach lacks a functionally realistic representation of drought responses of g_s and V_{cmax} . Largely due to the shortage of experimental studies describing the separate effects of drought on stomatal and non-stomatal processes, current models markedly differ in how they are represented. In models, drought may act either by increasing the marginal water use efficiency, which depends on the C_i/C_a ratio (the ratio of CO_2 concentration inside and outside the leaf); by reducing V_{cmax} and/or J_{max} ; or both. Moreover, most models simulate the drought effect on photosynthesis in a rough way simply by reducing the slope of the relationship between g_s and A , in a similar way for all PFTs. It is not known whether this method is adequate to capture the drought response, but there is a strong case to expect that it is not, as it does not account for either differences among species from different climatic origins, or for mechanisms of plant acclimation to drought.

The process of estimation of required model parameters (including g_s and V_{cmax} and their functions against soil moisture content) for global models is not straightforward and usually not transparent. Process-based modelling of the drought impacts on plants and ecosystems must be informed by experiments, which can help us to understand underlying processes.

Model evaluation and improvement must include the use of experimental observations, theory to explain the observations, quantitative parameterizations to describe the theory, and model simulations to test the impacts of environmental variables (Bonan et al., 2014) – necessary characteristics of ‘next-generation’ models as argued by Prentice et al. (2014b).

1.6 Philosophy and approach in this thesis

The research described in this thesis aimed at improving the representation of stomatal and non-stomatal responses to soil water potential within LSMs and DGVMs, based on the analysis of published and new experimental data on both the short- and long-term responses of gas exchange to drought, in species of contrasting climatic origins. The work also includes an exploratory study in which eddy covariance data (CO_2 and latent heat fluxes) from flux tower sites in different types of forests were compared to model simulations, including simulations with a LSM modified to include parameterizations of stomatal and non-stomatal drought response derived from experiments. In particular:

- (1) Existing, mainly published data were collected and analysed quantitatively in an explicit modelling framework based on combining the Farquhar et al. (1980) and Medlyn et al. (2011) models, in order to investigate how the stomatal and non-stomatal responses to drought differ across PFTs and climates.
- (2) Short-term experiments were conducted, and analysed in the same framework, in order to investigate how stomatal and non-stomatal drought sensitivity differ among tree species from contrasting environments.
- (3) Longer-term experiments were conducted in order to investigate the extent to which tree species from contrasting environments could acclimate (both in terms of stomatal and non-stomatal responses) to drought, and the hydraulic adjustments involved in acclimation.

(4) Observed responses of stomatal and non-stomatal sensitivity among PFTs were included within an LSM, and results compared to eddy covariance flux measurements.

The four research chapters sought to answer the following questions:

(1) Which photosynthetic processes are affected in short-term drought? What shape does each response function take? How do the responses vary across PFT membership and hydro-climates?

(2) How stomatal, mesophyll, and biochemical responses to short-term drought differ among species originating from different hydro-climates?

(3) Whether the plants acclimate to longer-term water stress? How riparian and xeric species differ in their degree of acclimation?

(4) Whether the inclusion of experimentally based and PFT-specific drought response functions of g_s and V_{cmax} would help LSMs to reproduce key features of ecosystems' responses to the heatwave?

The second chapter in this thesis (Zhou S, Duursma RA, Medlyn BE, Kelly JW, and Prentice IC, 2013. How should we model plant responses to drought? An analysis of stomatal and non-stomatal responses to water stress. *Agricultural and Forest Meteorology*, 182, 204-214) describes the characterization of stomatal and non-stomatal responses to drought with data sets from published experimental studies, and investigates how the response patterns vary with PFTs and climates. The starting point is to introduce a new analytical framework to disentangle stomatal and non-stomatal limitations. Drought effects on stomatal conductance are further partitioned into changes that represent an optimal response to a reduction in photosynthetic capacity, and changes driven by an increase in the marginal cost of water. The difference between this new framework and the traditional one introduced by Jones (1985) is

important, and discussed in this chapter, because any reduction in photosynthetic capacity will automatically generate a reduction in stomatal conductance both according to the optimal stomatal model (Cowan, 1977; Cowan & Farquhar, 1977) and empirical models (e.g. Ball et al. 1987, Leuning 1995) potentially resulting in confounding of biochemical and diffusional effects. The approach adopted in this chapter avoids this problem and has the advantage of being able to be translated directly into modelling terms. The results obtained describe in a common, consistent framework the drought sensitivity of stomatal conductance, mesophyll conductance, carboxylation capacity, and maximum electron transport rate, across a variety of PFTs and climates.

The third chapter in the thesis (Zhou S, Medlyn BE, Santiago S, Sperlich D, and Prentice IC, 2014. Short-term water stress impacts on stomatal, mesophyll, and biochemical limitations to photosynthesis differ consistently among tree species from contrasting climates. *Tree Physiology*. DOI: 10.1093/treephys/tpu072) systematically tests the simultaneous drought limitation on stomatal conductance, mesophyll conductance, and photosynthetic capacity across species and ecosystems in Australia and Europe with two glasshouse experiments. The rates of decline in stomatal conductance, mesophyll conductance, carboxylation capacity, and maximum electron transport rate are quantified in nine tree species along a strong hydro-climatic gradient. This chapter adopts the explicit and consistent definitions and analytical models introduced in the second chapter to characterize the stomatal and non-stomatal drought responses. It tests the hypothesis that there is a coordinated spectrum of increasing tolerance in plants from drier environments to wetter environments.

The fourth chapter in the thesis (Zhou S, Medlyn BE, Prentice IC. 2014. Long-term water stress leads to acclimation of drought sensitivity of photosynthetic capacity in xeric but not riparian *Eucalyptus* species) tests whether species from contrasting hydro-climates differ in their degree of acclimation to long-term drought. It compares gas exchange parameters

between xeric and riparian *Eucalyptus* species at two months and four months of partial drought (70 % field capacity) under glasshouse conditions. After four months, all of the plants enters a drying-down cycle starting at 100 % field capacity and proceeding to full stomatal closure, thus allowing comparison of their drought sensitivities (including stomatal conductance, mesophyll conductance and biochemical responses) during short-term drought after previous acclimation to long-term drought. Hydraulic adjustments at four months are also compared among the species.

The fifth chapter in the thesis (Zhou S, De Kauwe MG, Medlyn BE, Pitman AJ and Prentice IC. 2014. Representing observed plant responses to drought in a land surface model) tests the effects of representing empirically derived stomatal and non-stomatal drought responses within the Community Atmosphere Biosphere Land Exchange (CABLE) LSM. Experimentally derived stomatal and non-stomatal drought responses are used to define PFT-dependent relationships of stomatal sensitivity and photosynthetic capacity to soil water potential, as alternatives to the standard representation (a generic response to volumetric soil moisture content) of drought effects in CABLE. Comparisons are made between model simulations and CO₂ and latent heat flux measurements at six eddy covariance flux sites from different forest types and regions in Europe, across the heatwave that occurred in the summer of 2003.

1.7 Collaboration and candidate's role

Each main chapter in this thesis has been written as a journal article, and is either published, in review, or ready to submit.

Chapter 2 Zhou S., Duursma R.A., Medlyn B.E., Kelly J.W., and Prentice I.C., 2013. How should we model plant responses to drought? An analysis of stomatal and non-stomatal responses to water stress. *Agricultural and Forest Meteorology*, 182, 204-214.

Prentice I.C. and Medlyn B.E. proposed the original idea for this paper. Duursma R.A., Medlyn B.E., Prentice I.C. and Zhou S. were responsible for investigating the analytical models on stomatal and non-stomatal responses. Duursma R.A. instructed Zhou S. on plotting in R. Kelly J.W. offered two observational data sets from his glasshouse experiment. Zhou S collected all the published data sets, completed the quantitative characterizations, and wrote the first draft of the paper. Zhou S, Duursma R.A., Medlyn B.E., and Prentice I.C. contributed to the final version of the manuscript.

Chapter 3 Zhou S., Medlyn B.E., Santiago S., Sperlich D., and Prentice I.C., 2014. Short-term water stress impacts on stomatal, mesophyll, and biochemical limitations to photosynthesis differ consistently among tree species from contrasting climates. *Tree Physiology*. DOI: 10.1093/treephys/tpu072.

Zhou S., Medlyn B.E., and Prentice I.C. were responsible for the design of the glasshouse experiment in Macquarie University. Zhou S., Santiago S., and Prentice I.C. were responsible for the design of the glasshouse experiment in University of Barcelona. Santiago S. established the experiment platform in University of Barcelona. Sperlich D. contributed to the experiment University of Barcelona. Zhou S. completed all measurements in both experiments and all quantitative characterizations, statistical analyses and figure plotting, and wrote the first draft of the paper. All authors contributed to the final version of the manuscript.

Chapter 4 Zhou S., Medlyn B.E., Prentice I.C., 2014. Long-term water stress leads to acclimation of drought sensitivity of photosynthetic capacity in xeric but not riparian *Eucalyptus* species. In review with *Annals of Botany*.

All authors were responsible for the design of the glasshouse experiment in Macquarie University. Zhou S. designed the investigation on hydraulic adjustments. Zhou S. completed all measurements, quantitative characterizations, statistical analyses and figure plotting, and

wrote the first draft of the paper. All authors contributed to the final version of the manuscript.

Chapter 5 Zhou S., De Kauwe M.G., Medlyn B.E., Pitman A.J., and Prentice I.C., 2014. Representing observed plant responses to drought in a land surface model. In preparation for submission to *Ecological Modelling*.

The original idea for this study (with different choice of models) arose from separated discussions among Medlyn B.E., Prentice I.C., De Kauwe M.G., and Zhou S.. Medlyn B.E. and De Kauwe M.G. designed the simulations within the CABLE model. Zhou S. fitted the PFT-specific stomatal and non-stomatal response functions based on his experimental observations. De Kauwe M.G. incorporated these functions into CABLE and ran the simulations. Zhou S. and De Kauwe M.G. completed the statistical analyses and figure plotting. Zhou S. wrote the first draft of the paper. All authors contributed to the final version of the manuscript.

1.8 References

Adams, H. D., Germino, M. J., Breshears, D. D., et al. (2013) Nonstructural leaf carbohydrate dynamics of *Pinus edulis* during drought-induced tree mortality reveal role for carbon metabolism in mortality mechanism. *New Phytol.* 197, 1142–1151.

Adams, H. D., Guardiola-Claramonte, M., Barron-Gafford, G. A., et al. (2009) Temperature sensitivity of drought-induced tree mortality portends increased regional die-off under global-change-type drought. *Proc Natl Acad Sci USA* 106(17): 7063–7066.

Allen, C. D., Macalady, A. K., Chenchouni, H., et al. (2010) A global overview of drought and heat-induced tree mortality reveals emerging climate change risks for forests. *For Ecol Manage* 259(4): 660–684.

Allison, I., Bindoff, N. L., Bindenschadler, R. A., et al. (2009) The Copenhagen Diagnosis, 2009: Updating the World on the Latest Climate Science, The University of New South Wales Climate Change Research Centre.

Anderegg, W. R., Berry, J. A., Smith, D. D., et al. (2012) The roles of hydraulic and carbon stress in a widespread climate-induced forest die-off. *Proc. Natl Acad. Sci. USA* 109, 233–237.

Baldocchi, D. (1997) Measuring and modeling carbon dioxide and water vapor exchange over a temperate broad-leaved forest during the 1995 summer drought. *Plant Cell Environ.* 20,

1108-1122.

Baldocchi, D. (2008) TURNER REVIEW No. 15. 'Breathing' of the terrestrial biosphere: lessons learned from a global network of carbon dioxide flux measurement systems. *Aus. J. Bot.*, 56(1), 1-26.

Baldocchi, D., Hicks, B.B., Meyers, T.D. (1988) Measuring biosphere–atmosphere exchanges of biologically related gases with micrometeorological methods. *Ecology* 69, 1331–1340.

Ball JT, Woodrow IE, Berry JA (1987) A model predicting stomatal conductance and its contribution to the control of photosynthesis under different environmental conditions. In: *Progress in Photosynthesis Research* (ed. Biggins J), pp. 221–224. Martinus- Nijhoff Publishers, Dordrecht, the Netherlands

Berninger, F., Hari, P., 1993. Optimal regulation of gas exchange: evidence from field data. *Ann. Bot.* 71, 135–140.

Beniston, M., Stephenson, D.B., Christensen, O.B., Ferro, C.A.T., Frei, C., Goyette, S., Halsnaes, K., Holt, T., Jylha, K., Koffi, B., Palutikof, J., Schöll, R., Semmler, T., Woth, K. (2007) Future extreme events in European climate: an exploration of regional climate model projections. *Climatic Change* 81, 71-95.

Bernacchi, C. J., Bagley, J. E., Serbin, S. P., et al. (2013) Modelling C₃ photosynthesis from the chloroplast to the ecosystem. *Plant Cell Environ.* 36(9), 1641-1657.

Bonan, G. B. (1995) Land–atmosphere CO₂ exchange simulated by a land surface process model coupled to an atmospheric general circulation model, *J. Geophys. Res.*, 100, 2817–2831.

Bonan, G. B. (2008) Forests and climate change: forcings, feedbacks, and the climate benefits of forests. *Science*, 320(5882), 1444-1449.

Bonan, G. B., Lawrence, P. J., Oleson, K. W., Levis, S., Jung, M., Reichstein, M., ... & Swenson, S. C. (2011) Improving canopy processes in the Community Land Model version 4 (CLM4) using global flux fields empirically inferred from FLUXNET data. *J. Geophys. Res.: Biogeosciences* (2005–2012), 116(G2).

Bonan, G. B., Oleson, K. W., Fisher, R. A., Lasslop, G., & Reichstein, M. (2012) Reconciling leaf physiological traits and canopy flux data: Use of the TRY and FLUXNET databases in the Community Land Model version 4. *J. Geophys. Res.: Biogeosciences* (2005–2012), 117(G2).

Bonan, G. B., Williams, M., Fisher, R. A., & Oleson, K. W. (2014) Modeling stomatal conductance in the Earth system: linking leaf water-use efficiency and water transport along the soil-plant-atmosphere continuum. *Geoscientific Model Development Discussions*, 7(3), 3085-3159.

Bota J, Medrano H, Flexas J (2004) Is photosynthesis limited by decreased Rubisco activity and RuBP content under progressive water stress? *New Phytol* 162:671–681.

Breshears, D. D., Cobb, N. S., Rich, P. M., et al. (2005) Regional vegetation die-off in

- response to global-change-type drought. *Proc. Natl. Acad. Sci. U.S.A.* 102, 15144–15148.
- Castrillo, M., Fernandez, D., Calcagno, A. (2001) Responses of ribulose-1,5-bisphosphate carboxylase, protein content, and stomatal conductance to water deficit in maize, tomato, and bean. *Photosynthetica* 39: 221–226.
- Chaves, M.M., Maroco, J.P., Pereira, J.S. (2003) Understanding plant responses to drought – from genes to the whole plant. *Funct. Plant Biol.* 30(3): 239–264.
- Chen, H., Dickinson, R. E., Dai, Y., Zhou, L. (2011) Sensitivity of simulated terrestrial carbon assimilation and canopy transpiration to different stomatal conductance and carbon assimilation schemes. *Climate Dynamics*, 36(5-6), 1037-1054.
- Choat, B., Jansen, S., Brodribb, T.J., et al. (2012) Global convergence in the vulnerability of forests to drought. *Nature* 491(7426): 752-755.
- Ciais, P., Reichstein, M., Viovy, N., et al. (2005) Europe-wide reduction in primary productivity caused by the heat and drought in 2003. *Nature* 437, 529-533.
- Ciais, P., Sabine, C., Bala, G., Bopp, L., Brovkin, V., Canadell, J., Chhabra, A., DeFries, R., Galloway, J., Heimann, M., Jones, C., Le Quéré, C., Myneni, R. B., Piao, S., and Thornton, P.: Carbon and Other Biogeochemical Cycles, in *Climate Change 2013: The Physical Science Basis. Contribution of Working Group I to the Fifth Assessment Report of the Intergovernmental Panel on Climate Change*, edited by: T. F. Stocker, Qin, D., Plattner, G.-K., Tignor, M., Allen, S. K., Boschung, J., Nauels, A., Xia, Y., Bex, V., and Midgley, P. M., p. 1535, Cambridge University Press, Cambridge, United Kingdom and New York, NY, USA, 2013.
- Clark, J. S., Bell, D. M., Kwit, M., et al. (2012) Individual-scale inference to anticipate climate-change vulnerability of biodiversity. *Phil. Trans. R. Soc. Lond. B. Biol. Sci.* 367, 236–246.
- Collatz, G. J., Ball, J. T., Griivet, C., Berry, J. A. (1991) Physiological and environmental regulation of stomatal conductance, photosynthesis and transpiration: a model that includes a laminar boundary layer. *Agric. For. Meteorol.* 54: 107–136.
- Collatz, G. J., Ribas-Carbo, M., & Berry, J. A. (1992) Coupled photosynthesis-stomatal conductance model for leaves of C₄ plants. *Funct. Plant Biol.*, 19(5), 519-538.
- Cano, F.J., López, R., Warren, C.R. (2014) Implications of the mesophyll conductance to CO₂ for photosynthesis and water-use efficiency during long-term water stress and recovery in two contrasting *Eucalyptus* species. *Plant Cell Environ.* DOI: 10.1111/pce.12325.
- Cowan, I.R., 1977. Stomatal behaviour and environment. *Adv. Bot. Res.* 4, 117–288.
- Cowan, I.R., Farquhar, G.D., 1977. Stomatal function in relation to leaf metabolism and environment. *Symp. Soc. Exp. Biol.* 31, 471–505.
- Cox, P. M., Huntingford, C., and Harding, R. J. (1998) A canopy conductance and photosynthesis model for use in a GCM land surface scheme, *J. Hydrol.*, 212–213, 79–94.
- De Kauwe, M.G., Medlyn, B.E., Zaehle, S., et al. (2013) Forest water use and water use

efficiency at elevated CO₂: a model-data intercomparison at two contrasting temperate forest FACE sites. *Glob. Chang. Biol.* 19, 1759–1779.

Duan, H., Amthor, J. S., Duursma, R. A., O'Grady, A. P., Choat, B., & Tissue, D. T. (2013) Carbon dynamics of eucalypt seedlings exposed to progressive drought in elevated [CO₂] and elevated temperature. *Tree physiol.*, tpt061.

Egea, G, Verhoef, A, Vidale, PL. (2011) Towards an improved and more flexible representation of water stress in coupled photosynthesis–stomatal conductance models. *Agric. For. Meteorol.* 151: 1370–1384.

Engelbrecht, B. M., Comita, L. S., Condit, R., Kursar, T. A., Tyree, M. T., Turner, B. L., & Hubbell, S. P. (2007) Drought sensitivity shapes species distribution patterns in tropical forests. *Nature*, 447(7140), 80–82.

Evans, J.R., von Caemmerer, S. (2013) Temperature response of carbon isotope discrimination and mesophyll conductance in tobacco. *Plant Cell Environ.* 36: 745–756.

Farquhar, G.D., von Caemmerer, S., Berry, J.A. (1980). A biochemical model of photosynthetic CO₂ assimilation in leaves of C₃ species. *Planta* 149: 78–90.

Fischer, E. M., Seneviratne, S. I., Lüthi, D., Schär, C. (2007) Contribution of land-atmosphere coupling to recent European summer heat waves. *Geophys. Res. Lett.*, 34(6).

Flexas, J., Barbour, M.M., Brendel, O., et al. (2012) Mesophyll diffusion conductance to CO₂: an unappreciated central player in photosynthesis. *Plant Sci.* 193–194: 70–84.

Flexas, J., Bota, J., Loreto, F., Cornic, G., Sharkey, T.D. (2004) Diffusive and metabolic limitations to photosynthesis under drought and salinity in C₃ plants. *Plant Biol.* 6: 269–279.

Flexas, J., Diaz-Espejo, A., Galmés, J., Kaldenhoff, R., Medrano, H., Ribas-Carbo, M (2007) Rapid variations of mesophyll conductance in response to changes in CO₂ concentration around leaves. *Plant Cell Environ.* 30:1284–1298.

Flexas, J., Medrano, H. (2002) Drought-inhibition of photosynthesis in C₃ plants: Stomatal and non-stomatal limitations revisited. *Ann. Bot.* 89, 183–189.

Flexas, J., Ribas-Carbó, M., Bota, J., Galmés, J., Henkle, M., Martínez-Cañellas, S., Medrano, H. (2006) Decreased Rubisco activity during water stress is not induced by decreased relative water content but related to conditions of low stomatal conductance and chloroplast CO₂ concentration. *New Phytol.* 172: 73–82.

Flexas, J., Ribas-Carbó M, Diaz-Espejo A., Galmés J., & Medrano, H. (2008) Mesophyll conductance to CO₂: current knowledge and future prospects. *Plant Cell Environ.* 31(5), 602–621.

Galmés, J., Aranjuelo, I., Medrano, H., & Flexas, J. (2013) Variation in Rubisco content and activity under variable climatic factors. *Photosynthesis Res.*, 1–18.

Galmés, J., Flexas J, Keys AJ, Cifre J, Mitchell RAC, Madgwick PJ, Haslam RP, Medrano H, Parry MAJ (2005) Rubisco specificity factor tends to be larger in plant species from drier

- habitats and in species with persistent leaves. *Plant Cell Environ.* 28:571–579.
- Giorgi, F. (2006) Climate change hot-spots. *Geophysical Research Letters* 33, L08707.
- Giorgi, F., Bi, X., Pal, J., (2004) Mean, interannual variability and trends in a regional climate change experiment over Europe. II. Climate change scenarios (2071–2100). *Climate Dynamics* 23, 839–858.
- Granier, A., Reichstein, M., Bréda, N., et al. (2007) Evidence for soil water control on carbon and water dynamics in European forests during the extremely dry year: 2003. *Agric. For. Meteorol.* 143(1), 123–145.
- Grassi G, Magnani F (2005) Stomatal, mesophyll conductance and biochemical limitations to photosynthesis as affected by drought and leaf ontogeny in ash and oak trees. *Plant Cell Environ* 28:834–849.
- Groenendijk, M., Dolman, A.J., van der Molen, M.K., et al. (2011) Assessing parameter variability in a photosynthesis model with and between plant functional types using global Fluxnet eddy covariance data. *Agric. For. Meteorol.* 151, 22–38.
- Hall, A. E., SCHULZE, E. D. (1980). Stomatal response to environment and a possible interrelation between stomatal effects on transpiration and CO₂ assimilation. *Plant Cell Environ.* 3(6), 467–474.
- Hartmann, H., Ziegler, W., Kolle, O. & Trumbore, S (2013). Thirst beats hunger-declining hydration during drought prevents carbon starvation in Norway spruce saplings. *New Phytol.* 200, 340–349.
- Haxeltine, A., Prentice, I. C. (1996) BIOME3: An equilibrium terrestrial biosphere model based on ecophysiological constraints, resource availability, and competition among plant function types, *Global Biogeochemic. Cy.*, 10, 693–709.
- Hérault, A., Lin, Y-S., Bourne, A., Medlyn, B.E., Ellsworth, D.S. (2013) Optimal stomatal conductance in relation to photosynthesis in climatically contrasting *Eucalyptus* species under drought. *Plant Cell Environ.* 36: 262–274.
- IPCC (2014) Stocker TF et al. eds. *Climate Change 2013: The Physical Science Basis. Contribution of Working Group I to the Fifth Assessment Report of the Intergovernmental Panel on Climate Change.* Cambridge: Cambridge University Press.
- Jones, H.G. (1985) Partitioning stomatal and non-stomatal limitations to photosynthesis. *Plant Cell Environ.* 8:95–104.
- Kanechi, M., Uchida, N., Yasuda, T., Yamaguchi, T. (1996) Non-stomatal inhibition associated with inactivation of rubisco in dehydrated coffee leaves under unshaded and shaded conditions. *Plant Cell Physiol.* 37:455–460.
- Kattge J., Knorr W., Raddatz T., Wirth C. (2009) Quantifying photosynthetic capacity and its relationship to leaf nitrogen content for global-scale terrestrial biosphere models. *Glob. Chang. Biol.* 15, 976–991.
- Kljun, N, Black, TA, Griffis, TJ, Barr, AG, Gaumont-Guay, D., Morgenstern, K.,

- McCaughey, J.H., Nesic Z. (2006) Response of net ecosystem productivity of three boreal forest stands to drought. *Ecosystems* 9(7), 1128-1144.
- Knapp, A.K., Smith, M.D. (2001) Variation among biomes in temporal dynamics of aboveground primary production. *Science* 291(5503):481–484.
- Lawlor, D.W., Cornic, G. (2002) Photosynthetic carbon assimilation and associated metabolism in relation to water deficits in higher plants. *Plant, Cell and Environment*. 25, 275.
- Lawlor, D.W., Tezara, W. (2009) Causes of decreased photosynthetic rate and metabolic capacity in water-deficient leaf cells: a critical evaluation of mechanisms and integration of processes. *Ann. of Bot.* 103:561-579.
- Le Quéré, C., Andres, R. J., Boden, T., et al. (2013). The global carbon budget 1959–2011. *Earth System Science Data*, 5(1), 165-185.
- Lee, X., Massman, W., Law, B. (Eds.), 2004. *Handbook of Micrometeorology: A Guide for Surface Flux Measurement and Analysis*. Kluwer Academic Publishers.
- Leuning, R. (1995) A critical appraisal of a combined stomatal-photosynthesis model for C₃ plants. *Plant Cell Environ* 18:339–355.
- Limousin, J.M., Longepierre, D., Huc, R., Rambal, S. (2010a) Change in hydraulic traits of Mediterranean *Quercus ilex* subjected to long-term throughfall exclusion. *Tree Physiol* 30(8): 1026-1036.
- Limousin, J.M., Misson, L., Lavoie, A.V., Martin, N.K., Rambal, S. (2010b) Do photosynthetic limitations of evergreen *Quercus ilex* leaves change with long-term increased drought severity?. *Plant Cell Environ*. 33(5): 863-875.
- Long S.P., Ainsworth E.A., Leakey A.D.B., Nosberger J. & Ort D.R. (2006) Food for thought: lower than expected crop yield stimulation with rising CO₂ concentrations. *Science* 312, 1918–1921.
- Mäkelä, A., Berninger, F., Hari, P. (1996) Optimal control of gas exchange during drought : theoretical analysis. *Ann. Bot.* 77:461–467.
- Malhi, Y., Aragão, L. E., Galbraith, D., et al. (2009) Exploring the likelihood and mechanism of a climate-change-induced dieback of the Amazon rainforest. *Proc. Natl. Acad. Sci. U.S.A.* 106, 20610.
- Martin-StPaul, N.K., Limousin, J.M., Vogt-Schilb, H., Rodríguez-Calcerrada, J., Rambal, S., Longepierre, D., Misson, L. (2013) The temporal response to drought in a Mediterranean evergreen tree: comparing a regional precipitation gradient and a throughfall exclusion experiment. *Glob. Chang. Biol.* 19(8): 2413-2426.
- Martin-StPaul, N.K., Limousin, J.M., Rodríguez-Calcerrada, J., Ruffault, J., Rambal, S., Letts, M.G., Misson, L. (2012) Photosynthetic sensitivity to drought varies among populations of *Quercus ilex* along a rainfall gradient. *Funct. Plant Biol.* 39(1): 25-37.
- Maseda, P.H., Fernández, R.J. (2006). Stay wet or else: three ways in which plants can adjust hydraulically

to their environment. *J. Exp. Bot.* 57: 3963–3977.

Matusick, G., Ruthrof, K.X., Brouwers, N.C., Dell, B., Hardy, G.S.J., 2013. Sudden forest canopy collapse corresponding with extreme drought and heat in a mediterranean-type eucalypt forest in southwestern Australia. *European Journal of Forest Research*, 132(3): 497-510.

McDowell, N., Pockman, W. T., Allen, C. D., et al. (2008) Mechanisms of plant survival and mortality during drought: Why do some plants survive while others succumb to drought? *New Phytol.* 178(4): 719–739.

McDowell, N. G., Beerling, D. J., Breshears, D. D., et al. (2011). The interdependence of mechanisms underlying climate-driven vegetation mortality. *Trends in Ecology and Evolution*, 26(10): 523-532.

Medlyn, B.E., Duursma, R.A., Eamus, D. et al. (2011) Reconciling the optimal and empirical approaches to modelling stomatal conductance. *Glob. Chang. Biol.* 17:2134–2144.

Mencuccini, M. (2003) The ecological significance of long-distance water transport: short-term regulation, long-term acclimation and the hydraulic costs of stature across plant life forms. *Plant Cell Environ.* 26:163-182.

Nemani, R.R., Keeling, C.D., Hashimoto, H. et al. (2003) Climate-driven increases in global terrestrial net primary production from 1982 to 1999. *Science* 300: 1560–1563.

Niinemets, U., Penuelas, J., Flexas, J. (2011). Evergreens favored by higher responsiveness to increased CO₂. *Trends in Ecology and Evolution* 26: 136–142.

O'Brien, M. J., Leuzinger, S., Philipson, C. D., Tay, J., Hector, A. (2014) Drought survival of tropical tree seedlings enhanced by non-structural carbohydrate levels. *Nature Climate Change*, 4(8), 710-714.

Parry, M.A., Andralojc, P.J., Khan, S., Lea, P.J., Keys, A.J. (2002) Rubisco activity: effects of drought stress. *Ann. Bot.* 89:833–839.

Pan, Y., Birdsey, R. A., Fang, J., Houghton, R., Kauppi, P. E., Kurz, W. A., ... & Hayes, D. (2011). A large and persistent carbon sink in the world's forests. *Science*, 333(6045), 988-993.

Panković, D., Sakač, Z., Kevrešan, S., Plesničar, M. (1999) Acclimation to long-term water deficit in the leaves of two sunflower hybrids: photosynthesis, electron transport and carbon metabolism. *J. Exp. Bot.* 50: 127-138.

Pasho, E., Camarero, J.J., de Luis, M., Vicente-Serrano, S.M. (2011) Impacts of drought at different time scales on forest growth across a wide climatic gradient in north-eastern Spain. *Agric. For. Meteorol.* 151(12):1800–1811.

Pereira, J.S., Mateus, J., Aires, L., Pita, G., Pio, C., David, J., Andrade, V., Banza, J., David, T.S., Paco, T.A., Rodrigues, A. (2007) Net ecosystem carbon exchange in three contrasting Mediterranean ecosystems-the effect of drought. *Biogeosciences* 4, 791-802.

Sperry, J.S. (2004) Coordinating stomatal and xylem functioning – an evolutionary

perspective. *New Phytol.* 162, 568–570.

Pinheiro, C., Chaves M.M. (2011) Photosynthesis and drought: can we make metabolic connections from available data? *J. Exp. Bot.* 62:869-882.

Phillips, O. L., Aragão, L. E., Lewis, S. L., et al. (2009) Drought sensitivity of the Amazon rainforest. *Science*, 323(5919), 1344-1347.

Phillips, O. L., Van der Heijden, G., Lewis, S. L., et al. (2010) Drought-mortality relationships for tropical forests. *New Phytol.* 187, 631–646.

Pitman, A. J.: The evolution of, and revolution in, land surface schemes designed for climate models, *Int. J. Climatol.*, 23, 479–510, 2003.

Pockman WT, Sperry JS (2000) Vulnerability to xylem cavitation and the distribution of Sonoran desert vegetation. *Am. J. Bot.* 87, 1287-1299.

Potts, M. (2003) Drought in a Bornean everwet rain forest. *J. Ecol.* 91, 467–474.

Powell, T. L., Galbraith, D. R., Christoffersen, B. O., Harper, A., Imbuzeiro, H., Rowland, L., Samuel Almeida S., Brando P. M., da Costa, A. C. L., Costa M. H., N. M. Levine, Y. Malhi, S. R. Saleska, E. Sotta, M. Williams, P. Meir, and Moorcroft, P. R. (2013) Confronting model predictions of carbon fluxes with measurements of Amazon forests subjected to experimental drought. *New Phytol.*, 200(2), 350-365.

Prentice, I. C., Cowling, S. A. (2013) Dynamic global vegetation models, in: *Encyclopedia of Biodiversity*, 2nd edition, edited by: Levin, S. A., Academic Press, 607–689.

Prentice, I.C., N. Dong, S.M. Gleason, V. Maire and I.J. Wright (2014a) Balancing the costs of carbon gain and water loss: testing a new quantitative framework for plant functional ecology. *Ecology Letters* 17: 82-91.

Prentice, I.C., X. Liang, B. Medlyn and Y. Wang (2014b) Reliable, robust and realistic: the three R's of next-generation land-surface modelling. *Atmospheric Chemistry and Physics Discussions* 14: 24811-24861.

Rambal, S., Ourcival, J-M., Joffre, R., Mouillot, F., Nouvellon, Y., Reichstein, M., Rocheteau, A. (2003) Drought controls over conductance and assimilation of a Mediterranean evergreen ecosystem: Scaling from leaf to canopy. *Glob. Chang. Biol.* 9, 1813-1824.

Reich, P.B. (2014) The world-wide 'fast-slow' plant economics spectrum: a traits manifesto. *J. of Ecol.* 102:275-301.

Reichstein, M., Tenhunen, J.D., Rouspard, O., Ourcival, J.M., Rambal, S., Dore, S., Valentini, R. (2002a) Ecosystem respiration in two Mediterranean evergreen holm oak forests: Drought effects and decomposition dynamics. *Funct. Ecol.* 16, 27-39.

Reichstein, M., Tenhunen, J.D., Rouspard, O., et al. (2002b) Severe drought effects on ecosystem CO₂ and H₂O fluxes at three Mediterranean evergreen sites: Revision of current hypotheses? *Glob. Chang. Biol.* 8, 999.

Reichstein, M., Ciais, P., Papale, D., et al. (2007). Reduction of ecosystem productivity and

- respiration during the European summer 2003 climate anomaly: A joint flux tower, remote sensing and modelling analysis. *Glob. Chang. Biol.* 13, 634–651.
- Rogers, A., Medlyn, B. E., Dukes, J. S. (2014). Improving representation of photosynthesis in Earth System Models. *New Phytol.* 204(1), 12–14.
- Sala, A., Piper, F. & Hoch, G (2010). Physiological mechanisms of drought-induced tree mortality are far from being resolved. *New Phytol.* 186, 274–281.
- Sala, A., Woodruff, D. R., & Meinzer, F. C. (2012) Carbon dynamics in trees: Feast or famine? *Tree Physiol.* 32, 764–775.
- Sellers, P. J., Randall, D. A., Collatz, G. J., Berry, J. A., Field, C. B., Dazlich, D. A., Zhang, C., Collelo, G. D., and Bounoua, L. (1996) A revised land surface parameterization (SiB2) for atmospheric GCMs, Part I: Model formulation, *J. Climate*, 9, 676–705.
- Sevanto, S., McDowell, N. G., Dickman, L. T., Pangle, R. & Pockman, W. T. How do trees die? (2014) A test of the hydraulic failure and carbon starvation hypotheses. *Plant Cell Environ.* 37, 153–161.
- Sperry, J.S. (2004) Coordinating stomatal and xylem functioning – an evolutionary perspective. *New Phytol.* 162, 568–570.
- Tezara, W. (2002) Effects of water deficit and its interaction with CO₂ supply on the biochemistry and physiology of photosynthesis in sunflower. *J. Exp. Bot.* 53:1781–1791.
- Tezara, W., Mitchell, V.J., Driscoll, S.D., Lawlor, D.W. (1999) Water stress inhibits plant photosynthesis by decreasing coupling factor and ATP. *Nature* 401: 914–917.
- Thimmanaik, S., Kumar, S.G., Kumari, G.J., Suryanarayana, N., Sudhakar, C. (2002) Photosynthesis and the enzymes of photosynthetic carbon reduction cycle in mulberry during water stress and recovery. *Photosynthetica* 40:233–236.
- Vicente-Serrano, S. M., Gouveia, C., Camarero, J. J., et al., (2013). Response of vegetation to drought time-scales across global land biomes. *Proceedings of the National Academy of Sciences*, 110(1), 52–57.
- Webb WL, Lauenroth WK, Szarek SR, Kinerson RS (1983) Primary production and abiotic controls in forests, grasslands, and desert ecosystems in the United States. *Ecology* 64(1):134–151.
- Williams, C. A., Albertson, J. D. (2005). Contrasting short- and long-timescale effects of vegetation dynamics on water and carbon fluxes in water-limited ecosystems. *Water Resources Research*, 41(6).
- Williams, A.P., Allen, C. D., Macalady, A. K., et al. (2013) Temperature as a potent driver of regional forest drought stress and tree mortality. *Nature Climate Change*, 3(3), 292–297.
- Wilson, K.B., Baldocchi, D.D., Hanson, P.J. (2000) Quantifying stomatal and non-stomatal limitations to carbon assimilation resulting from leaf aging and drought in mature deciduous tree species. *Tree Physiol.* 20:787–797.

Wright, I.J., Reich, P.B., Westoby, M., et al. (2004) The worldwide leaf economics spectrum. *Nature*. 428: 821-827.

Xu, L., Baldocchi, D.D. (2003) Seasonal trends in photosynthetic parameters and stomatal conductance of blue oak (*Quercus douglasii*) under prolonged summer drought and high temperature. *Tree Physiol.* 23:865–877.

Xu, L., Baldocchi, D.D. (2004) Seasonal variation in carbon dioxide exchange over a Mediterranean annual grassland in California. *Agric. For. Meteorol.* 123, 79-96.

Yachi, S. & Loreau, M. (1999) Biodiversity and ecosystem productivity in a fluctuating environment: the insurance hypothesis. *Proc. Natl Acad. Sci. USA* 96, 1463–1468.

Zeppel, M.J.B., Wilks, J., Lewis, J.D. (2014). Impacts of extreme precipitation and seasonal changes in precipitation on plants. *Biogeosciences*, 11: 1-11. doi:10.5194/bg-11-1-2014.

Chapter 2

How should we model plant responses to drought? An analysis of stomatal and non-stomatal responses to water stress

S. Zhou^{1*}, R. A. Duursma², B. E. Medlyn¹, J. W. G. Kelly¹, I. C. Prentice^{1,3}

¹Department of Biological Sciences, Macquarie University, North Ryde, NSW 2109, Australia

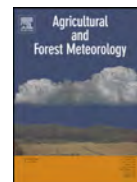
²Hawkesbury Institute for the Environment, University of Western Sydney, Locked Bag 1797, Penrith 2751, NSW, Australia.

³AXA Chair of Biosphere and Climate Impacts, Grand Challenges in Ecosystems and the Environment and Grantham Institute – Climate Change and the Environment, Department of Life Sciences, Imperial College London, Silwood Park Campus, Buckhurst Road, Ascot SL5 7PY, UK

*Corresponding author: shuangxi.zhou@students.mq.edu.au

This chapter is presented as the published journal article:

Zhou, S., Duursma, R. A., Medlyn, B. E., Kelly, J. W., & Prentice, I. C. (2013). How should we model plant responses to drought? An analysis of stomatal and non-stomatal responses to water stress. *Agricultural and Forest Meteorology*, 182, 204-214.



How should we model plant responses to drought? An analysis of stomatal and non-stomatal responses to water stress

Shuangxi Zhou^{a,*}, Remko A. Duursma^b, Belinda E. Medlyn^a,
Jeff W.G. Kelly^a, I. Colin Prentice^{a,c}

^a Department of Biological Sciences, Macquarie University, North Ryde, NSW 2109, Australia

^b Hawkesbury Institute for the Environment, University of Western Sydney, Locked Bag 1797, Penrith, NSW 2751, Australia

^c Grantham Institute and Division of Ecology and Evolution, Imperial College, Silwood Park Campus, Ascot SL5 7PY, UK

ARTICLE INFO

Article history:

Received 15 November 2012

Received in revised form 19 February 2013

Accepted 16 May 2013

Keywords:

Photosynthetic limitation

Stomatal conductance

V_{cmax}

Mesophyll conductance

Drought

Model

ABSTRACT

Models disagree on how to represent effects of drought stress on plant gas exchange. Some models assume drought stress affects the marginal water use efficiency of plants (marginal WUE = $\partial A/\partial E$; i.e. the change in photosynthesis per unit of change in transpiration) whereas others assume drought stress acts directly on photosynthetic capacity. We investigated drought stress in an analysis of results from 22 experimental data sets where photosynthesis, stomatal conductance and predawn leaf water potential were measured at increasing levels of water stress.

Our analysis was framed by a recently developed stomatal model that reconciles the empirical and optimal approaches to predicting stomatal conductance. The model has single parameter g_1 , a decreasing function of marginal WUE. Species differed greatly in their estimated g_1 values under moist conditions, and in the rate at which g_1 declined with water stress. In some species, particularly the sclerophyll trees, g_1 remained nearly constant or even increased.

Photosynthesis was found almost universally to decrease more than could be explained by the reduction in g_1 , implying a decline in apparent carboxylation capacity (V_{cmax}). Species differed in the predawn water potential at which apparent V_{cmax} declined most steeply, and in the steepness of this decline. Principal components analysis revealed a gradient in water relation strategies from trees to herbs. Herbs had higher apparent V_{cmax} under moist conditions but trees tended to maintain more open stomata and higher apparent V_{cmax} under dry conditions. There was also a gradient from malacophylls to sclerophylls, with sclerophylls having lower g_1 values under well-watered conditions and a lower sensitivity of apparent V_{cmax} to drought.

Despite the limited amount of data available for this analysis, it is possible to draw some firm conclusions for modeling: (1) stomatal and non-stomatal limitations to photosynthesis must both be considered for the short-term response to drought and (2) plants adapted to arid climate respond very differently from others.

© 2013 Elsevier B.V. All rights reserved.

1. Introduction

Soil water deficit or “ecological drought” is considered to be the main environmental factor limiting global plant photosynthesis (Nemani et al., 2003). Modeling the effect of drought on photosynthesis (A) and stomatal conductance (g_s) is crucial to understand and project the consequences of global environmental change for plants and ecosystems. However, there is disagreement among models in how to represent drought effects. Many models simply reduce the slope of the g_s/A relationship (e.g. Battaglia et al.,

2004; Kirschbaum, 1999; Friend and Kiang, 2005; Medlyn, 2004; Sala and Tenhunen, 1996; Wang and Leuning, 1998), whereas others assume drought affects A directly by reducing V_{cmax} (maximum rate of carboxylation) and/or J_{max} (maximum rate of electron transport) in the Farquhar et al. (1980) C_3 photosynthesis model (e.g. Calvet et al., 2004; Keenan et al., 2009; Krinner et al., 2005; Moorcroft et al., 2001; Sellers et al., 1996). Only a few models include both effects (e.g. the Sheffield Dynamic Global Vegetation Model, SDGVM) (Woodward and Lomas, 2004). Recent studies have suggested that both effects ought to be included (Egea et al., 2011), but it is not known which approach best captures the drought response, nor is it known how drought responses vary among species and plant functional types (PFTs). The goal of this paper is to investigate drought responses in a range of species. Datasets of photosynthesis, stomatal conductance and pre-dawn leaf water

* Corresponding author.

E-mail addresses: shuangxi.zhou@students.mq.edu.au,
shuangxi.zhou2014@gmail.com (S. Zhou).

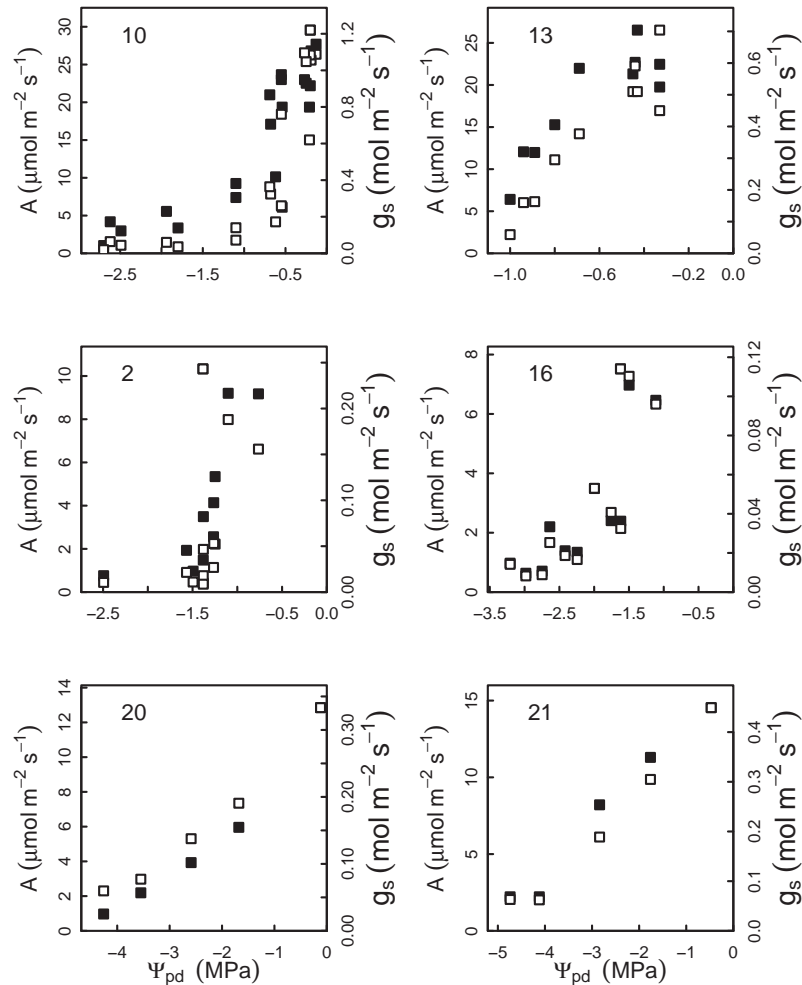


Fig. 1. A (filled squares) and g_s (open squares) responses to Ψ_{pd} , from two data sets representative for each of three PFTs. Herbs: (10) *Helianthus annuus* and (13) *Mediterranean Herbs*; Malacophyll angiosperm tree: (2) *Broussonetia papyrifera* and (16) *Platycarya longipes*; Sclerophyll angiosperm tree: (20) *Quercus ilex* and (21) *Quercus suber*.

potential during drying cycles were obtained from the literature (Fig. 1.) and were analyzed in the framework of a model of optimal stomatal conductance.

The theory of optimal stomatal behavior has been influential in explaining how carbon gain and water loss are balanced. Optimality theory hypothesizes that plants regulate stomatal opening and closing in such a way as to maximize $(A - \lambda E)$ where A is photosynthesis, E is transpiration, and λ is the marginal carbon cost of water to the plant (Cowan, 1977; Cowan and Farquhar, 1977). When water availability decreases, it is hypothesized that λ increases, due to the risk of damage from hydraulic failure if plants maintain high transpiration rate, and/or the increased cost of building structures that are more hydraulically efficient (Berninger and Hari, 1993). Theoretical analysis by Mäkelä et al. (1996) indicated that $1/\lambda$ should be expected to decline exponentially with decreasing soil moisture availability, and the rate of decline with soil moisture should increase with the probability of rain.

We use the term stomatal limitation to refer to this idea that the optimal stomatal conductance declines in response to drought causing a decline in photosynthesis. There can also be non-stomatal limitation of photosynthesis, which involves a reduction in apparent V_{cmax} . If A declines with drought more steeply than can be explained by the observed stomatal limitation, this indicates the

presence of non-stomatal limitation. Thus we interpret stomatal limitation as involving a change in the leaf-internal concentration of CO_2 (C_i) and non-stomatal limitation as a change in the $A-C_i$ curve (Fig. 2). Note that our approach differs from one traditional way of analysing the drought effect on photosynthesis in terms of stomatal and non-stomatal limitations, using the equations from Jones (1985) (e.g. Grassi and Magnani, 2005; Keenan et al., 2009; Kubiske and Abrams, 1993; Ni and Pallardy, 1992; Wilson et al., 2000). Our method differs from that of Jones (1985) because the evidence for stomatal limitation is considered to be reduced C_i and not just reduced g_s , which could also arise a response to biochemical limitation. The difference is important because, in the optimal stomatal model and similar empirical models (e.g. Ball et al., 1987; Leuning, 1995), any reduction in apparent V_{cmax} will drive a reduction in stomatal conductance. Our approach partitions drought effects on stomatal conductance into changes that are an optimal response to a reduction in V_{cmax} , and reductions that are driven by an increase in the marginal cost of water. This way of thinking about stomatal conductance has the advantage of being able to be translated directly into modeling terms.

There has been controversy – perhaps fueled by this ambiguity over definitions – over the extent to which photosynthesis

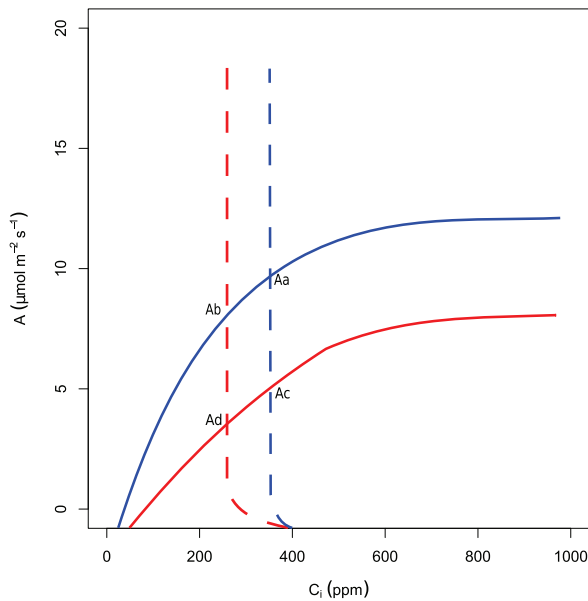


Fig. 2. Framework for the analysis of stomatal and non-stomatal limitations to photosynthesis. The non-stomatal limitation is represented by the solid lines, which shows the response of A to C_i . This curve depends on the apparent V_{cmax} . The stomatal limitation is represented by the dashed lines, which depend on g_1 . Blue lines represent well-watered conditions and red lines represent drought conditions. Under drought, a reduction in g_1 (stomatal limitation only) leads to a trajectory of A from Aa to Ab; a reduction in apparent V_{cmax} (non-stomatal limitation only) leads to a trajectory from Aa to Ac; and reduction in both parameters leads to a trajectory from Aa to Ad. (For interpretation of the references to color in this figure legend, the reader is referred to the web version of this article.)

is more restricted by stomatal or non-stomatal limitations under drought conditions (e.g. Grassi and Magnani, 2005; Lawlor and Tezara, 2009). One strand of the literature has suggested that with increasing drought severity, non-stomatal limitations (due to either mesophyll conductance or leaf biochemistry or both) on photosynthesis come to predominate over stomatal limitation (e.g. Grassi and Magnani, 2005). Proposed non-stomatal mechanisms include reduced Rubisco activity (e.g. Medrano et al., 1997; Parry et al., 2002), reduced electron transport capacity (e.g. Cornic et al., 1989; Epron and Dreyer, 1992), and reduced mesophyll conductance (e.g. Egea et al., 2011): see Flexas et al. (2012) for a review. We refer to the concept of ‘apparent’ carboxylation capacity (V_{cmax}) recognizing that changes in V_{cmax} , when measured in the standard way, can arise either from changes in the actual capacity for carboxylation within the chloroplast, or from changes in g_m .

The objective of this work was to analyze available experimental data in a model-oriented framework in order to answer the question of how best to model the drought responses of gas exchange. In particular: (1) Which processes are affected? (2) What shape does the response function take? (3) How do the responses vary across species and hydro-climates? We have consistently used pre-dawn leaf water potential as the indicator of plant water stress (except one data set with only data on soil water potential). We investigated how the g_s/A relationship changes with experimental drought, and analyzed the potential role of changes in apparent V_{cmax} . The starting point for our study was the analysis by Manzoni et al. (2011), which describes marginal water use efficiency ($\partial A/\partial E$) as increasing monotonically with more negative leaf water potential (when finite cuticular conductance is taken into account). Our analysis was conducted in the framework of a recently derived and simple representation of the optimal stomatal model (Medlyn et al., 2011).

The model's single parameter g_1 is directly related to the marginal carbon cost of water (λ). To quantify the role of stomatal limitation, we examine the response of fitted values of g_1 to soil water deficit. To quantify the role of non-stomatal limitation, we examine the effect of water stress on apparent V_{cmax} , calculated from observed values of g_s and A .

2. Materials and methods

2.1. Sources of data

We analyzed 22 experimental data sets (two unpublished) that include concurrent measurement of net assimilation (A), stomatal conductance (g_s), and pre-dawn leaf water potential (Ψ_{pd}) (except two data sets on *Glycine max*: Huang et al., 1975 with soil water potential data and Liu et al., 2005 with root water potential data, which allow us to estimate Ψ_{pd}) spanning well-watered to water-stressed conditions. We confined our attention to studies that reported either Ψ_{pd} (except two allowing us to estimate Ψ_{pd}), because daytime leaf water potentials depend strongly on transpiration as well as soil water status. Ψ_{pd} is the best measure of water availability to the plant, since it integrates soil water potential over the root zone (Schulze and Hall, 1982) and is not influenced by daytime transpiration. It is also independent of soil texture, unlike volumetric soil moisture content, enabling us to compare species from experiments using different soil types.

Fourteen data sets were derived from Manzoni et al. (2011) via tables and digitized figures in the original sources. Six data sets were derived from two studies on species from karst substrates in southwest China. Two unpublished data sets were added, derived from drought experiments on two *Eucalyptus* species conducted in glasshouses at Macquarie University in 2011 (Kelly, unpublished data).

Most studies were under controlled conditions with plants growing in pots. Water stress was manipulated by withholding irrigation, and leaf gas exchange was measured on the same plant during a single drying cycle. Data on atmospheric CO_2 concentration (C_a) and vapor pressure deficit (D) were also derived from the reports. For a few studies where D was not reported, we assumed $D = 2$ kPa (Peguero-Pina et al., 2009), or $D = 2.1$ kPa (Liu et al., 2010). These D values are consistent with the sites' climate during the measurement period. We assumed dark respiration (R_d) to be negligible for our purpose. As a test of this assumption we estimated R_d as 7% of maximum photosynthesis rate recorded in each data set (Givnish, 1988), and found that this had a negligible effect on the results. The database spans tropical to boreal species, and herbaceous annuals to woody gymnosperms and angiosperms. Thus, the species are broadly representative of the PFTs commonly employed in ecosystem modeling. Species were classified into five PFTs (herb, shrub and liana, sclerophyll angiosperm tree, malacophyll angiosperm tree, gymnosperm), defined by a combination of phylogeny (angiosperm, gymnosperm), life form (tree, herb, shrub, liana), phenology (evergreen and deciduous) and leaf consistency (sclerophyll and malacophyll: sclerophyll leaves are hard, tough and stiffened; malacophyll leaves are soft).

2.2. Analytical models

2.2.1. Stomatal limitation

Medlyn et al. (2011) showed that the theory of optimal stomatal conductance leads, with some approximations, to a simple theoretical model that is closely analogous to widely used empirical models (Ball et al., 1987; Leuning, 1995; Arneeth et al., 2002):

$$g_s \approx g_0 + 1.6 \left(1 + \frac{g_1}{\sqrt{D}} \right) \frac{A}{C_a}, \quad (1)$$

Table 1
Parameter values across 22 species and 5 PFTs.

Species	PFT	No.	Literature source	b	g_1^*	V_{cmax}	S_f	Ψ_f
<i>Allocasuarina luehmannii</i>	Sclerophyll angiosperm tree	1	Posch and Bennett (2009)	1.08	1.99	50.7	2.12	−2.16
<i>Cinnamomum bodinieri</i>	Sclerophyll angiosperm tree	4	Liu et al. (2010)	−0.4	3.11	34.1	4.52	−1.52
<i>Eucalyptus pilularis</i>	Sclerophyll angiosperm tree	5	Kelly (unpublished)	0.94	2.22	69.38	1.82	−1.14
<i>Eucalyptus populnea</i>	Sclerophyll angiosperm tree	6	Kelly (unpublished)	0.15	3.15	52.94	2.06	−3.36
<i>Olea europaea</i> var. <i>Chemlali</i>	Sclerophyll angiosperm tree	14	Ennajeh et al. (2008)	1.28	2.72	125.83	0.4	−0.69
<i>Olea europaea</i> var. <i>Meski</i>	Sclerophyll angiosperm tree	15	Ennajeh et al. (2008)	0.49	3.16	72.52	0.51	−1.95
<i>Quercus coccifera</i>	Sclerophyll angiosperm tree	19	Peguero-Pina et al. (2009)	0.02	6.06	81.2	4.89	−1.66
<i>Quercus ilex</i>	Sclerophyll angiosperm tree	20	Peguero-Pina et al. (2009)	−0.11	6.12	75.62	0.73	−0.17
<i>Quercus suber</i>	Sclerophyll angiosperm tree	21	Peguero-Pina et al. (2009)	0.14	7.55	89.97	1.2	−3
<i>Broussonetia papyrifera</i>	Malacophyll angiosperm tree	2	Liu et al. (2010)	1.14	5.88	50.06	7.16	−1.32
<i>Platycarya longipes</i>	Malacophyll angiosperm tree	16	Liu et al. (2010)	0.66	5.85	37.16	2.53	−2.01
<i>Pteroceltis tatarinowii</i>	Malacophyll angiosperm tree	18	Liu et al. (2010)	−0.14	3.7	33.49	3.49	−1.79
<i>Ficus tikoua</i>	Shrub and liana	7	Liu et al. (2011)	0.07	6.17	42.78	3.34	−1.6
Medit. deciduous shrubs	Shrub and liana	11	Galmés et al. (2007)	0.49	4.82	61.87	3.89	−1.82
Medit. evergreen shrubs	Shrub and liana	12	Galmés et al. (2007)	0.68	4.72	27.81	2.02	−2
<i>Rosa cymosa</i>	Shrub and liana	22	Liu et al. (2010)	0.22	3.07	52.6	1.62	−2.35
<i>Glycine max</i>	Herb	8	Liu et al. (2005)	0.09	3.74	71	1.89	−1.37
<i>Glycine max</i>	Herb	9	Huang et al. (1975)	0.41	3.77	84.2	7.93	−0.65
<i>Helianthus annuus</i>	Herb	10	Tezara et al. (2008)	2.07	4.64	105.4	1.7	−1.03
Medit. herbs	Herb	13	Galmés et al. (2007), Medrano et al. (2009)	1.61	4.72	71.23	11.97	−0.99
<i>Cedrus atlantica</i>	Gymnosperm	3	Grieu et al. (1988)	0.46	3.18	13.31	5.28	−2.31
<i>Pseudotsuga menziesii</i>	Gymnosperm	17	Grieu et al. (1988)	0.79	3.13	13.16	–	–
PFT median values								
Sclerophyll angiosperm tree				0.15	3.15	72.52	1.82	−1.66
Malacophyll angiosperm tree				0.66	5.85	37.16	3.49	−1.79
Shrub and liana				0.35	4.77	47.69	2.68	−1.91
Herb				1.01	4.2	77.72	4.91	−1.01
Gymnosperm				0.63	3.16	13.23	5.28	−2.31

where D is the vapor pressure deficit at the leaf surface (kPa); C_a is the atmospheric CO_2 concentration at the leaf surface ($\mu\text{mol mol}^{-1}$); g_s is stomatal conductance to water vapor ($\text{mol m}^{-2} \text{s}^{-1}$), and g_0 is the leaf water vapor conductance when photosynthesis is zero ($\text{mol m}^{-2} \text{s}^{-1}$). The derivation of the model (Medlyn et al., 2011) provides an interpretation for the single model parameter g_1 ($\text{kPa}^{-0.5}$):

$$g_1 \propto \sqrt{\frac{\Gamma^*}{\lambda}}, \quad (2)$$

where Γ^* is the CO_2 compensation point in the absence of dark respiration ($\mu\text{mol mol}^{-1}$), and λ is the marginal water use efficiency ($\partial A / \partial E$, $\text{mol C mol}^{-1} \text{H}_2\text{O}$) (Medlyn et al., 2011). We estimated g_1 for each predawn leaf water potential from values of A and g_s by rearranging Eq. (1). The parameter g_0 is not part of the optimization. In the analysis, g_0 was estimated as the minimum value of g_s in each data set, similar to Manzoni et al. (2011) who set cuticular conductance to water vapor at 90% of the minimum measured g_s . The gas exchange data corresponding to the minimum measured g_s in each data set were excluded.

An exponential response curve of g_1 to Ψ_{pd} was fitted to each set of observations. Instead of setting the function shape responses in advance (e.g. Egea et al., 2011), we inferred them based on the data set. We attempted to fit the logistic function (cf. Tuzet et al., 2003), but the exponential function suggested by Mäkelä et al. (1996) fitted better:

$$g_1 = a \exp(b/\Psi_{pd}), \quad (3)$$

where a and b are fitted parameters: a is the g_1 value at $\Psi_{pd} = 0$, and b represents the sensitivity of g_1 to Ψ_{pd} . Species adopting different water use strategies might be expected to differ in their estimated g_1 values under moist conditions (defined here as the value of g_1 when $\Psi_{pd} = -0.5$ MPa), and might also differ in their sensitivity to water stress as represented by b .

2.2.2. Non-stomatal limitation

The apparent effect of water stress on V_{cmax} was quantified from the measurements of A and g_s as follows. Firstly, we assumed that photosynthesis was Rubisco-limited under the conditions of the experiments. Note that it is alternatively possible to assume that photosynthesis was electron transport-limited, leading to an estimate of the apparent effect of water stress on J_{max} . Results (Fig. 4 in Appendix B) were closely similar, indicating that this method effectively estimates the effect of drought stress on the photosynthetic biochemistry. We estimated the maximum apparent V_{cmax} value when $\Psi_{pd} = 0$ (V_{cmax}^*). This estimate was obtained by inverting the expression for photosynthesis as follows:

$$V_{cmax} = \frac{(A + R_d)(C_i + K_m)}{(C_i - \Gamma^*)}, \quad (4)$$

where the value of C_i is obtained from measurements (Appendix A). We then estimated, for each data point, the photosynthesis (A_c) that would be obtained if drought stress only affected C_i , by calculating the photosynthetic rate obtained with maximum V_{cmax}^* and the observed C_i . The ratio of observed photosynthesis to the estimated photosynthesis (A/A_c) measures the apparent effect of water stress on V_{cmax} , as this ratio gives the decline in V_{cmax} that would be needed to obtain the observed photosynthetic rate.

The sensitivity of V_{cmax} to water availability was quantified using the logistic function (Tuzet et al., 2003):

$$f(\Psi_{pd}) = \frac{1 + \exp[S_f \Psi_f]}{1 + \exp[S_f (\Psi_f - \Psi_{pd})]}. \quad (5)$$

The function $f(\Psi_{pd})$ accounts for the relative effect of water stress on the apparent V_{cmax} . The form of this function allows a relatively flat response of apparent V_{cmax} under wet conditions, followed by a steeper decline, with a flattening again (toward zero) under the driest conditions. S_f is a sensitivity parameter indicating the steepness of the decline, while Ψ_f is a reference value indicating the water potential at which $f(\Psi_{pd})$ decreases to half of its maximum value. Species adopting different water use strategies might

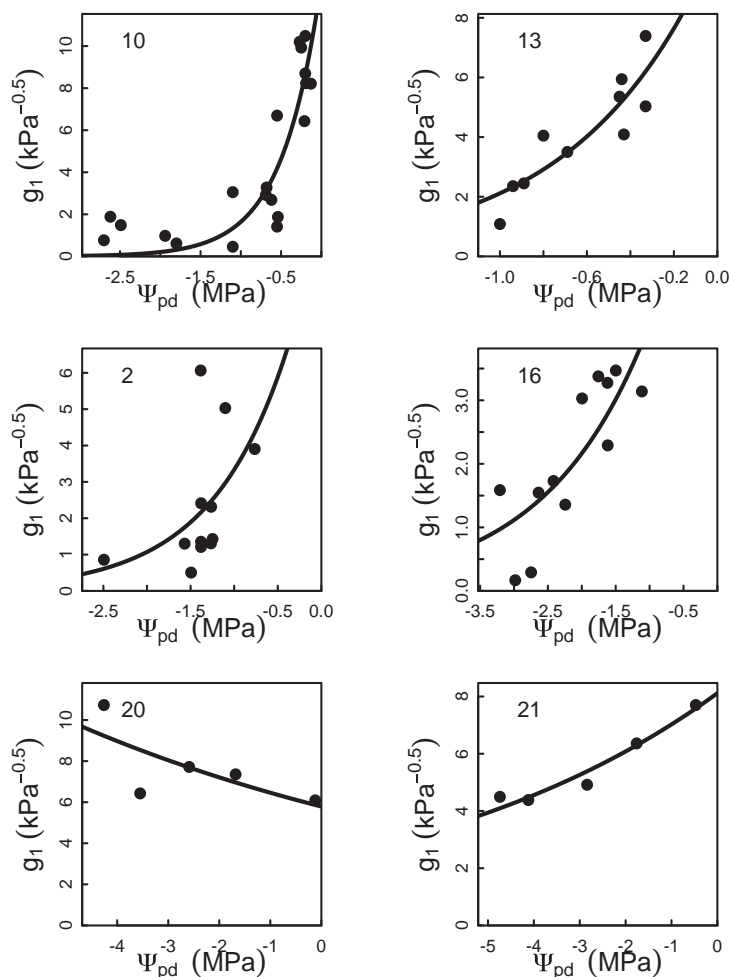


Fig. 3. Variability of g_1 responses to Ψ_{pd} from two data sets representative for each of three PFTs. Herbs: (10) *Helianthus annuus* and (13) *Mediterranean Herbs*; Malacophyll angiosperm tree: (2) *Broussonetia papyrifera* and (16) *Platycarya longipes*; Sclerophyll angiosperm tree: (20) *Quercus ilex* and (21) *Quercus suber*.

be expected to differ in their estimated V_{cmax} values under moist conditions, and might also differ in the sensitivity of apparent V_{cmax} to water stress (S_f) and reference water potential (Ψ_f).

There are two possible classes of causes for a reduction in apparent V_{cmax} : biochemical reductions in enzyme activity, or reductions in mesophyll conductance (g_m). With the data available, we are not able to distinguish between these two effects. However, we investigated the potential role of the two effects by calculating the implied drought response of one parameter when the other parameter was held constant. Firstly, we assumed g_m as constant at $0.15 \text{ mol m}^{-2} \text{ s}^{-1}$ (Niinemets et al., 2009a), and then estimated the decline of true V_{cmax} needed to account for observed photosynthesis decline with drought. Secondly, we assumed true V_{cmax} as unchanged from its fitted value at $\Psi_{pd} = 0$, and then estimated the decline in g_m needed to account for observed photosynthesis decline with drought.

2.3. Multivariate analysis

The fitted values of five parameter, S_f , Ψ_f , b , g_1^* (g_1 estimated at $\Psi_{pd} = -0.5 \text{ MPa}$) and V_{cmax}^* (apparent V_{cmax} estimated at $\Psi_{pd} = 0$), were entered as variables (traits) in a principal components analysis (PCA) based on their correlations across species, grouped

by PFTs. The results were interpreted in terms of emergent patterns of differences among PFTs. The analysis was written and run in R (R Development Core Team, 2010).

3. Results

3.1. Response of g_1 to water stress

Estimated parameter values from each data set, and median values for each PFT, are given in Table 1. Species differed greatly in their estimated g_1 values under moist conditions (parameter g_1^*), and the rates at which g_1 declined with water stress (parameter b). Differences in the response curves are shown in Fig. 3 (which shows selected species in detail; see also Fig. 2 in Appendix B) and Fig. 4 (which compares response curves for all species). Malacophylls generally (except *Pteroceltis tatarinowii*) had higher g_1^* values than sclerophylls (5.85 versus 3.15, based on PFT median values in Table 1; Fig. 3).

The rate of decline in g_1 with drought varied considerably among species, with g_1 remaining nearly constant in some species and declining severely with drought in others. For herbaceous species (except *Glycine max*), g_1 was found to decline more steeply with water stress than in trees. Shrubs and lianas showed intermediate

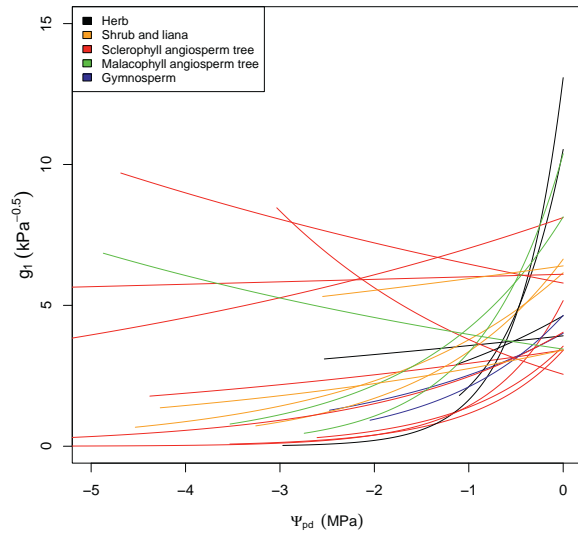


Fig. 4. g_1 responses to Ψ_{pd} from 22 data sets, grouped by PFT (herb, shrub and liana, sclerophyll angiosperm tree, malacophyll angiosperm tree, gymnosperm).

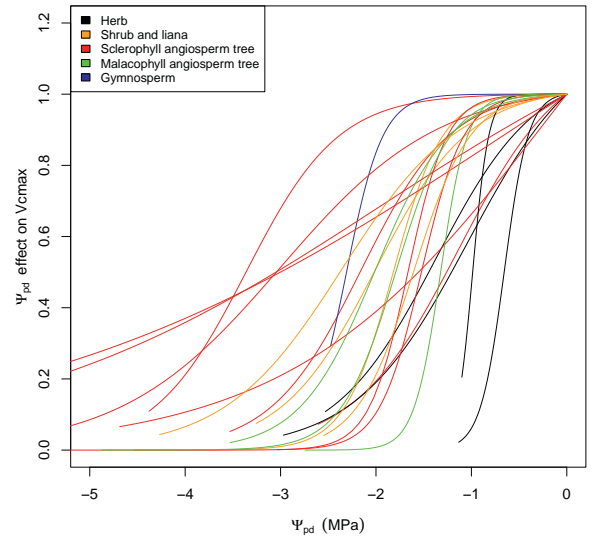


Fig. 6. V_{cmax} responses to Ψ_{pd} from 21 data sets, grouped by PFT (herb, shrub and liana, sclerophyll angiosperm tree, malacophyll angiosperm tree, gymnosperm).

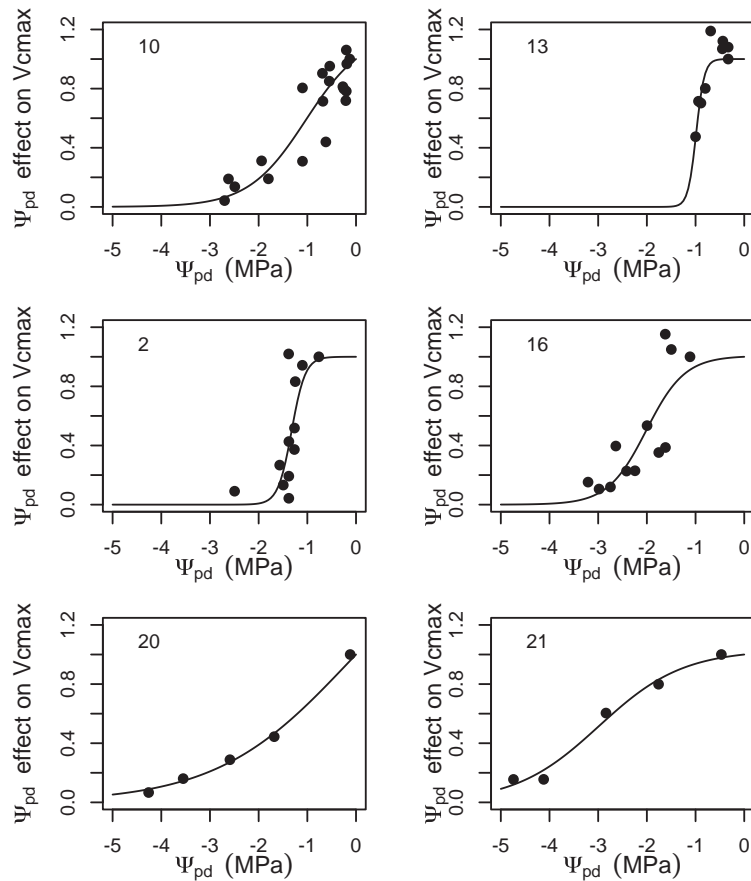


Fig. 5. Relative effect of Ψ_{pd} on V_{cmax} from two data sets representative for each of three PFTs. Herbs: (10) *Helianthus annuus* and (13) *Mediterranean Herbs*; Malacophyll angiosperm tree: (2) *Broussonetia papyrifera* and (16) *Platycarya longipes*; Sclerophyll angiosperm tree: (20) *Quercus ilex* and (21) *Quercus suber*.

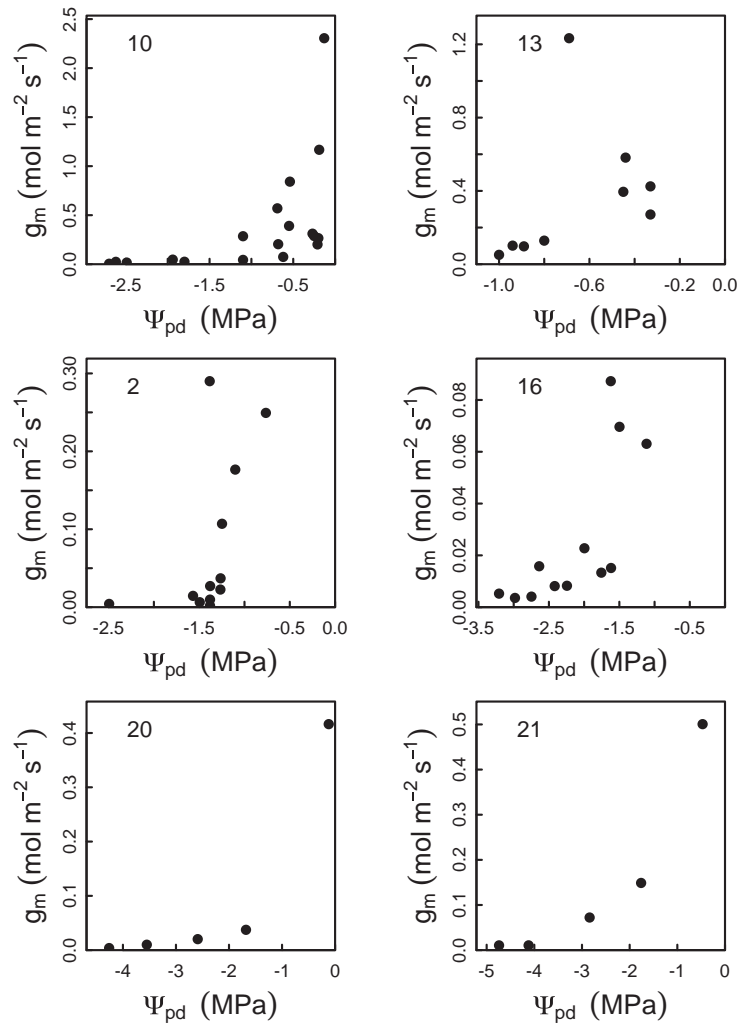


Fig. 7. Estimated responses of mesophyll conductance (g_m) to Ψ_{pd} under the assumption that true V_{cmax} is constant, for two data sets representative of each of three PFTs. These curves were estimated from data by assuming that true V_{cmax} is constant and equal to its observed value at $\Psi_{pd}=0$, and calculating the reduction in g_m that would be needed to explain the observed reduction in apparent V_{cmax} .

responses. Woody species varied in their g_1 responses to drought. In the Mediterranean sclerophyll *Quercus* species (*Quercus ilex*, *Quercus suber*, *Quercus coccifera*) g_1 remained nearly constant or even increased with drought. The g_1 of *Cinnamomum bodinieri* increased with drought. The two *Eucalyptus* species (*Eucalyptus pilularis*, *Eucalyptus populnea*) had very different drought responses, according to their ecological niches: in the mesic tall-forest species *E. pilularis*, g_1 decreased rapidly with drought ($b=0.94$) whereas in the semi-arid woodland species *E. populnea*, g_1 barely changed with drought ($b=0.15$).

3.2. Response of apparent V_{cmax} to water stress

We quantified the non-stomatal limitation to photosynthesis by calculating Rubisco-limited photosynthesis (A_c) values for each species assuming that V_{cmax} is constant at the value shown under moist conditions. The ratio of measured A and estimated A_c then indicates the degree of non-stomatal limitation. The observations consistently show a decline in apparent V_{cmax} , and thus

a progressive increase in non-stomatal limitation, with increasing water stress (Fig. 5; see also Fig. 3 in Appendix B).

We explored the relative impact of drought-induced reductions on apparent V_{cmax} and g_1 on photosynthesis. The effect of water stress on measured photosynthesis was compared (1) with the effect on estimated photosynthesis when V_{cmax} was fixed (on the V_{cmax} value at the least negative Ψ_{pd} in each data set) and only g_1 changed, and (2) with the effect on estimated photosynthesis when g_1 was fixed and only V_{cmax} changed (see Fig. 5 in Appendix B). This analysis confirmed the strong inhibitory effect of water stress on apparent V_{cmax} .

All species showed a decline of apparent V_{cmax} as water availability declined, but species differed considerably in the parameters (Ψ_f and S_f) of this response. Different PFTs varied in the sensitivity to Ψ_{pd} . Trees had generally more negative Ψ_f than that of herbaceous species (Table 1), i.e. they showed the ability to continue active photosynthesis down to lower soil water potentials than herbaceous species. Among woody species, malacophylls showed higher V_{cmax} sensitivity (S_f) to drought than most sclerophylls (3.49 versus 1.82, based on PFT median values in Table 1; Fig. 5).

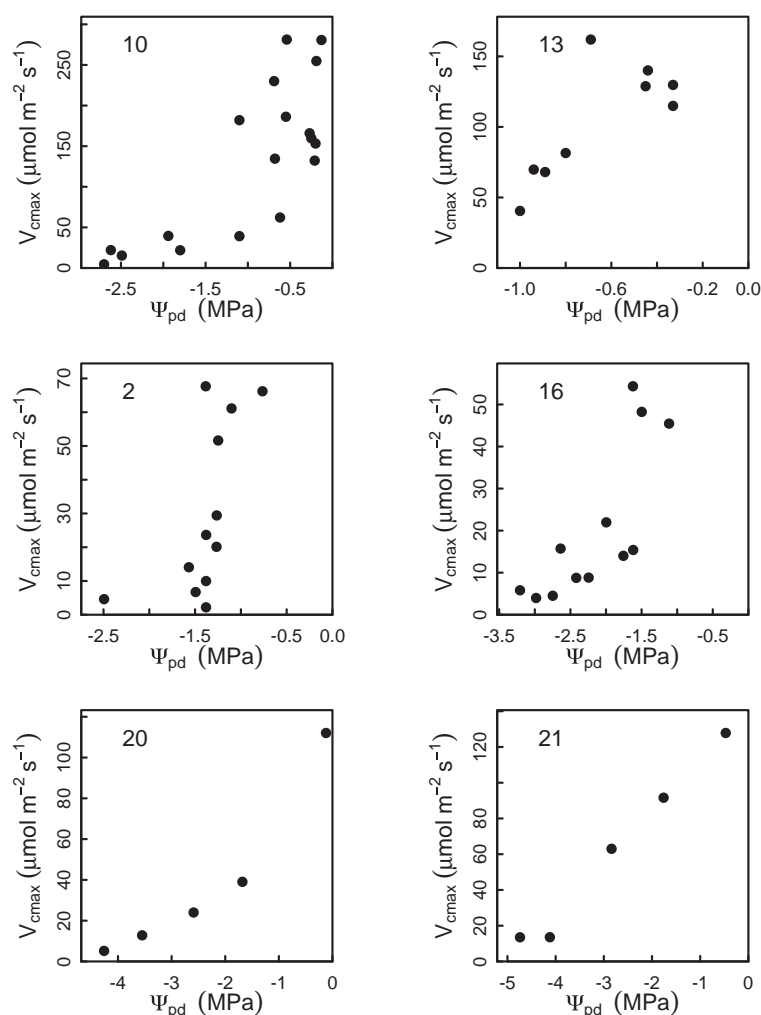


Fig. 8. Estimated responses of true V_{cmax} to Ψ_{pd} under the assumption that mesophyll conductance is constant, for two data sets representative of each of three PFTs. These curves were estimated from data by assuming that g_m is constant and equal to $0.15 \text{ mol m}^{-2} \text{ s}^{-1}$, and calculating the reduction in true V_{cmax} that would be needed to explain the observed reduction in apparent V_{cmax} .

Separate estimates of the response of either g_m (Fig. 7) or V_{cmax} (Fig. 8) to water stress show that both could equally well explain the declines in apparent V_{cmax} (Fig. 9).

3.3. Water relation strategies

PCA was conducted on 21 data sets that allowed estimation of all five parameters. *Pseudotsuga menziesii* was excluded because the $f(\Psi_{pd})$ curve could not be fitted, owing to the small number of data points.

The first principal component (PC1) shows the existence of one independent gradient, characterized by the positive correlation among V_{cmax}^* , b and Ψ_f (Fig. 9). It indicates that species with high V_{cmax}^* also tend to have a high sensitivity of both g_1 and V_{cmax} to drought. Species with this combination of traits are aligned to the right part of Fig. 9, with positive scores on the first principal component. The second principal component (PC2) shows the existence of another independent gradient, characterized by the positive correlation between g_1^* and S_f . Species with high values of g_1^* and S_f are aligned in the upper part of Fig. 9, with positive scores on the second principal component. The two principal components

together account for 58.7% of the total variation in these five parameters.

This analysis shows species scattered through a continuum, but nevertheless suggests some systematic patterns related to PFT membership. The first principal component (PC1) can be interpreted as a gradient in water relation strategies from woody to herbaceous species (explaining 35.2% of total variance). Compared with the herbaceous species, most of the woody species tended to have lower values of b (decreasing g_1 slowly to maintain more open stomata) and Ψ_f (maintaining high apparent V_{cmax}) down to lower water potential, and also lower V_{cmax} under wet conditions.

The second principal component (PC2) can be interpreted as a second gradient in water relation strategies from malacophyll to sclerophyll tree species (explaining 23.5% of total variance). Compared with malacophyll species (except *P. tatarinowii*, which has drought-adapted leaf anatomical structure and epidermal characteristics), sclerophyll species have lower values of g_1^* and S_f , corresponding to a combination of relatively low stomatal conductance under wet conditions, but with a slow decline of photosynthetic capacity under drought.

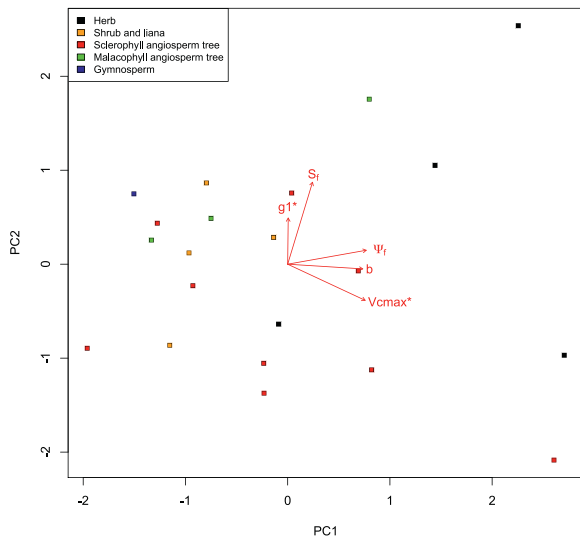


Fig. 9. Principal components analysis of the five traits, S_f , Ψ_f , b , g_1^* (g_1 estimated at $\Psi_{pd} = -0.5$ MPa) and V_{cmax}^* (apparent V_{cmax} estimated at $\Psi_{pd} = 0$). The first principal component (PC1) explained 35.2% of total variance, and the second principal component (PC2) explained 23.5% of total variance. The two principal components together accounted for 58.7% of the total variation in these five parameters.

4. Discussion

The goal of this analysis was to compare data sets in a modeling framework to identify key aspect for modeling drought effects on plant gas exchange. The results are consistent with other studies showing that both stomatal and non-stomatal processes are affected by drought (e.g. Egea et al., 2011; Keenan et al., 2010). Our analysis shows that non-stomatal limitation is considerable and has in general a greater impact than that of stomatal limitation on photosynthetic rates. Photosynthesis under drought would be greatly overestimated if the decline in apparent V_{cmax} was not taken into account. Both assimilation rate and stomatal conductance decrease as pre-dawn leaf water potential declines, but assimilation rate usually decreases more – often many times more – than could be explained by a reduction in stomatal conductance (and g_1) alone (see Figs. 1 and 2 in Appendix B).

The analysis showed large variation among species and PFTs in drought effect on g_1 . This finding is consistent with those of Manzoni et al. (2011) who showed the shape of $\partial A/\partial E$ response curves to soil water availability varies according to PFT and climate. The near-constancy (or slight increase) of g_1 values with declining Ψ_{pd} , as shown in Mediterranean oaks, is consistent with their evident ability to thrive in a climate with a long summer dry season; this departs from Manzoni et al.'s (2011) generalization that $\partial A/\partial E$ increases monotonically with increasing water stress. Among the *Eucalyptus* species studied, *E. populnea* (from a xeric climate) and *E. pilularis* (from a mesic climate) notably differ in their g_1 responses (see Fig. 2 in Appendix B), consistent with Manzoni et al.'s (2011) indication of lower marginal WUE (i.e. higher g_1) in species from dry climates.

The large variation among PFTs in the drought effect on apparent V_{cmax} , as shown in our analysis, has not been reported before. It appears that species with high V_{cmax}^* under moist conditions also tend to be most sensitive to moisture stress, and that responses to moisture stress of g_1 and apparent V_{cmax} are correlated. The consistency between g_1^* and S_f (PC2 in Fig. 6) also suggests that water stress is associated with consistent limitations on g_1 and apparent V_{cmax} . However, the lack of correlation between V_{cmax}^* and

g_1^* indicates that photosynthetic capacity and water use strategy under moist conditions are not correlated. Our results also highlight the different strategies of drought response shown by species of different PFTs and from different hydro-climates.

Variation between species and PFTs in their responses to water deficit may relate to species-specific trade-offs between transpiration and vulnerability to hydraulic failure (Berninger and Hari, 1993). The Ψ_{pd} at which the g_s of sclerophyll trees (especially the Mediterranean oaks) approaches zero was often well below that of malacophyll trees, and was much lower than that of the herbs (see Fig. 1 in Appendix B). Sclerophyll trees are particularly noted for their larger turgor maintenance capacity (e.g. Myers et al., 1997; Prior et al., 1997), and maintaining high stomatal conductance and photosynthetic capacity at low water potentials (e.g. Turner, 1994; Groom and Lamont, 1997; Niinemets et al., 2009b). Deciduous trees usually display greater stomatal sensitivity to increasing water deficit than semi-deciduous and evergreen sclerophyll trees (Myers et al., 1997). Malacophyll, even when “evergreen”, may have to shed their leaves to regulate water loss during prolonged drought (Prior et al., 1997).

The exponential decline of g_1 with decreasing soil water availability is consistent with the theoretical analysis on optimal stomatal response by Mäkelä et al. (1996). However, in their analysis, Mäkelä et al. (1996) assumed no drought effect on photosynthetic capacity. Future analysis of optimal stomatal responses to drought should consider how the reduction in apparent V_{cmax} with water limitation alters the optimal stomatal behavior. Our finding that apparent V_{cmax} is reduced is consistent with recent studies of mesophyll conductance (g_m) which report that g_m decreases with soil water deficit, and this effect may also contribute as much as the reduction in g_s to the decrease of A under water stress (Flexas et al., 2012; Keenan et al., 2010; Perez-Martin et al., 2009). The available data did not allow us to calculate the extent of g_m limitation on photosynthesis under water-stressed condition. However, declines in apparent V_{cmax} could be equally well explained by declines in either g_m (Fig. 7) or V_{cmax} (Fig. 8). Either way, the responses can be modeled adequately using the concept of apparent V_{cmax} .

The data available for this analysis were limited. Noise might have been introduced by digitizing figures in original publications, setting D values when not reported, and differences in experimental methods (especially given the large time span among the experiments). Although thousands of experiments have been done on plant response to drought, data sets containing enough information for model improvement are rare. Thus, the analysis highlights a need for further model-oriented experimental work to better define quantitative relationships between the several different aspects of drought response and other plant traits. Nevertheless, this study permits some strong conclusion for modeling: (1) it is necessary to represent non-stomatal limitation to carbon assimilation during drought, and (2) there are large differences among plant species in the values of key drought-response parameters, which appear to be related to PFT membership and climate. Without consideration of these two points, it is likely that models will underestimate short-term (within-season) response of primary production to drought while also underestimating the ability of drought-adapted taxa to maintain their function.

Acknowledgments

We thank Dr. Chang-cheng Liu (Institute of Botany, Chinese Academy of Sciences) for providing published data on karst species. Thanks also to Dr. Stefano Manzoni for making his digitized database freely available.

Appendix A. Supplementary data

Supplementary data associated with this article can be found, in the online version, at <http://dx.doi.org/10.1016/j.agrformet.2013.05.009>.

References

- Arneth, A., Lloyd, J., Santruckova, H., Bird, M., Grigoryev, S., Kalaschnikov, Y.N., Gleixner, G., Schulze, E., 2002. Response of central Siberian Scots pine to soil water deficit and long-term trends in atmospheric CO₂ concentration. *Global Biogeochem. Cycles* 16, 1005.
- Ball, J.T., Woodrow, I.E., Berry, J.A., 1987. A model predicting stomatal conductance and its contribution to the control of photosynthesis under different environmental conditions. In: Biggins, J. (Ed.), *Progress in Photosynthesis Research*. Martinus-Nijhoff Publishers, Dordrecht, the Netherlands, pp. 221–224.
- Battaglia, M., Sands, P., White, D., Mummery, D., 2004. CABALA: a linked carbon, water and nitrogen model of forest growth for silvicultural decision support. *Forest Ecol. Manag.* 193, 251–282.
- Berninger, F., Hari, P., 1993. Optimal regulation of gas exchange: evidence from field data. *Ann. Bot.* 71, 135–140.
- Calvet, J.C., Rivalland, V., Picon-Cochard, C., Guehl, J.M., 2004. Modelling forest transpiration and CO₂ fluxes-response to soil moisture stress. *Agric. For. Meteorol.* 124, 143–156.
- Cornic, G., Gouallec, J.L.L., Briantais, J.M., Hodges, M., 1989. Effect of dehydration and high light on photosynthesis of two C₃ plants (*Phaseolus vulgaris* L. and *Elatostema repens* (Lour.) Hall f.). *Planta* 177, 84–90.
- Cowan, I.R., 1977. Stomatal behaviour and environment. *Adv. Bot. Res.* 4, 117–288.
- Cowan, I.R., Farquhar, G.D., 1977. Stomatal function in relation to leaf metabolism and environment. *Symp. Soc. Exp. Biol.* 31, 471–505.
- Egea, G., Verhoef, A., Vidale, P.L., 2011. Towards an improved and more flexible representation of water stress in coupled photosynthesis–stomatal conductance models. *Agric. For. Meteorol.* 151, 1370–1384.
- Ennajeh, M., Tounekti, T., Vadel, A.M., Khemira, H., Cochard, H., 2008. Water relations and drought-induced embolism in olive (*Olea europaea*) varieties Meski and Chemlali during severe drought. *Tree Physiol.* 28, 971–976.
- Epron, D., Dreyer, E., 1992. Effects of severe dehydration on leaf photosynthesis in *Quercus petraea* (Matt.) Liebl.: photosystem II efficiency, photochemical and nonphotochemical fluorescence quenching and electrolyte leakage. *Tree Physiol.* 10, 273–284.
- Farquhar, G.D., Caemmerer, S.V., Berry, J.A., 1980. A biochemical model of photosynthetic CO₂ assimilation in leaves of C₃ species. *Planta* 149, 78–90.
- Flexas, J., Barbour, M.M., Brendel, O., Cabrera, H.M., Carriqui, M., Díaz-espejo, A., Douthe, C., Dreyer, E., Ferrio, J.P., Gago, J., Gallé, A., Galmés, J., Kodama, N., Medrano, H., Niinemets, Ü., Peguero-pina, J.J., Pou, A., Ribas-carbó, M., Tomás, M., Tosens, T., Warren, C.R., 2012. Mesophyll diffusion conductance to CO₂: An unappreciated central player in photosynthesis. *Plant Sci.* 194, 70–84.
- Friend, A.D., Kiang, N.Y., 2005. Land surface model development for the GISS GCM: Effects of improved canopy physiology on simulated climate. *J. Clim.* 18, 2883–2902.
- Galmés, J., Flexas, J., Savé, R., Medrano, H., 2007. Water relations and stomatal characteristics of Mediterranean plants with different growth forms and leaf habits: responses to water stress and recovery. *Plant Soil* 290, 139–155.
- Givnish, T.J., 1988. Adaptation to sun and shade: a whole-plant perspective. *Aust. J. Plant Physiol.* 15, 63–92.
- Grassi, G., Magnani, F., 2005. Stomatal, mesophyll conductance and biochemical limitations to photosynthesis as affected by drought and leaf ontogeny in ash and oak trees. *Plant Cell Environ.* 28, 834–849.
- Grieu, P., Guehl, J.M., Aussenac, G., 1988. The effects of soil and atmospheric drought on photosynthesis and stomatal control of gas exchange in three coniferous species. *Physiol. Plantarum* 73, 97–104.
- Groom, P.K., Lamont, B.B., 1997. Xerophytic implications of increased sclerophyll: interactions with water and light in *Hakea psilorrhyncha* seedlings. *New Phytol.* 136, 231–237.
- Huang, C.Y., Boyer, J.S., Vanderhoef, L.N., 1975. Acetylene reduction (nitrogen fixation) and metabolic activities of soybean having various leaf and nodule water potential. *Plant Physiol.* 56, 222–227.
- Jones, H.G., 1985. Partitioning stomatal and non-stomatal limitations to photosynthesis. *Plant Cell Environ.* 8, 95–104.
- Keenan, T., Garcia, R., Friend, A.D., Zaehle, S., Gracia, C., Sabate, S., 2009. Improved understanding of drought controls on seasonal variation in Mediterranean forest canopy CO₂ and water fluxes through combined in situ measurements and ecosystem modelling. *Biogeosciences* 6, 1423–1444.
- Keenan, T., Sabate, S., Gracia, C., 2010. The importance of mesophyll conductance in regulating forest ecosystem productivity during drought periods. *Global Change Biol.* 16, 1019–1034.
- Kirschbaum, M.U.F., 1999. CenW, a forest growth model with linked carbon, energy, nutrient and water cycles. *Ecol. Model.* 118, 17–59.
- Krinner, G., Viovy, N., Noblet-Ducoudre, N., Ogée, J., Polcher, J., Friedlingstein, P., Ciais, P., Sitch, S., Prentice, I.C., 2005. A dynamic global vegetation model for studies of the coupled atmosphere–biosphere system. *Global Biogeochem. Cycles* 19, GB1015.
- Kubiske, M.E., Abrams, M.D., 1993. Stomatal and nonstomatal limitations of photosynthesis in 19 temperate tree species on contrasting sites during wet and dry years. *Plant Cell Environ.* 16, 1123–1129.
- Lawlor, D.W., Tezara, W., 2009. Causes of decreased photosynthetic rate and metabolic capacity in water-deficient leaf cells: a critical evaluation of mechanisms and integration of processes. *Ann. Bot.* 103, 561–579.
- Leuning, R., 1995. A critical appraisal of a combined stomatal-photosynthesis model for C₃ plants. *Plant Cell Environ.* 18, 339–355.
- Liu, C.C., Liu, Y.G., Guo, K., Fan, D.Y., Yu, L.F., Yang, R., 2011. Exploitation of patchy soil water resources by the clonal vine *Ficus tikoua* in karst habitats of southwestern China. *Acta Physiol. Plantarum* 33, 93–102.
- Liu, C.C., Liu, Y.G., Guo, K., Zheng, Y.R., Li, G.Q., Yu, L.F., Yang, R., 2010. Influence of drought intensity on the response of six woody karst species subjected to successive cycles of drought and rewetting. *Physiol. Plantarum* 139, 39–54.
- Liu, F., Andersen, M.N., Jacobsen, S.-E., Jensen, C.R., 2005. Stomatal control and water use efficiency of soybean (*Glycine max* L. Merr.) during progressive soil drying. *Environ. Exp. Bot.* 54, 33–40.
- Manzoni, S., Vico, G., Katul, G., Fay, P.A., Polley, W., Palmroth, S., Porporato, A., 2011. Optimizing stomatal conductance for maximum carbon gain under water stress: a meta-analysis across plant functional types and climates. *Funct. Ecol.* 25, 456–467.
- Medlyn, B.E., 2004. A MAESTRO retrospective. In: Mencuccini, M., Grace, J., Moncrieff, J., McNaughton, K.G. (Eds.), *Forests at the Land–Atmosphere Interface*. CAB International, Wallingford, pp. 105–121.
- Medlyn, B.E., Duursma, R.A., Eamus, D., Ellsworth, D.S., Prentice, I.C., Barton, C.V.M., Crous, K.Y., Angelis, P.D., Freeman, M., Wingate, L., 2011. Reconciling the optimal and empirical approaches to modelling stomatal conductance. *Global Change Biol.* 17, 2134–2144.
- Medrano, H., Flexas, J., Galmés, J., 2009. Variability in water use efficiency at the leaf level among Mediterranean plants with different growth forms. *Plant Soil* 317, 17–29.
- Medrano, H., Parry, M.A.J., Socías, X.D.W.L., 1997. Long term water stress inactivates Rubisco in subterranean clover. *Ann. Appl. Biol.* 131, 491–501.
- Moorcroft, P.R., Hurtt, G.C., Pacala, S.W., 2001. A method for scaling vegetation dynamics: the ecosystem demography model (ED). *Ecol. Monographs* 71, 557–585.
- Myers, B.A., Duff, G.A., Eamus, D., Fordyce, I.R., O'Grady, A., Williams, R.J., 1997. Seasonal variation in water relations of trees of differing leaf phenology in a wet–dry tropical savanna near Darwin, northern Australia. *Aust. J. Bot.* 45, 225–240.
- Mäkelä, A., Berninger, F., Hari, P., 1996. Optimal control of gas exchange during drought: theoretical analysis. *Ann. Bot.* 77, 461–467.
- Nemani, R.R., Keeling, C.D., Hashimoto, H., Jolly, W.M., Piper, S.C., Tucker, C.J., Myneni, R.B., Running, S.W., 2003. Climate-driven increases in global terrestrial net primary production from 1982 to 1999. *Science* 300, 1560–1563.
- Ni, B.R., Pallardy, S.G., 1992. Stomatal and nonstomatal limitations to net photosynthesis in seedlings of woody angiosperms. *Plant Physiol.* 99, 1502–1508.
- Niinemets, U., Diaz-Espejo, A., Flexas, J., Galmés, J., Warren, C.R., 2009a. Role of mesophyll diffusion conductance in constraining potential photosynthetic productivity in the field. *J. Exp. Bot.* 60, 2249–2270.
- Niinemets, U., Wright, I.J., Evans, J.R., 2009b. Leaf mesophyll diffusion conductance in 35 Australian sclerophylls covering a broad range of foliage structural and physiological variation. *J. Exp. Bot.* 60, 2433–2449.
- Parry, M.A.J., Andralojc, P.J., Khan, S., Lea, P.J., Keys, A.J., 2002. Rubisco activity: effects of drought stress. *Ann. Bot.* 89, 833–839.
- Peguero-Pina, J.J., Sancho-Knapik, D., Morales, F., Flexas, J., Gil-Pelegrín, E., 2009. Differential photosynthetic performance and photoprotection mechanisms of three Mediterranean evergreen oaks under severe drought stress. *Funct. Plant Biol.* 36, 453–462.
- Perez-Martin, A., Flexas, J., Ribas-Carbó, M., Bota, J., Tomás, M., Infante, J.M., Diaz-Espejo, A., 2009. Interactive effects of soil water deficit and air vapour pressure deficit on mesophyll conductance to CO₂ in *Vitis vinifera* and *Olea europaea*. *J. Exp. Bot.* 60, 2391–2405.
- Posch, S., Bennett, L.T., 2009. Photosynthesis, photochemistry and antioxidative defence in response to two drought severities and with re-watering in *Allo-casuarina luehmannii*. *Plant Biol.* 11 (Suppl. 1), 83–93.
- Prior, L.D., Eamus, D., Duff, G.A., 1997. Seasonal trends in carbon assimilation, stomatal conductance, pre-dawn leaf water potential and growth in *Terminalia ferdinandiana*, a deciduous tree of northern Australian savannas. *Aust. J. Bot.* 45, 53–69.
- R Development Core Team, 2010. R: A Language and Environment for Statistical Computing. R Foundation for Statistical Computing, Vienna, Austria, ISBN 3-900051-07-0, <http://www.R-project.org>
- Sala, A., Tenhunen, J.D., 1996. Simulations of canopy net photosynthesis and transpiration in *Quercus ilex* L. under the influence of seasonal drought. *Agric. For. Meteorol.* 78, 203–222.
- Schulze, E.D., Hall, A.E., 1982. Stomatal responses, water loss and CO₂ assimilation rates of plants in contrasting environments. In: Lange, O.L., Nobel, P.S., Osmond, C.B., Ziegler, H. (Eds.), *Physiological Plant Ecology II Water Relations and Carbon Assimilation*. Springer-Verlag, Berlin, pp. 181–230.
- Sellers, P.J., Randall, D.A., Collatz, G.J., Berry, J.A., Field, C.B., Dazlich, D.A., Zhang, C., Collelo, G.D., Bounoua, L., 1996. A revised land surface parameterization (SiB2) for atmospheric GCMs. Part I. Model formulation. *J. Clim.* 9, 676–705.
- Tezara, W., Driscoll, S., Lawlor, D.W., 2008. Partitioning of photosynthetic electron flow between CO₂ assimilation and O₂ reduction in sunflower plants under water deficit. *Photosynthetica* 46, 127–134.
- Turner, I.M., 1994. Sclerophyll: primarily protective? *Funct. Ecol.* 8, 669–675.

Tuzet, A., Perrier, A., Leuning, R., 2003. A coupled model of stomatal conductance, photosynthesis and transpiration. *Plant Cell Environ.* 26, 1097–1116.
 Wang, Y., Leuning, R., 1998. A two-leaf model for canopy conductance, photosynthesis and partitioning of available energy I: Model description and comparison with a multi-layered model. *Agric. For. Meteorol.* 91, 89–111.

Wilson, K.B., Baldocchi, D.D., Hanson, P.J., 2000. Quantifying stomatal and non-stomatal limitations to carbon assimilation resulting from leaf aging and drought in mature deciduous tree species. *Tree Physiol.* 20, 787–797.
 Woodward, F.I., Lomas, M.R., 2004. Vegetation dynamics – simulating responses to climatic change. *Biol. Rev.* 79, 643–670.

2.S1 Supplementary Information

How should we model plant responses to drought? An analysis of stomatal and non-stomatal responses to water stress

S. Zhou^{1*}, R. A. Duursma², B. E. Medlyn¹, J. W. G. Kelly¹, I. C. Prentice^{1,3}

¹Department of Biological Sciences, Macquarie University, North Ryde, NSW 2109, Australia

²Hawkesbury Institute for the Environment, University of Western Sydney, Locked Bag 1797, Penrith 2751, NSW, Australia.

³AXA Chair of Biosphere and Climate Impacts, Grand Challenges in Ecosystems and the Environment and Grantham Institute – Climate Change and the Environment, Department of Life Sciences, Imperial College London, Silwood Park Campus, Buckhurst Road, Ascot SL5 7PY, UK

*Corresponding author: shuangxi.zhou@students.mq.edu.au

Supplementary model estimation of A_c and V_{cmax} .

The biochemically based photosynthesis model by Farquhar *et al.* (1980) was used to understand how photosynthesis responds to drought. Net photosynthesis, A_n , is modelled as the minimum of two different limiting rates:

$$A_n = \min(A_c, A_j) - R_d, \quad (1)$$

where A_c is the rate of photosynthesis when Rubisco activity is limiting and A_j the rate when ribulose-1,5-bisphosphate (RuBP)-regeneration is limiting. R_d is the rate of mitochondrial respiration. We focus on Rubisco-limited photosynthesis, given by:

$$A_c = \frac{V_{cmax}(C_i - \Gamma^*)}{(C_i + K_m)} - R_d, \quad (2)$$

where C_i is the intercellular concentrations of CO_2 . We assumed R_d to be negligible, because we estimated R_d as 7% of maximum photosynthesis rate recorded in each data set (Givinish, 1988), and found that this had a negligible effect on the results. K_m , the effective Michaelis-Menten coefficient for Rubisco kinetics, and Γ ($\mu\text{mol mol}^{-1}$), the CO_2 compensation point in the absence of mitochondrial respiration, were estimated by Bernacchi *et al.* (2001) as follows:

$$K_m = K_c \left(1 + \frac{O_i}{K_o}\right), \quad (3)$$

$$K_c = \exp\left(38.05 - \frac{79.43}{RT_k}\right), \quad (4)$$

$$K_o = \exp\left(20.30 - \frac{36.38}{RT_k}\right), \quad (5)$$

$$\Gamma^* = 42.75 \exp\left[\frac{37830(T_k - 298)}{(298RT_k)}\right], \quad (6)$$

where O_i is the intercellular O_2 concentration ($210 \text{ mmol mol}^{-1}$), and K_c and K_o are the Michaelis–Menten coefficients of Rubisco activity for CO_2 and O_2 , respectively. R is the universal gas constant ($8.314 \text{ J mol}^{-1} \text{ K}^{-1}$), and T_k denotes leaf temperature in K .

The net mass transpot of CO_2 (A) through stomata is described by Fickian diffusion (Farquhar & Sharkey 1982) as

$$A = g_c (C_a - C_i), \quad (7)$$

from which C_i was estimated as

$$C_i = C_a - \frac{A}{g_c}, \quad (8)$$

where g_c is the stomatal conductance to CO_2 . We assumed cuticular conductance has a negligible impact on CO_2 exchange. From these equations we can estimate the A_c value from the C_i , Γ and K_m values at a given leaf temperature and at the different observed g_s values, on the assumption that V_{cmax} was unchanged from the moist state. The ratio of measured A to this estimated A_c measures the relative effect of water stress on apparent V_{cmax} .

Supplementary figures

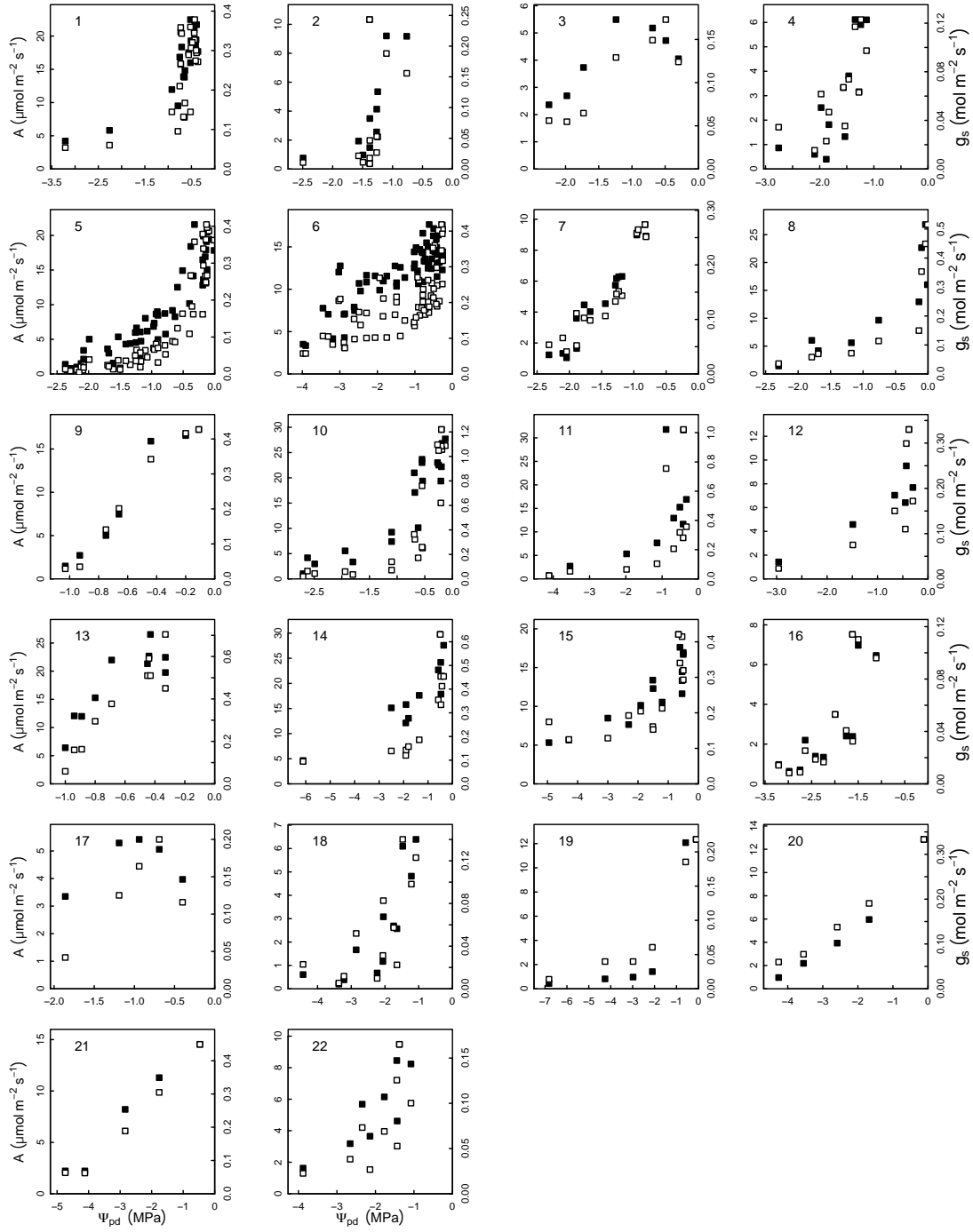


Fig.1 A (filled squares) and g_s (open squares) responses to Ψ_{pd} , from 22 data sets.

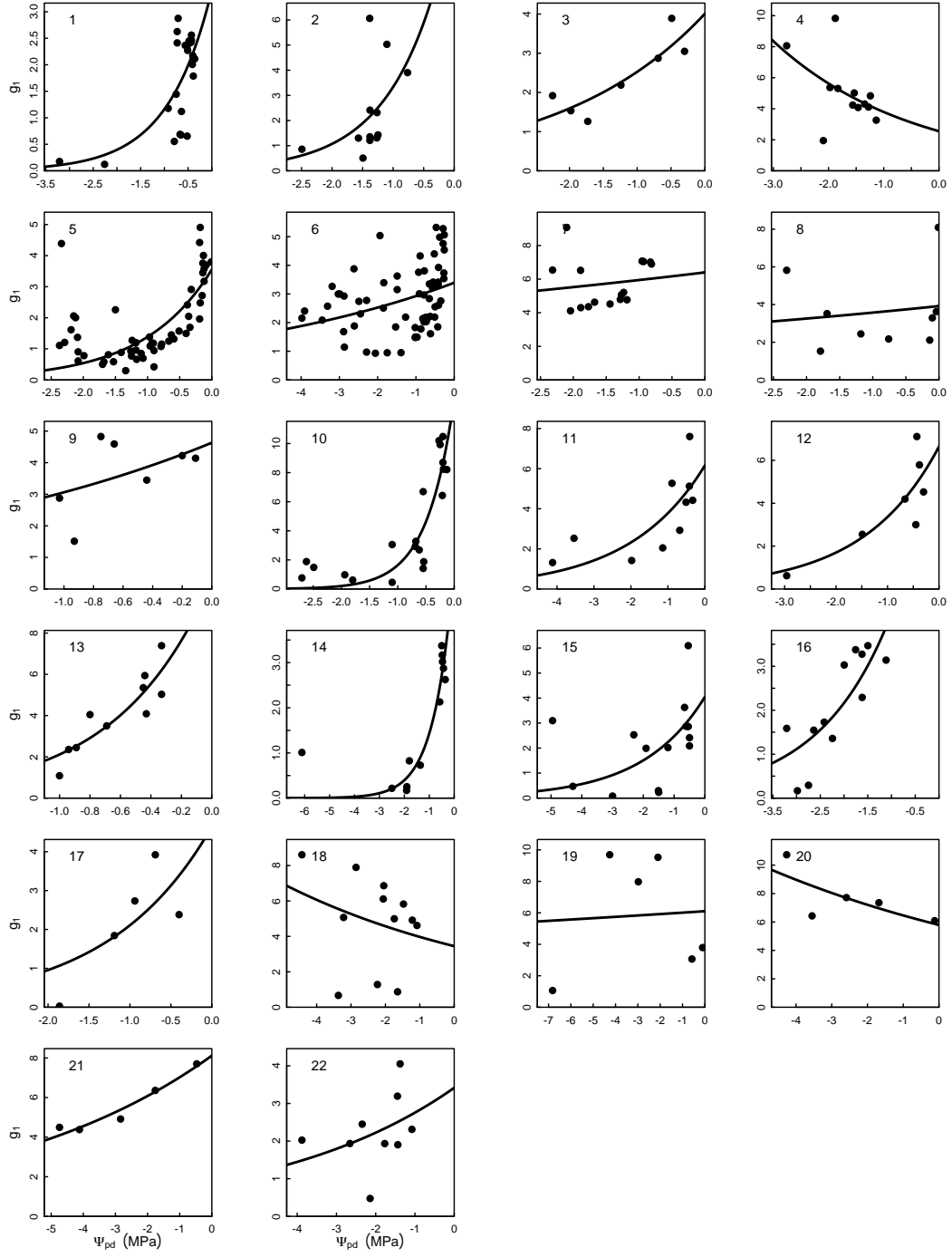


Fig. 2 g_1 responses to Ψ_{pd} from 22 data sets.

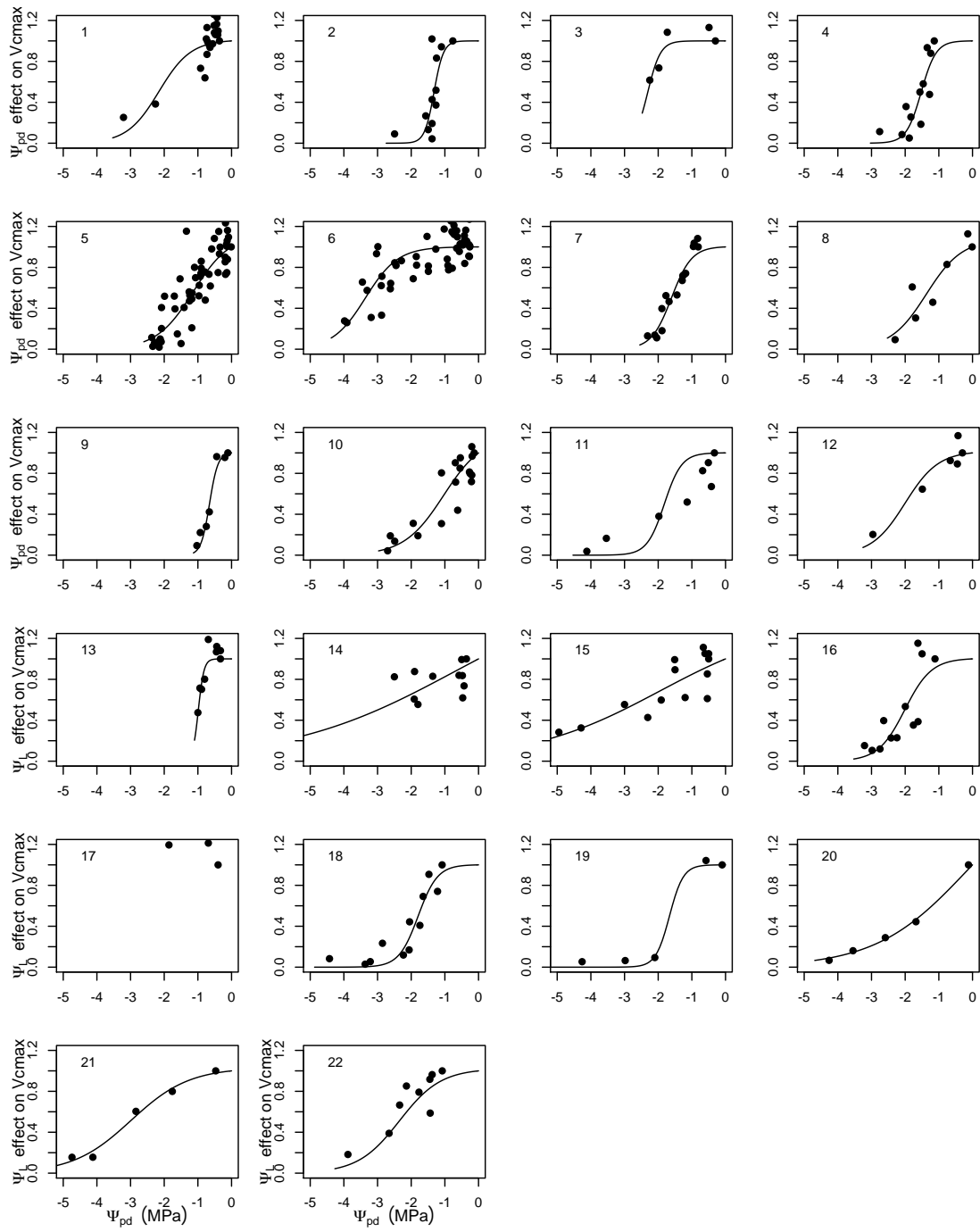


Fig. 3 Relative effect of Ψ_{pd} on V_{cmax} from 21 data sets.

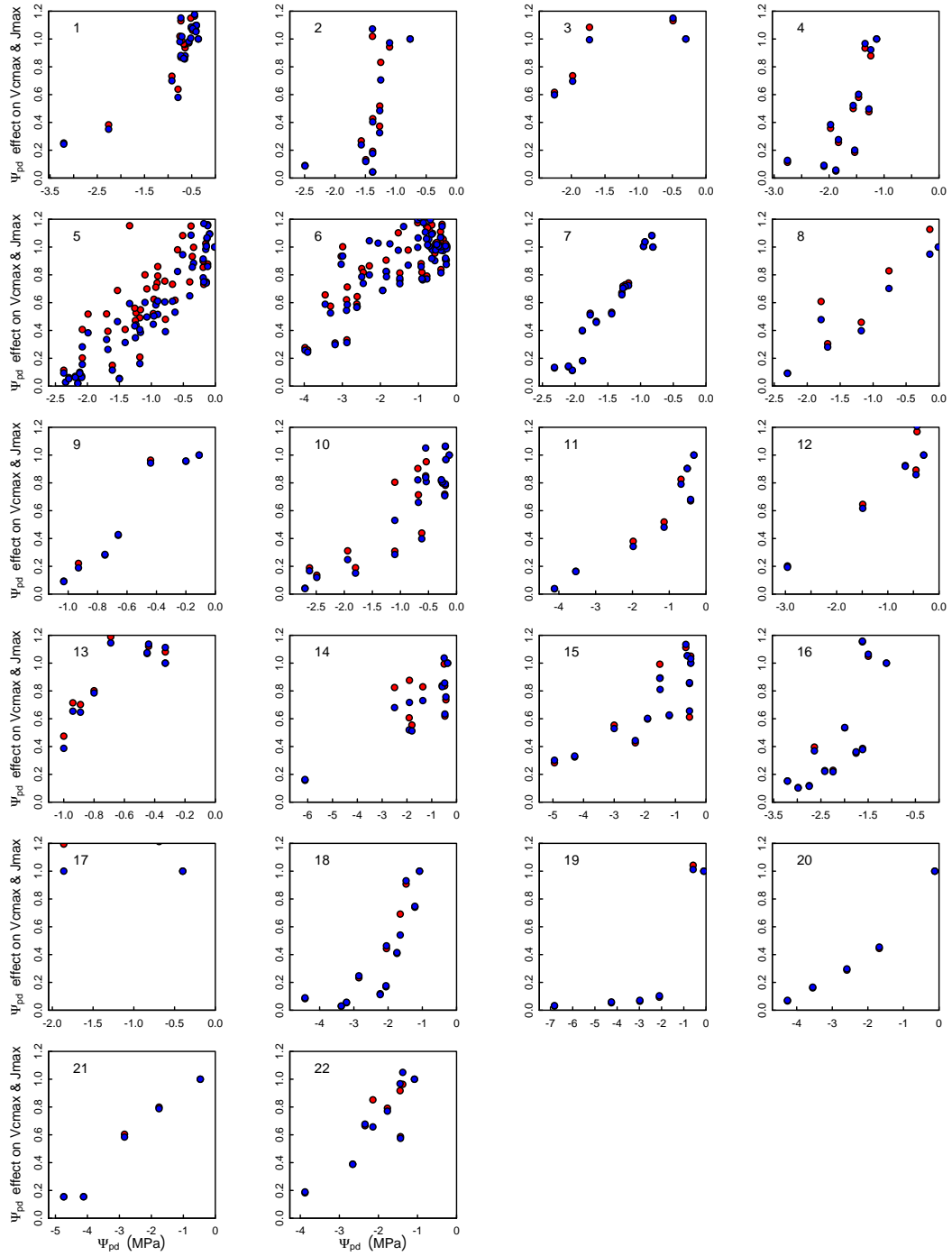


Fig. 4 The apparent effect of water stress on V_{cmax} (red point), and the apparent effect of water stress on J_{max} (blue point).

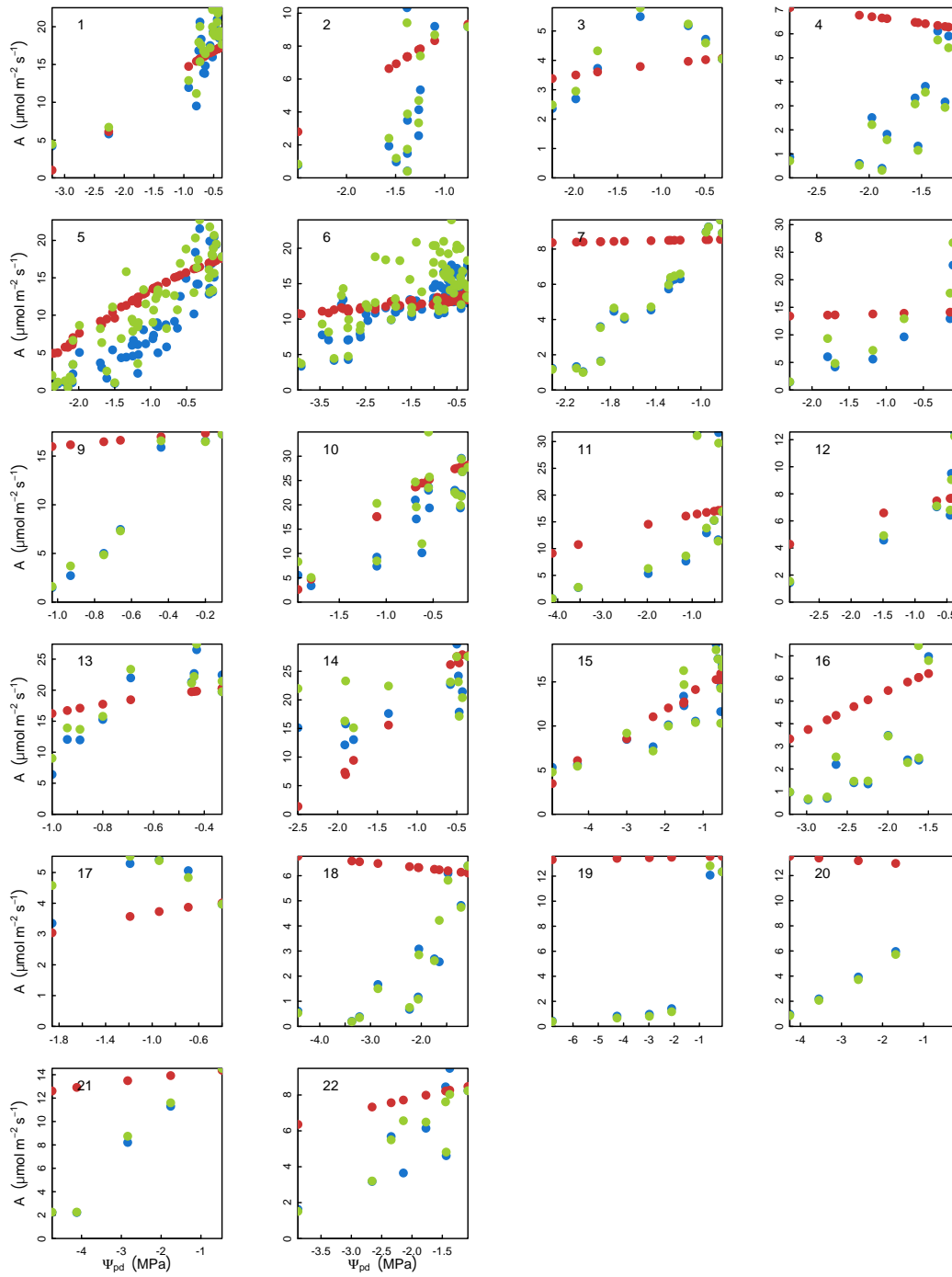


Fig. 5 The effect of water stress on measured photosynthesis (blue point) was compared with the effect on estimated photosynthesis when V_{cmax} was fixed and only g_1 changed (brown point), and with the effect on estimated photosynthesis when g_1 was fixed and only V_{cmax} changed (green point).

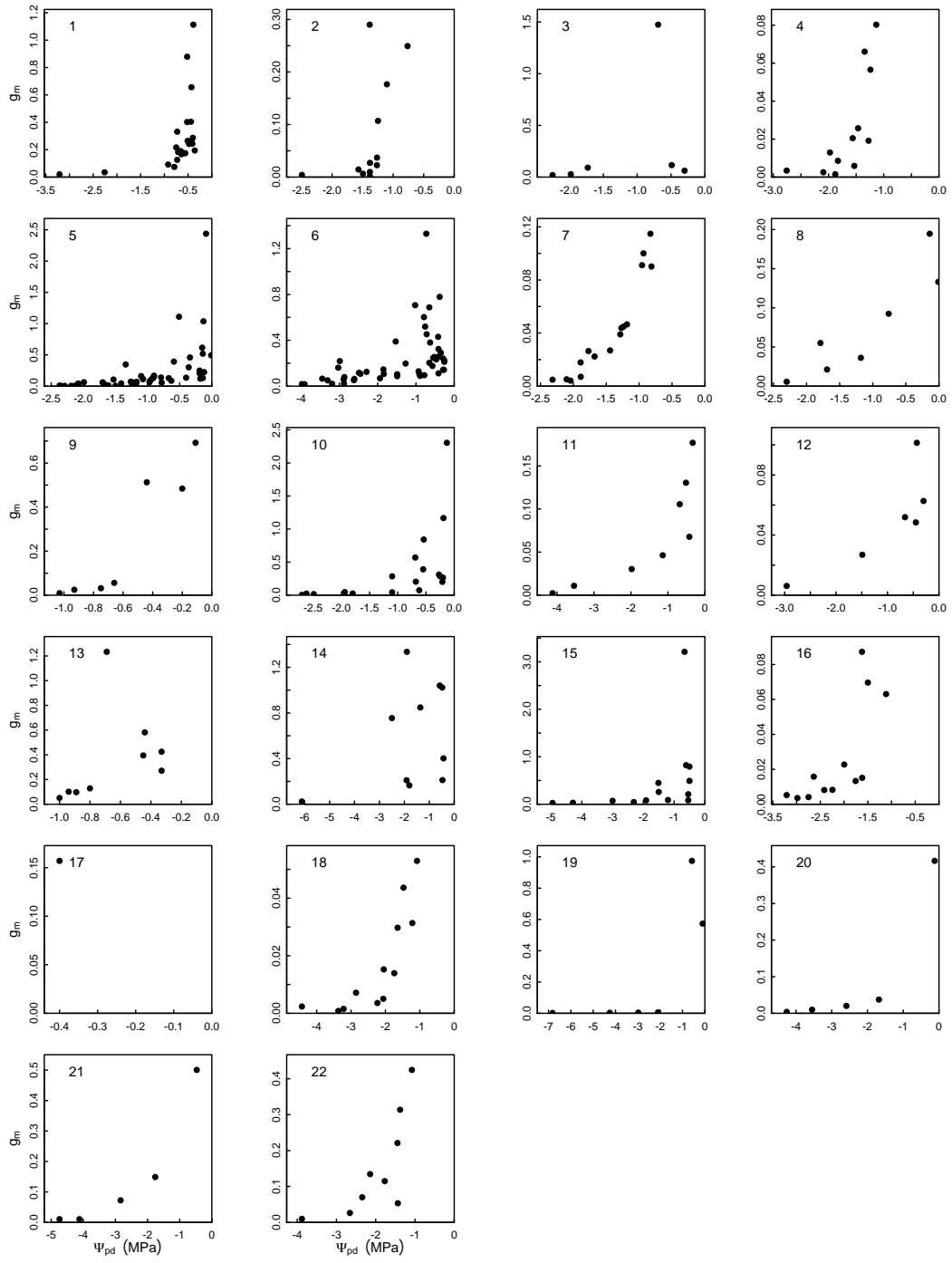


Fig. 6 Estimated g_m responses to Ψ_{pd} from 22 data sets.

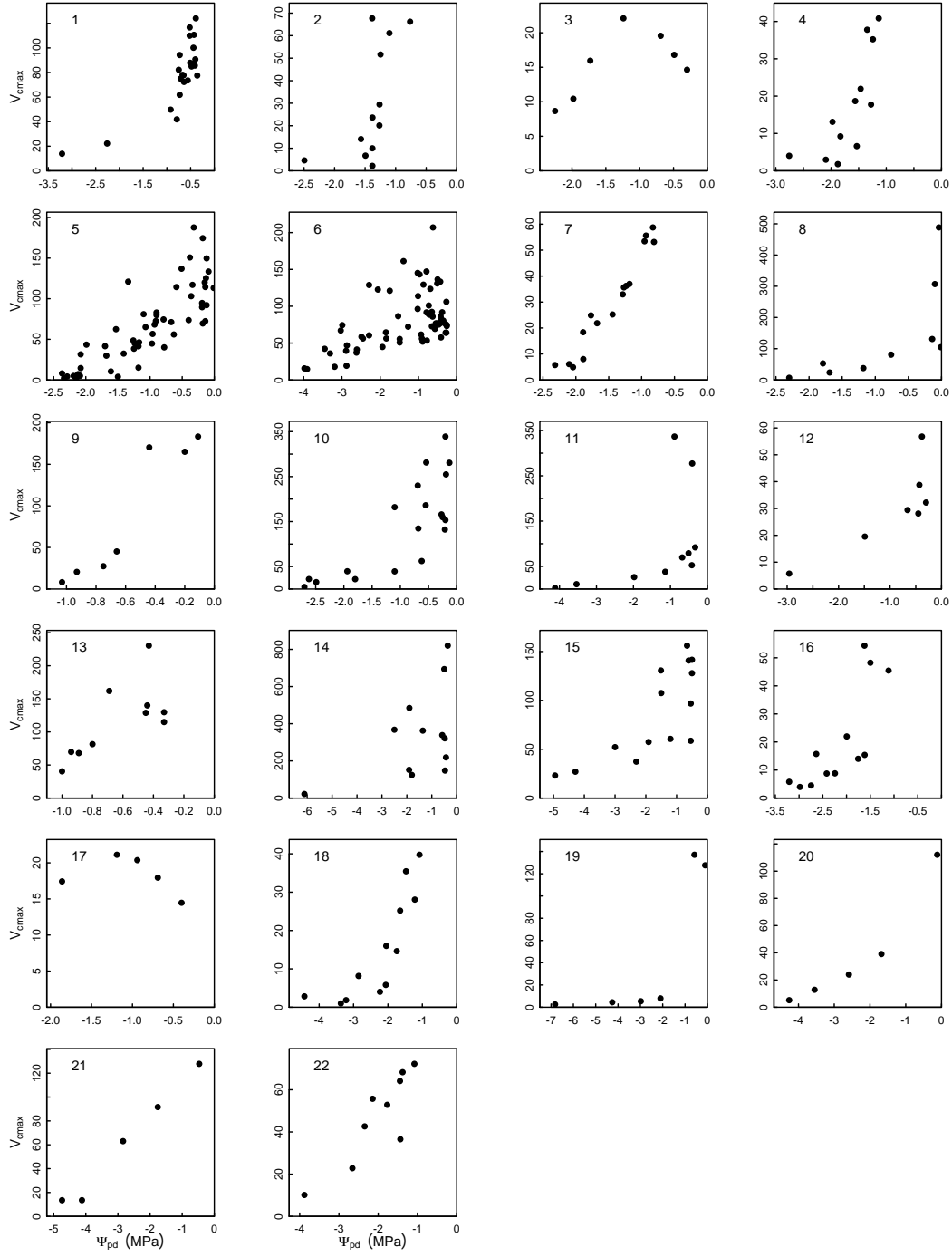


Fig. 7 Estimated V_{cmax} responses to Ψ_{pd} from 22 data sets.

Chapter 3

Short-term water stress impacts on stomatal, mesophyll, and biochemical limitations to photosynthesis differ consistently among tree species from contrasting climates

S. Zhou^{1*}, B. E. Medlyn¹, Santiago Sabaté^{2,3}, Dominik Sperlich^{2,3}, I. C. Prentice^{1,4}

¹Department of Biological Sciences, Macquarie University, North Ryde, NSW 2109, Australia

²Ecology Department, University of Barcelona, Avgda. Diagonal 643, 08028 Barcelona

³CREAF (Centre de Recerca Ecològica i Aplicacions Forestals) Universitat Autònoma de Barcelona, 08193 Barcelona

⁴AXA Chair of Biosphere and Climate Impacts, Grand Challenges in Ecosystems and the Environment and Grantham Institute – Climate Change and the Environment, Department of Life Sciences, Imperial College London, Silwood Park Campus, Buckhurst Road, Ascot SL5 7PY, UK

*Corresponding author: shuangxi.zhou@students.mq.edu.au

This chapter is presented as the published journal article:

Zhou S., Medlyn B. E., Santiago S., Sperlich D., and Prentice I. C., 2014. Short-term water stress impacts on stomatal, mesophyll, and biochemical limitations to photosynthesis differ consistently among tree species from contrasting climates. *Tree Physiology*. DOI: 10.1093/treephys/tpu072.

Pages 50-82 of this thesis have been removed as they contain published material. Please refer to the following citation for details of the article contained in these pages.

Shuangxi Zhou, Belinda Medlyn, Santiago Sabaté, Dominik Sperlich, I. Colin Prentice, David Whitehead, Short-term water stress impacts on stomatal, mesophyll and biochemical limitations to photosynthesis differ consistently among tree species from contrasting climates, *Tree Physiology*, Volume 34, Issue 10, October 2014, Pages 1035–1046,

DOI: [10.1093/treephys/tpu072](https://doi.org/10.1093/treephys/tpu072)

Chapter 4

Long-term water stress leads to acclimation of drought sensitivity of photosynthetic capacity in xeric but not riparian *Eucalyptus* species

S. Zhou¹, B. E. Medlyn¹, I. C. Prentice^{1,2}

¹Department of Biological Sciences, Macquarie University, North Ryde, NSW 2109,
Australia

²AXA Chair of Biosphere and Climate Impacts, Grand Challenges in Ecosystems and the
Environment and Grantham Institute – Climate Change and the Environment, Department of
Life Sciences, Imperial College London, Silwood Park Campus, Buckhurst Road, Ascot SL5
7PY, UK

This chapter is in review with *Annals of Botany*.

This article has been published in [Journal Title] Published by Oxford University Press. *Annals of Botany*, Volume 117, Issue 1, January 2016, Pages 133–144, <https://doi.org/10.1093/aob/mcv161>

4.1 Abstract

Experimental drought is well documented to induce a decline in photosynthetic capacity. However, given time to acclimate to drought, the photosynthetic responses of plants in field could differ from those found in short-term experiments. We compared shorter- and longer-term drought responses of gas exchange in three *Eucalyptus* taxa from contrasting habitats. Photosynthetic parameters were measured after two and four months of watering treatments – field capacity or partial drought. At four months, all plants were watered to field capacity, then watering was ceased. Further measurements were made during subsequent ‘drying down’, continuing until stomata were closed. Two months of partial drought consistently reduced assimilation rate, stomatal sensitivity parameter (g_1), apparent maximum Rubisco activity (V_{cmax}') and maximum electron transport rate (J_{max}'). *E. occidentalis* from the xeric habitat showed the smallest decline in V_{cmax}' and J_{max}' . However, after four months, V_{cmax}' and J_{max}' had recovered. Species differed in their degree of V_{cmax}' acclimation. *E. occidentalis* showed significant acclimation of the predawn leaf water potential at which the V_{cmax}' and ‘true’ V_{cmax} (accounting for mesophyll conductance) declined most steeply during drying-down. It is concluded that carbon loss under prolonged drought could be overestimated without accounting for acclimation. In particular: (i) species from contrasting habitats differed in the magnitude of V_{cmax}' reduction in short-term drought; (ii) long-term drought allowed the possibility of acclimation, such that V_{cmax}' reduction was mitigated; (iii) the degree of V_{cmax}' acclimation was greater in xeric species; and (iv) photosynthetic acclimation would involve hydraulic adjustments to reduce water loss while maintaining photosynthesis.

Keywords: drought acclimation, Huber value, hydraulic adjustment, J_{max} , mesophyll conductance, stomatal conductance, V_{cmax} , water use efficiency

4.2 Introduction

Drought duration and intensity are predicted to increase in future in some regions, particularly in Mediterranean and subtropical climates (IPCC, 2014). The mechanisms underlying plant response to water stress are different for different time scales of stress (Maseda and Fernández, 2006). Short-term water stress reduces plant photosynthesis (A) through limitation of stomatal conductance (g_s) and/or mesophyll conductance to CO_2 (g_m) (Flexas et al., 2004, 2006, 2012; Bota et al., 2004; Grassi and Magnani, 2005; Egea et al., 2011; Galmés et al., 2013; Zhou et al., 2013, 2014), reduction of the maximum carboxylation rate (V_{cmax}) (Kanechi et al., 1996; Castrillo et al., 2001; Parry et al., 2002; Tezara, 2002; Zhou et al., 2013, 2014), and/or reduction of the maximum electron transport rate (J_{max}) (Tezara et al., 1999; Thimmanaik et al., 2002; Zhou et al., 2014). Zhou *et al.* (2014) reported that short-term water stress led to concurrent stomatal, mesophyll, and biochemical limitations on photosynthesis, while species from contrasting hydro-climates differed in the drought sensitivity of each process – reflecting inherent differences in drought tolerance. During longer-term water stress in long-lived plants such as trees, acclimation can take place, rendering the xylem less vulnerable to cavitation. Acclimation can include adjustments at different levels including leaf physiology, anatomy, morphology, chemical composition, xylem hydraulics, growth, and/or carbon partitioning among organs (Maseda and Fernandez, 2006; Limousin et al., 2010*a, b*; Martin StPaul et al., 2012, 2013). However, most of our knowledge about plant drought responses comes from short-term studies (Cano et al., 2014). If we were to predict drought effects on trees based on the drought-induced diffusional and biochemical limitations to photosynthesis found in short-term experiments, we might overestimate the long-term drought impacts because we would be ignoring potentially important acclimation processes.

Among long-term studies, there is disagreement about whether or not plants acclimate to long-term water stress by modifying the functional relationships between photosynthetic traits and water stress. Limousin et al. (2010*b*) and Misson et al. (2010) compared the responses of

Quercus ilex under different long-term manipulative precipitation regimes, and found high sensitivity of g_s , g_m , V_{cmax} , and J_{max} to decreased predawn leaf water potential but no clear trend of acclimation in the drought treatment. In contrast, Martin StPaul et al. (2012) compared the responses of three populations of *Quercus ilex* in sites differing in mean annual rainfall, and found steeper declines of g_s , g_m , V_{cmax} , and J_{max} as predawn leaf water potential declined in the wettest site than in the drier sites. There are also studies reporting that long-term water stress causes an acclimation response through decreased mesophyll limitation on CO₂ supply to the chloroplasts (Galle et al., 2009; Cano et al., 2014).

Another important but largely unexplored question is whether species of contrasting climate origin differ in their degree of acclimation in photosynthetic traits during long-term water stress. Cano et al. (2014) reported that long-term water stress led to decreased mesophyll limitation in a xeric species, but not mesic species. A synthesis study (Choat et al. 2012) showed that vulnerability to drought is equally high in plants from both mesic and xeric ecosystems, despite soil water availability being lower in xeric ecosystems – indicating that there must be important differences between the responses of mesic and xeric species to prolonged drought.

In this paper, we test three general hypotheses on the long-term water stress impacts on photosynthesis of contrasting tree species. (i) Long-term water stress should allow the possibility of acclimation, such that the diffusional and/or biochemical limitations found in short-term water stress are mitigated. (ii) Relative to species from riparian habitats, species from xeric habitats should show a greater degree of acclimation. (iii) Plants would respond to water stress by controlling stomatal openness in the shorter-term, but longer-term acclimation to water stress would involve hydraulic adjustments to reduce water loss while maintaining photosynthesis. We tested these hypotheses in a common glasshouse experiment with three congeneric (*Eucalyptus*) taxa originating from riparian and xeric habitats. Plants were maintained under either field capacity or partial drought treatment, and gas exchange was

monitored after shorter-and longer-term treatment. After the longer-term treatment, we watered all plants to field capacity and then withheld water and compared their stomatal, mesophyll, and biochemical responses during the ‘drying down’ process. We investigated whether the plants acclimate to the partial drought treatment. We then investigated whether the plants could better tolerate water stress during the drying-down process after the longer-term water stress, and how the contrasting taxa differed in their degree of photosynthetic acclimation to water stress. We also assessed the hydraulic adjustments after the longer-term water stress.

4.3 Materials and methods

4.3.1 Choice of plant taxa

Three evergreen taxa were selected from the widely distributed Australian genus *Eucalyptus* (Table 1). The selected taxa were *E. occidentalis* from southwestern Australia, *E. camaldulensis* subsp. *subcinerea* from central Australia, and *E. camaldulensis* subsp. *camaldulensis* from southeastern Australia. *E. camaldulensis* subsp. *Camaldulensis* and *E. camaldulensis* subsp. *subcinerea* are strongly riparian.

Table 1. Description of the seed origin for the three taxa.

Species	Seed source; Latitude, Longitude ^a
<i>E.occidentalis</i>	Spa Bundaleer, West Australia; 33.19°S, 138.33°E
<i>E.camaldulensis</i> subsp. <i>subcinerea</i>	Arthur Creek, Northern Territory; 22.40°S, 136.38°E
<i>E.camaldulensis</i> subsp. <i>camaldulensis</i>	Barmah SF, New South Wales; 35.50°S, 145.07°E

^a Data source: Australian Tree Seed Centre at Canberra

4.3.2 Plant material, growth conditions, and experimental design

Seeds of the three *Eucalyptus* taxa were directly collected from their natural habitats by the Australian Tree Seed Centre at Canberra (Table 1) and were germinated in May 2012 at Macquarie University. At three months, the seedlings were transplanted into 90-litre pots containing 80 kg of loamy soil (collected from the Robertson area in New South Wales,

Australia), evenly mixed with slow-release fertilizer. The plants were grown in the open air with regular watering and full sunshine for three months to allow natural establishment. At six months (December 2012), the plants were placed in a glasshouse under a 25°C/18°C diurnal temperature cycle and maintained in a moist condition (100% field capacity). In February 2013, plants of each taxon were subjected to one of two treatments – full watering (100% field capacity) or partial drought (70% field capacity). Three plants of each taxon were randomly assigned to each treatment. Soil water content was maintained based on pot weighting. The soil surface was covered with gravel to minimize water loss. Pots were randomly located in the glasshouse, and randomly relocated twice a week.

Leaf gas exchange measurements were conducted after two months (April 2013) and four months (June 2013) of treatment. After four months, all pots were watered to 100% field capacity. Then watering was ceased, and plants were subjected to drying down until stomatal conductance was close to zero. Daily measurements on predawn leaf water potential, leaf gas exchange, carbon response curves, and chlorophyll fluorescence were conducted throughout the drying-down process.

4.3.3 Pre-dawn leaf water potential

Pre-dawn leaf water potential (Ψ_{pd}) was adopted as the consistent measure of soil moisture across plants. Ψ_{pd} is the best measure of plant water availability because it integrates soil water potential over the root zone (Schulze and Hall, 1982). In particular: (i) Ψ_{pd} is not influenced by daytime transpiration, while daytime leaf water potential depends strongly on transpiration as well as soil water status; (ii) Ψ_{pd} is independent of differences in rooting depth and soil water access; (iii) unlike volumetric soil moisture content, Ψ_{pd} is independent of soil texture. Ψ_{pd} was measured using a pressure chamber (PMS 1000, PMS Instruments, Corvallis, OR, USA). All measurements were completed before sunrise. Two leaves per sapling were sampled. When the observed difference between the two leaves was > 0.2 MPa,

a third leaf was measured.

4.3.4 Leaf gas exchange, carbon response curve, chlorophyll fluorescence, and mesophyll conductance

Leaf gas exchange measurements were performed on current-year, fully expanded sun-exposed leaves, using a portable photosynthesis system (LI-6400, Li-Cor Inc., Lincoln, NE, USA) equipped with a LI-6400-40 Leaf Chamber Fluorometer. Before each measurement, the leaf was acclimated in the chamber for 20 to 30 minutes to achieve stable gas exchange, with leaf temperature maintained at 25 °C, reference CO₂ concentration at 400 µmol CO₂ mol⁻¹ air, and a saturating photosynthetic photon flux density (Q) of 1800 µmol photon m⁻² s⁻¹. Vapour pressure deficit (D) was held as constant as possible during the measurement. After the leaf acclimated to the cuvette environment, light-saturated net CO₂ assimilation rate (A_{sat}) and stomatal conductance were measured. A - C_i curves were then measured with the cuvette reference CO₂ concentration set as follows: 300, 200, 150, 100, 50, 400, 400, 600, 800, 1000, 1400 and 2000 µmol CO₂ mol⁻¹ air. The leaf was allowed to equilibrate for at least three minutes at each C_i step. After completion of these measurements, the light was switched off for 3 minutes and then leaf respiration rate was measured at the ambient CO₂ concentration. A and C_i values at each step were corrected for CO₂ diffusion leaks with a diffusion correction term (k) of 0.445 µmol m⁻² s⁻¹, following the manufacturer's recommendation (Li-Cor Inc.).

At each measurement step, steady-state fluorescence (F_s) and maximum fluorescence (F_m') were measured during a light-saturating pulse, allowing calculation of the photochemical efficiency of PSII as $\Phi_{\text{PSII}} = (F_m' - F_s)/F_m'$. The rate of photosynthetic electron transport from fluorescence (J_{ETR}) was then calculated following Krau and Edwards (1992), as $J_{\text{ETR}} = 0.5 \cdot \Phi_{\text{PSII}} \cdot \alpha \cdot Q$, whereas 0.5 is a factor accounting for the light distribution between the two photosystems and α is the leaf absorptance (assumed to be 0.85-0.88 in the calculations of LI-

6400).

Mesophyll conductance was quantified following the variable electron transport rate method by Harley et al.(1992):

$$g_m = \frac{A}{C_i - \frac{\Gamma^* [J_{ETR} + 8(A + R_d)]}{J_{ETR} - 4(A + R_d)}}, \quad (1)$$

where the Γ^* value was taken from Bernacchi et al. (2002), and the rate of non-photorespiratory respiration continuing in the light (R_d) was taken as half of the rate of respiration measured in the dark (Niinemets *et al.*, 2005). Thereafter, g_m was quantified for every step of the carbon response curves, and then used to calculate the CO_2 concentration at the chloroplast (C_c) as follows:

$$C_c = C_i - A/g_m. \quad (2)$$

4.3.5 Estimation of V_{cmax}' , J_{max}' , V_{cmax} , and J_{max}

Estimation of V_{cmax}' , J_{max}' , V_{cmax} , and J_{max} (the terms without primes being ‘true’ values, accounting for g_m) followed methods described in detail by Zhou et al. (2014). In brief, the values were quantified from CO_2 response curves using the leaf photosynthesis model of Farquhar et al. (1980), based on the curve fitting routine was that introduced by Domingues et al. (2010) using the least-squares fitting method in the ‘R’ environment (R Development Core Team, 2010).

4.3.6 Conduit anatomy, HV , sapwood-specific and leaf-specific hydraulic conductivity

One current-year branch 25 cm long from the distal apex was collected from each plant for measurements on xylem conduit anatomy. A cross-section at 25 cm from the apex was made by hand, stained with methylene blue, and mounted in water for immediate microphotography. The microscope (Olympus BX53, Olympus America Inc.) was interfaced with a digital camera at $\times 4$ magnification in order to record the whole sapwood area, and at $\times 20$

magnification in order to record the conduit diameter. Both measurements were made using ImageJ image analysis software (<http://rsb.info.nih.gov/ij/>; ImageJ 1.48; U. S. National Institutes of Health, Bethesda, Maryland, USA). Huber Values (HV) were calculated as the ratio between the cross-sectional sapwood area and the leaf area supplied. The hydraulically weighted vessel diameter was calculated for each plant to determine the relative contribution of the conduit to hydraulic conductivity. Calculation of hydraulically weighted diameter and sapwood-specific hydraulic conductivity (K_S , $\text{kg m}^{-1} \text{s}^{-1} \text{MPa}^{-1}$) was performed as described by Lewis and Boose (1995). Leaf-specific conductivity (K_L) was calculated as the product of K_S and HV.

4.3.7 LMA, intrinsic water use efficiency, leaf nitrogen content, height and basal diameter

After four months of treatment, three current-year fully-expanded sun-exposed leaves of each plant were collected, scanned, and measured with the ImageJ image analysis software. The leaves were then oven-dried at 60 °C for at least 48 h and weighed in order to calculate leaf mass per area (LMA, kg m^{-2}). The dried leaf tissue was analysed for stable carbon isotope composition ($\delta^{13}\text{C}$, ‰) and nitrogen content on a mass basis (N_{mass} , %) as described in Mitchell et al. (2008). $\delta^{13}\text{C}$ provides a time-integrated measure of intrinsic water-use efficiency over the period in which the leaf carbon is assimilated. Nitrogen content on an area basis (N_{area} , g m^{-2}) was calculated as the product of N_{mass} and LMA. The height and trunk basal diameter of each plant were also measured.

4.3.8 Stomatal sensitivity to water stress

The g_1 parameter ($\text{kPa}^{-0.5}$) was introduced by Medlyn et al. (2011) to represent the stomatal behaviour. Medlyn et al. (2011) showed that a stomatal optimality hypothesis results in a simple theoretical model of very similar form to the widely used empirical stomatal models (Ball et al., 1987; Collatz et al., 1991; Leuning, 1995; Arneeth et al., 2002):

$$g_s \approx g_0 + 1.6 \left(1 + \frac{g_1}{\sqrt{D}}\right) \frac{A}{C_a}, \quad (3)$$

where C_a is the atmospheric CO_2 concentration at the leaf surface ($\mu\text{mol mol}^{-1}$) and g_0 is the leaf water vapour conductance when photosynthesis is zero ($\text{mol H}_2\text{O m}^{-2} \text{s}^{-1}$). The derivation of the model by Medlyn *et al.* (2011) provides an interpretation for g_1 as being inversely proportional to the marginal carbon cost of water. An alternative derivation of the same expression, and further empirical support, were provided by Prentice *et al.* (2014). The g_1 parameter has proved to be a useful, experimentally-determined measure of stomatal sensitivity across climates and plant functional types (PFTs) (H  roult *et al.* 2013; Zhou *et al.* 2013, 2014). Its response to water stress is consistent with the theoretical analysis by M  kel   *et al.* (1996) suggesting that the marginal water cost of carbon gain should decline exponentially with decreasing soil moisture availability, and the rate of decline with soil moisture should increase with the probability of rain (Zhou *et al.* 2013, 2014).

We estimated g_1 for each predawn leaf water potential from measurements of A , g_s , C_a , and D by re-arranging equation (3). The parameter g_0 is not part of the optimization and was assigned the value $0.001 \text{ mol m}^{-2} \text{s}^{-1}$.

4.3.9 Analytical model for the function of stomatal, mesophyll, and biochemical responses during the drying-down process

We used equations introduced by Zhou *et al.* (2013, 2014) to analyse the response functions of g_1 , g_m , V_{cmax}' , and J_{max}' to Ψ_{pd} during the drying-down process. An exponential decrease of g_1 and g_m with declining Ψ_{pd} was fitted to each set of observations:

$$g_1 = g_1^* \exp(b_1 (\Psi_{\text{pd}} + 0.3)), \quad (4)$$

$$g_m = g_m^* \exp(b_2 (\Psi_{\text{pd}} + 0.3)), \quad (5)$$

where g_1^* , b_1 , g_m^* , and b_2 are fitted parameters: g_1^* is the g_1 value at $\Psi_{pd} = -0.3$ MPa, and b_1 represents the sensitivity of g_1 to Ψ_{pd} . g_m^* is the g_m value at $\Psi_{pd} = -0.3$ MPa, and b_2 represents the sensitivity of g_m to Ψ_{pd} . Species adopting different water use strategies are expected to differ in their g_1 sensitivity (b_1) and g_m sensitivity (b_2) to water stress. The responses of V_{cmax}' and J_{max}' were quantified using the logistic function (Tuzet *et al.*, 2003):

$$f(\Psi_{pd}) = K \frac{[1 + \exp(S_f \Psi_f)]}{1 + \exp[S_f(\Psi_f - \Psi_{pd})]}. \quad (6)$$

We also quantified all parameters defining the drought response of V_{cmax} . The function $f(\Psi_{PD})$ accounts for the relative effect of water stress on V_{cmax} , V_{cmax}' , and J_{max}' . The form of this function allows a relatively flat response of V_{cmax} , V_{cmax}' , and J_{max}' under moist conditions, followed by a steep decline, with a flattening again (towards zero) under the driest conditions. K is the value of $f(\Psi_{PD})$ under moist conditions. S_f is a sensitivity parameter indicating the steepness of the decline, while Ψ_f is a reference value indicating the water potential at which K decreases to half of its maximum value. Species adopting different water use strategies might be expected to differ in the sensitivity of V_{cmax} , V_{cmax}' , and J_{max}' to water stress (S_{fV} , S_{fV}' , and S_{fJ}') and reference water potential (Ψ_{fV} , Ψ_{fV}' , and Ψ_{fJ}').

4.3.10 Statistical analyses

The analysis of variance package `anova()` in R was used to assess treatment effects, interactions between species and treatment and between treatment and duration. The nonlinear least-squares package `nls()` in R was used to find initial values (least-squares estimates) of the parameters of the exponential functions for responses of g_1 and g_m (g_1^* , b_1 , g_m^* , and b_2); the alternative nonlinear least-squares package `nls2()` was used to find initial values of the parameters of the logistic functions for responses of V_{cmax} , V_{cmax}' , and J_{max}' (V_{cmax}^* , $V_{cmax}'^*$, $J_{max}'^*$, S_{fV} , S_{fV}' , S_{fJ}' , Ψ_{fV} , Ψ_{fV}' , and Ψ_{fJ}') (Table 2). These initial values were then input into the

maximum likelihood estimation package `bblme()` in R to yield best estimates and standard errors for each parameter. The package `glht()` was used to conduct multi-comparison analysis on response curves of each parameter across the three contrasting *Eucalyptus* taxa in the drying down process after four months of treatments. Principal components analysis (PCA) was conducted on the best estimates of parameters to investigate the correlations among the key traits defining the longer-term drought responses of g_1 , g_m , V_{cmax}' , and J_{max}' of three contrasting taxa.

4.4 Results

4.4.1 Effect of partial drought on A_{sat} , g_s , g_1 , V_{cmax}' , and J_{max}' after two and four months

The partial drought consistently reduced the light-saturated CO_2 assimilation rate (A_{sat}) after two months ($P < 0.001$) and four months ($P < 0.01$). There was a significant interaction between species and treatment ($P < 0.01$), indicating that partial drought had a greater impact on photosynthesis in the riparian *E. camaldulensis* than the xeric *E. occidentalis* (Fig.1a). There was also a significant interaction between treatment and duration ($P < 0.05$), indicating that in both riparian and xeric species, the effect of water stress on photosynthesis recovered over time. Compared to *E. camaldulensis* subsp. *camaldulensis* and *E. camaldulensis* subsp. *subcinerea*, *E. occidentalis* from the xeric habitat showed the smallest decline in A_{sat} after two months (Fig.1a). In *E. occidentalis*, A_{sat} recovered completely after four months, such that there was no difference in A_{sat} between the droughted and well-watered plants (Fig.1a). The partial drought significantly reduced g_s in all taxa after two months ($P < 0.01$) and four months ($P < 0.001$) (Fig.1b), and reduced g_1 after four months ($P < 0.01$) (Fig.2a).

V_{cmax}' was significantly reduced by the partial drought after two months ($P < 0.001$) but not after four months. There were significant interactions between species and treatment ($P < 0.05$) and between treatment and duration ($P < 0.05$) (Fig.2b). Compared to the two riparian

taxa, *E. occidentalis* showed the smallest decline in V_{cmax}' after two months, and the V_{cmax}' recovered after four months (Fig.2b). The partial drought significantly reduced the J_{max}' ($P < 0.01$) and increased the ratio between J_{max}' and V_{cmax}' ($P < 0.05$) after two months, while there was no significant reduction after four months (Fig.2c; Fig.2d).

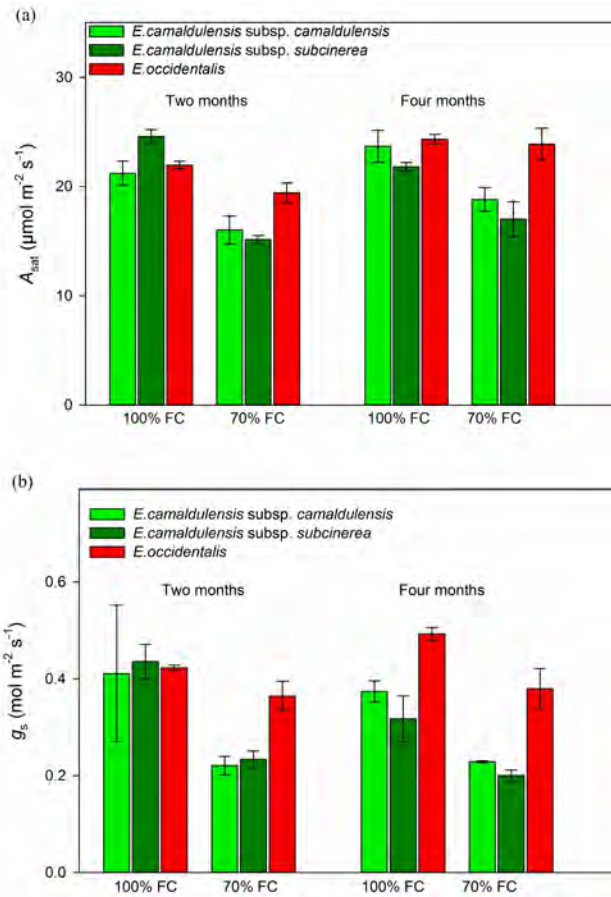


Figure 1. (a) Leaf net photosynthesis at saturating light (A_{sat}) and (b) stomatal conductance (g_s) of three *Eucalyptus* taxa exposed to watering treatments of 100% and 70% field capacity (FC), measured after 2 months and 4 months of treatment. Values are means \pm SE (n = 3).

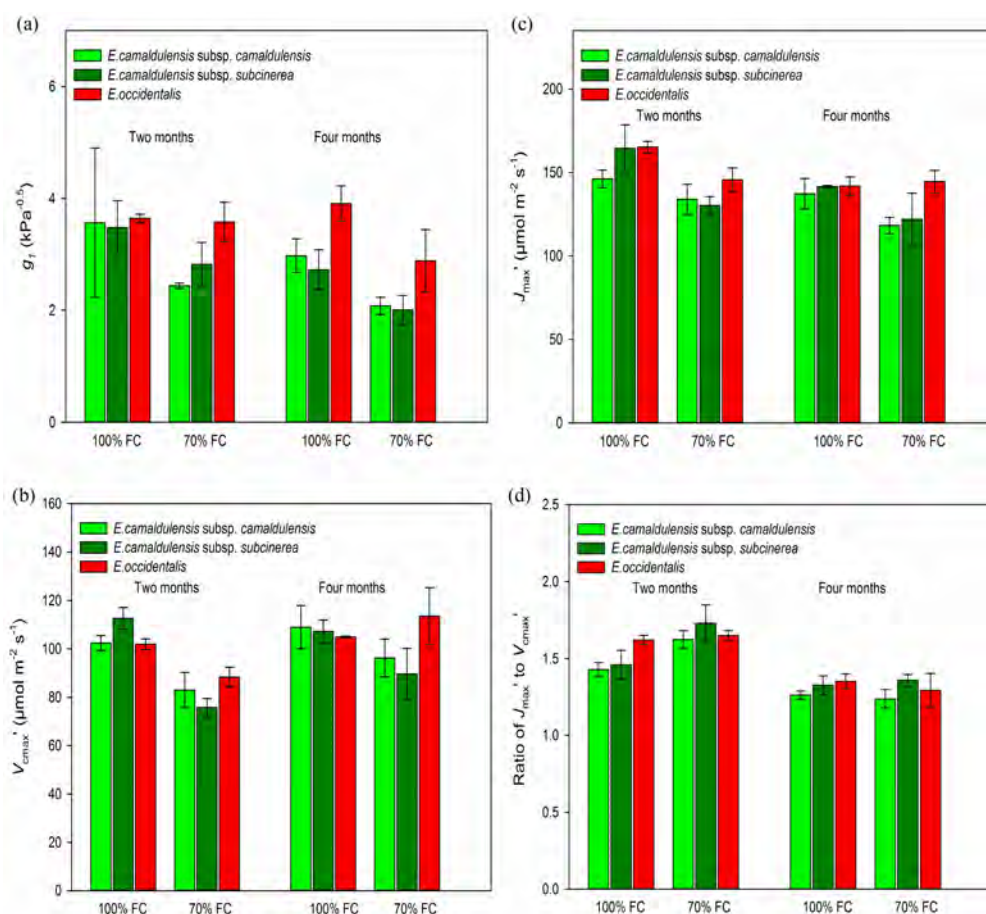


Figure 2. Components of leaf gas exchange in three *Eucalyptus* taxa exposed to watering treatments of 100% and 70% FC, after 2 months and 4 months of treatment. (a) Stomatal sensitivity parameter g_1 ; (b) Apparent Rubisco activity V_{cmax}' ; (c) Apparent maximum electron transport rate J_{max}' ; (d) Ratio of J_{max}' to V_{cmax}' . Values are means \pm SE ($n = 3$).

4.4.2 Effect of partial drought on $\delta^{13}C$, K_L , K_S , HV , height, basal diameter, LMA, and N_{area} after four months

Compared to plants of three taxa kept under 100% FC for four months, plants kept under 70% FC showed less negative $\delta^{13}C$ ($P < 0.05$) (Fig.3a), larger K_L ($P < 0.01$) (Fig.3b), larger HV ($P < 0.001$) (Fig.3d), smaller height (marginally significant, $P < 0.1$) (Fig.3e) and basal diameter ($P < 0.001$) (Fig.3f). There was no effect of growth treatment on the K_S (Fig.3c), LMA (Fig.3g), N_{weight} and N_{area} (Fig.3h), or the hydraulically weighted vessel diameter (Supplementary Fig.2). These long-term responses to partial drought did not differ significantly among species.

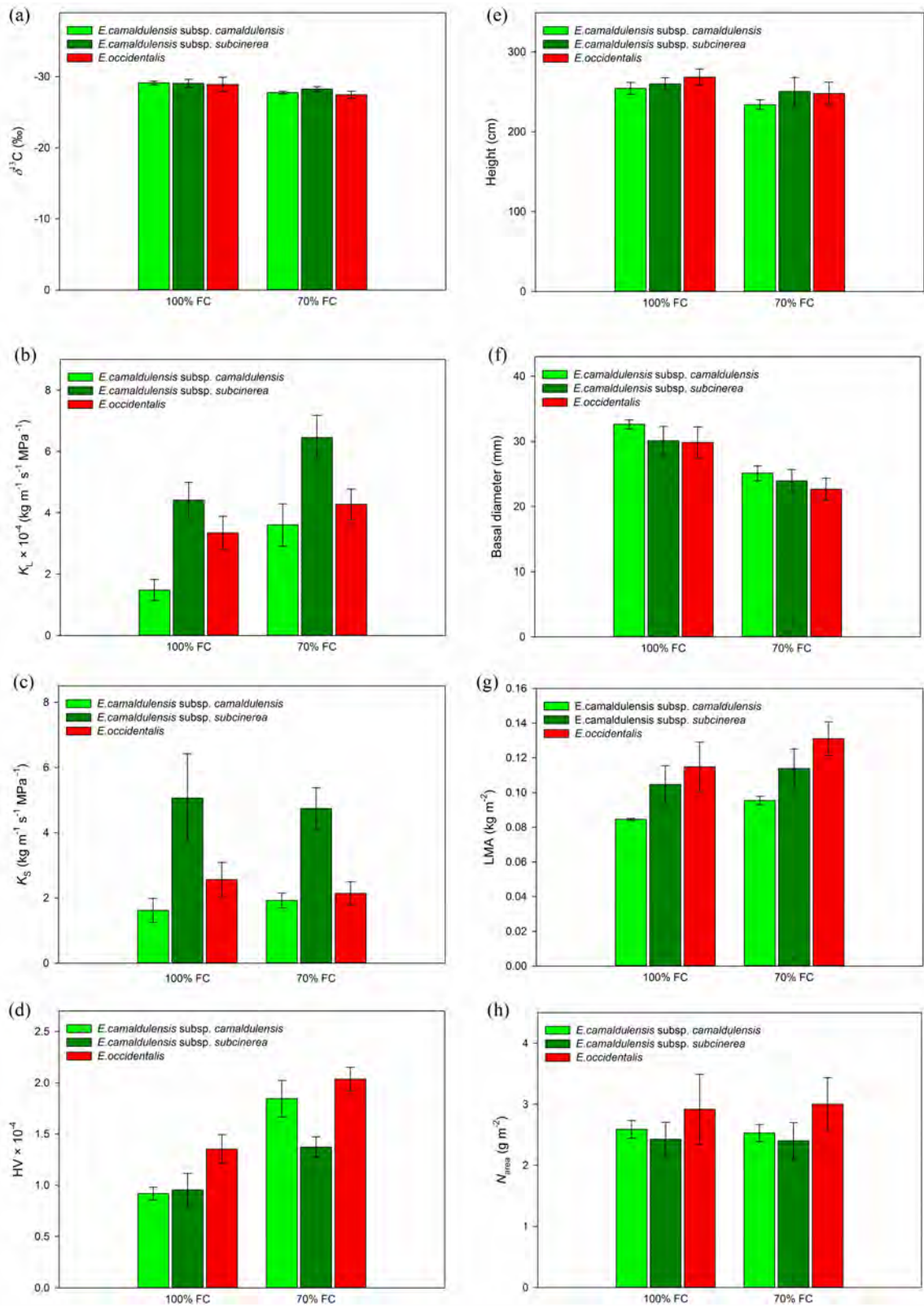


Figure 3. Hydraulic traits, growth status, and leaf nitrogen content of three *Eucalyptus* taxa exposed to watering treatments of 100% and 70% field capacity (FC), measured after 2 months and 4 months of treatment. (a) Carbon-isotope composition $\delta^{13}\text{C}$; (b) leaf-specific conductivity; (c) sapwood-specific conductivity; (d) Huber value (sapwood area per unit leaf

area); (e) height; (f) basal diameter; (g) leaf mass per area; (h) leaf nitrogen content on an area basis. Values are means \pm SE (n = 3).

4.4.3 Response of g_1 , g_m , V_{cmax}' , and J_{max}' in the drying-down process after four months

In the drying-down process after four months of treatments, all plants showed considerable decline of A_{sat} , g_s , g_1 , g_m , V_{cmax}' , and J_{max}' as water availability declined (Fig. 4; 5). There was no effect of growth treatment (100% FC vs 70% FC) on the response of g_1 , g_m , and J_{max}' to declining Ψ_{PD} (Fig. 5a; 5b; 5d; Table 2). There was a significant effect of growth treatment on the response curve of V_{cmax}' to declining Ψ_{PD} in xeric *E. occidentalis* but not in either subspecies of riparian *E. camaldulensis* (Fig. 5c; Table 2). Compared to plants from 100% FC, *E.occidentalis* plants from 70% FC treatment had significantly more negative Ψ_{FV}' (the water potential at which V_{cmax}' decreases to half of its maximum value) ($P < 0.01$; Table 2). Similarly, there was a difference between these contrasting taxa when comparing the effect of growth treatment on the response curve of V_{cmax} , which was consistent with the contrasting responses of V_{cmax}' (SI Fig.1; Table 2). *E.occidentalis* plants from 70% FC had more negative Ψ_{FV} (marginally significant, $P = 0.07$) than plants from 100% FC (Table 2). Estimated parameter values for each *Eucalyptus* taxa from each treatment are given in Table 2.

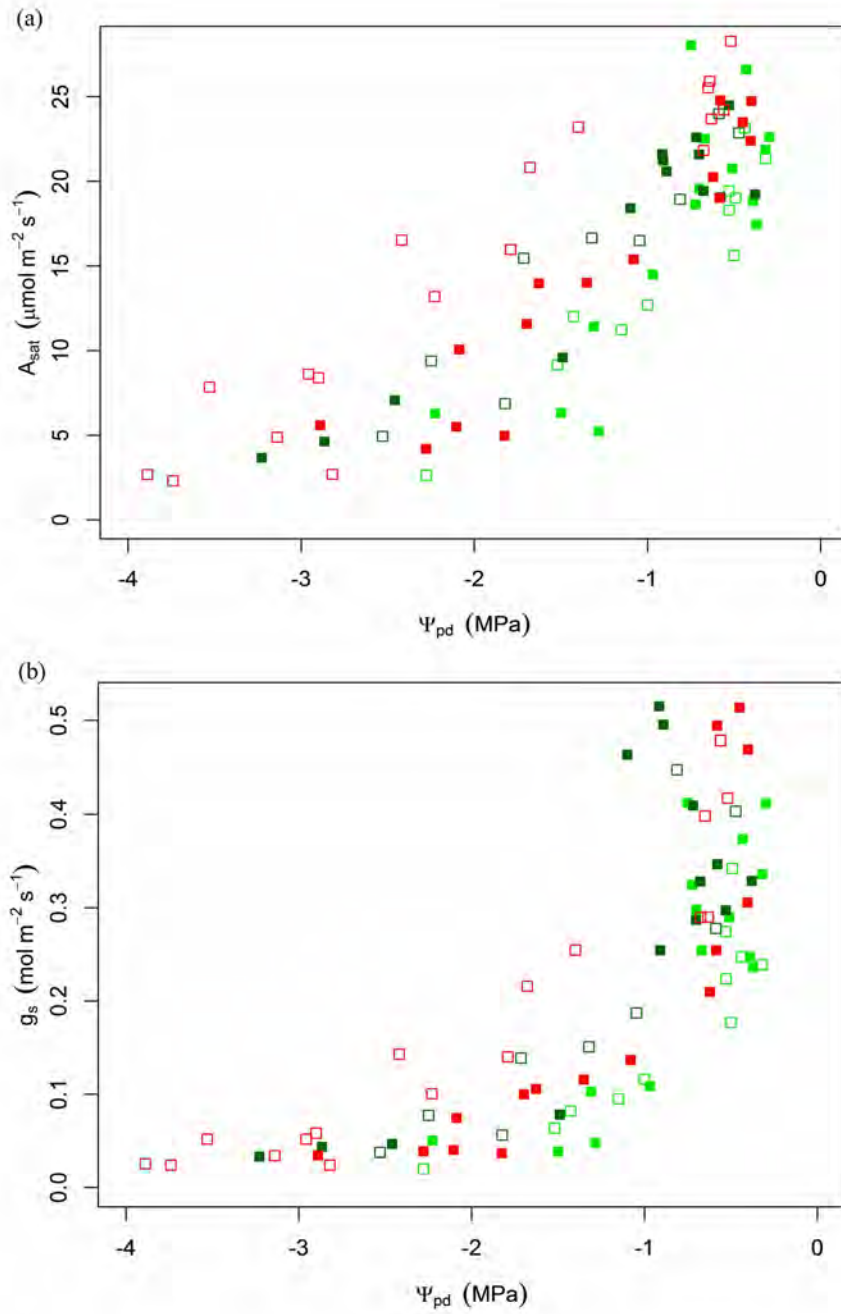


Figure 4. (a) Light-saturated CO_2 assimilation rate (A_{sat}) and (b) stomatal conductance as a function of pre-dawn leaf water potential during a drying cycle following 4 months of treatment at 100% FC (solid squares) or 70% FC (open squares). Dark green: *E. camaldulensis* subsp. *camaldulensis*; Light green: *E. camaldulensis* subsp. *subcinerea*; Red: *E. camaldulensis* subsp. *occidentalis*.

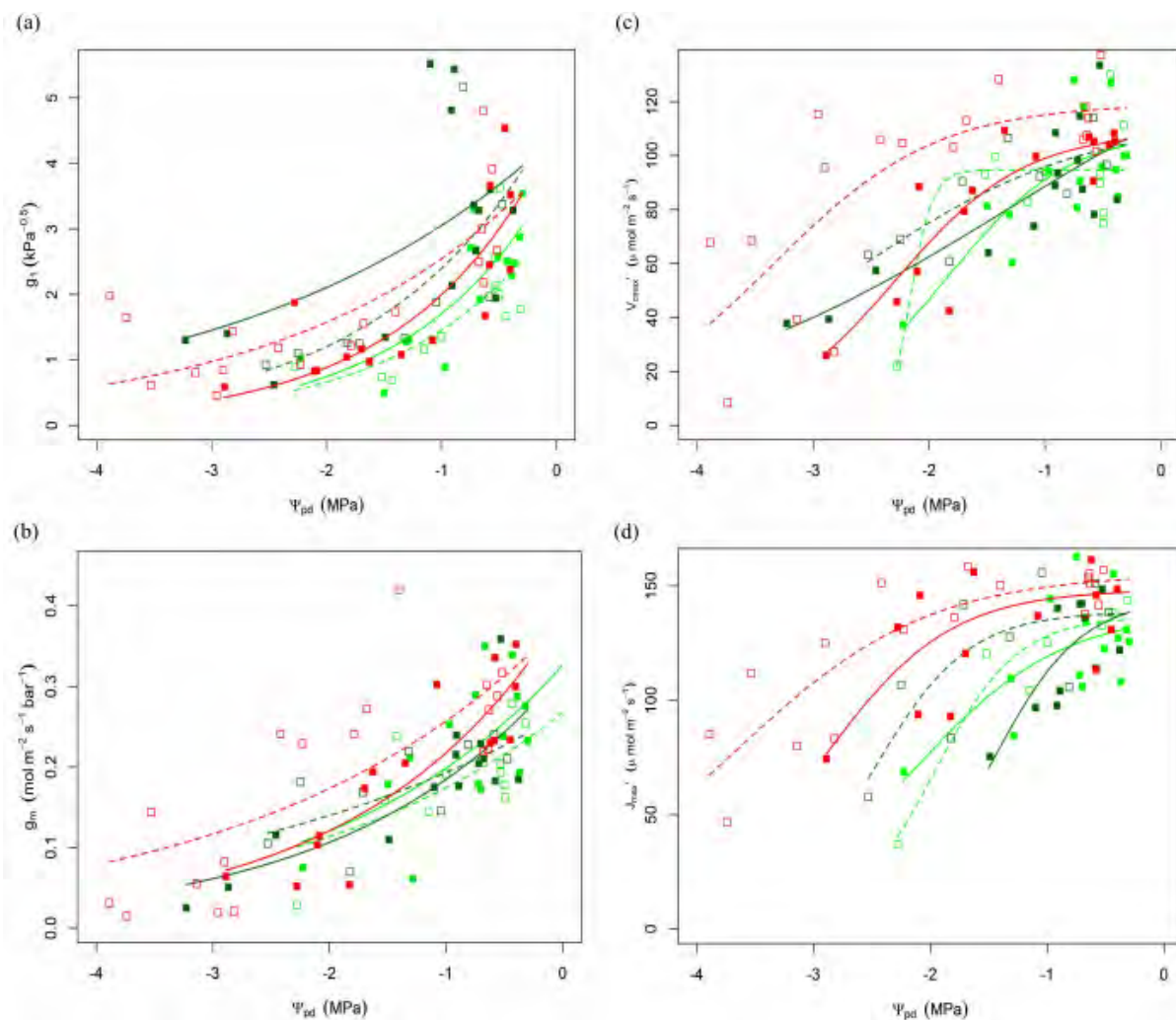


Figure 5. Components of leaf gas exchange as a function of pre-dawn leaf water potential during a drying cycle following 4 months of treatment at 100% FC (solid squares for raw data; solid lines for fitted curves) or 70% FC (open squares for raw data; solid lines for fitted curves). (a) Stomatal sensitivity parameter g_1 ; (b) Mesophyll conductance g_m ; (c) Apparent Rubisco activity V_{cmax}' ; (d) Apparent maximum electron transport rate J_{max}' . Dark green: *E. camaldulensis* subsp. *camaldulensis*; Light green: *E. camaldulensis* subsp. *subcinerea*; Red: *E. occidentalis*.

4.4.4 Water relation strategies

PCA (Fig.6) showed strong dominance by the first principal component (PC1), which explained 49.2% of total variation. PC1 showed a continuum from the most xeric *Eucalyptus* taxon (*E. occidentalis* towards the left) to the most mesic taxon (*E. camaldulensis* subsp.

camaldulensis towards the right), characterized by the positive correlation among b_1 , S_{fv}' , S_{fl}' , Ψ_{fv}' , and Ψ_{fl}' , and by their negative correlations with g_1^* , g_m^* , V_{cmax}^* , and J_{max}^* (Fig. 6). *E. camaldulensis* subsp. *camaldulensis*, found to the right of PC1, was characterized by (i) lower initial g_1 , g_m , V_{cmax}' , and J_{max}' values under moist conditions, (ii) a relatively higher rate of decline in g_1 , V_{cmax}' , and J_{max}' in the drying-down process, and (iii) the decrease of V_{cmax}' and J_{max}' commencing at a more negative predawn leaf water potential (Fig. 6; Table 2).

The second principal component (PC2) explained 24.1% of total variation. Along PC2, the plants were arranged into two loose groups along another continuum from the *Eucalyptus* taxa kept under 70% FC for four months (towards the bottom) to the *Eucalyptus* taxa kept under 100% FC (towards the top), characterized by the positive correlation with b_2 . The *Eucalyptus* taxa kept under 70% FC for four months were characterized by a slower rate of decline of g_m in the drying-down process. PC1 and PC2 suggested a direction of acclimation from plants kept under 100% FC to that of 70% FC in long-term water stress. Compared with plants kept under 100% FC, plants kept under 70% FC for four months tended to have lower values of b_2 and Ψ_{fv}' . Parameter values of the three *Eucalyptus* taxa from two treatments are shown in Table 2.

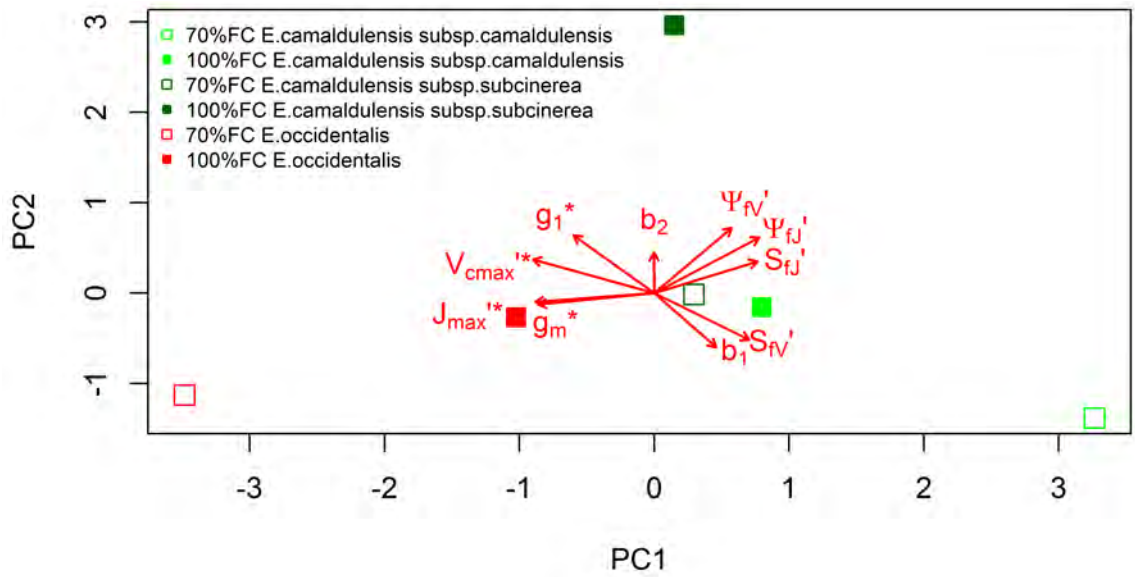


Figure 6. Principal components analysis of ten drought-response traits, b_1 (sensitivity of g_1), g_1^* (g_1 estimated at $\Psi_{pd} = -0.3$ MPa), b_2 (sensitivity of g_m), g_m^* (g_m estimated at $\Psi_{pd} = -0.3$ MPa), V_{cmax}^{*} (V_{cmax}' estimated at $\Psi_{pd} = 0$), S_{fv}' , Ψ_{fv}' , J_{max}^{*} (J_{max}' estimated at $\Psi_{pd} = 0$), S_{fj}' , and Ψ_{fj}' . The first principal component (PC1) showed a continuum of species from more mesic to more xeric species, which explained 49.2% of total variation. The second principal component (PC2) showed a continuum of plants from 70% FC to 100% FC treatment, which explained 24.1% of total variation. Values of traits are shown in Table 2.

4.5 Discussion

When given time to acclimate to water stress, the photosynthetic response of plants could differ from that of plants in short-term water stress. However, the photosynthetic responses of plants to long-term water stress and its variation among species of contrasting climate of origin are poorly understood. In the present study, we investigated the varied photosynthetic responses of three contrasting *Eucalyptus* taxa in shorter- and longer-term water stress, and then compared their degree of acclimation of g_1 , g_m , V_{cmax}' , and J_{max}' – if any occurred in the longer-term water stress – by imposing a drying-down process. We also investigated the

hydraulic adjustments after the longer-term water stress. This study provides important experimental evidence that the photosynthetic acclimation can occur in longer-term water stress, and highlights the significant acclimation of V_{cmax} ' in xeric but not riparian *Eucalyptus* taxa.

4.5.1 Differential acclimation of photosynthetic responses in contrasting *Eucalyptus* taxa to long-term water stress

After two months of 70% FC treatment, we observed a significant reduction in A_{sat} , g_s , V_{cmax} ', and J_{max} ' in all taxa (Fig.1; Fig.2). However, the effect of partial drought on photosynthesis differed among species, such that *E.occidentalis* from xeric habitat showed less stomatal and biochemical limitations than the riparian *E. camaldulensis* at two months.

Meanwhile, the effect of partial drought differed at the different time points, being smaller at four months than at two months. Four months of 70% FC treatment allowed for acclimation of V_{cmax} ' and J_{max} ' such that the biochemical limitations found in short-term water stress in all taxa are mitigated (Fig.2). However, *E.occidentalis* showed more recovery of V_{cmax} ' and J_{max} ' than *E. camaldulensis* after four months of water stress (Fig.2).

In the subsequent drying-down process, all plants consistently showed a progressive increase in stomatal, mesophyll, and biochemical limitation with increasing water stress (Fig.4; Fig.5; Table 2), which is consistent with previous studies where a drying-down process was imposed without the longer-term water stress (Zhou et al. 2013, 2014). The response functions of g_1 , g_m , V_{cmax} ', and J_{max} ' to declining Ψ_{PD} were compared between plants from 70% FC and 100% FC using a multi-comparison analysis. We investigated two possible classes of causes accounting for mitigation of limitation on V_{cmax} ' in longer-term water stress: (i) mitigation of limitation on g_m as reported by Galle et al. (2009) and Cano et al. (2014); (ii) mitigation of limitation on V_{cmax} which has never been reported before according to our knowledge. The

results showed the three contrasting *Eucalyptus* taxa differed notably in their degree of modification of the functional relationship of V_{cmax}' (and V_{cmax}) with declining Ψ_{PD} (Fig. 5; Table 2). When comparing the plants kept under 70% FC and 100% FC, *E. occidentalis* showed a significantly higher degree of V_{cmax}' (and V_{cmax}) acclimation than the two riparian taxa in the longer-term water stress, by significantly displacing the start of severe limitations on V_{cmax}' (and V_{cmax}) to lower Ψ_{FV}' (and Ψ_{FV}) (Fig. 5; Table 2). *E. occidentalis* plants kept under 70% FC for four months – during which the significant acclimation process occurred – showed the ability to continue active photosynthesis down to much lower soil water potential (–3.9 MPa) than plants of the two riparian taxa kept under 70% FC for four months (Fig.4; Fig.5).

For the first time, we report significant acclimation of drought sensitivity of V_{cmax} in xeric but not riparian *Eucalyptus* (Fig.2; Fig.5; Supplementary Fig.1; Table 2). This study adds novel information to previous studies investigating whether or not plants acclimate to long-term water stress by modifying the functional relationships between photosynthetic traits and water stress (Limousin et al. 2010b; Misson et al. 2010; Martin StPaul et al. 2012). After long-term water stress during which the acclimation process occurred, the xeric but not riparian *Eucalyptus* taxa could significantly modify the functional relationship between Rubisco activity and declined Ψ_{PD} . The inherent differences among the three *Eucalyptus* taxa of contrasting climatic origin were not only reflected in their contrasting degree of tolerance in short-term water stress, but also in their contrasting degree of acclimation in long-term water stress.

Short-term water stress could lead to the decrease of Rubisco activity, associated with down-regulation of the activation state of the enzyme (Galmés et al., 2013), reduction in Rubisco content and/or soluble protein content (Hanson and Hitz 1982; Wilson et al., 2000; Xu and Baldocchi, 2003; Grassi et al., 2005; Misson et al., 2006). However, the longer-term water

stress might lead to significantly higher protein content and/or protein allocated to Rubisco in leaves of the drought-tolerant taxa than drought-sensitive taxa (Tezara and Lawlor, 1995; Pankovic et al., 1999), indicating that higher Rubisco content could be one factor in conferring higher drought tolerance and acclimation in xeric species than mesic species. In this study, there was no difference on leaf N_{mass} or N_{area} between plants from two treatments (Fig.3), but we were unable to further test if the plants kept under 70% FC had higher nitrogen allocation to Rubisco than that of plants kept under 100% FC.

We did not find significant higher g_m in xeric species than mesic species after longer-term water stress as reported by Cano et al. (2014). Species-specific physiology may be of particular importance in comparing their responses to longer-term water stress, leading to varied findings among studies investigating the comparative acclimation in contrasting species (Ogaya and Peñuelas, 2003; Cano et al., 2014). It remains to be shown whether or not the same patterns found in the present study exist for mature *Eucalyptus* trees in field, and also for contrasting species of other genus and/or in other biomes.

4.5.2 Hydraulic adjustments after the longer-term water stress

Without sufficient control of water loss during severe drought, xylem embolism and damage could occur and lead to hydraulic failure. However, maintaining water potentials through stomatal closure during severe drought reduces photosynthesis, potentially leading to carbon starvation and mortality (Sala et al., 2012; Adams et al., 2013). Our results showed an adjustment of hydraulic properties in plants exposed to four months of 70% FC treatment (Fig.2; Fig.3; Fig. 6; Table 2), which would reduce the vulnerability of xylem to cavitation while maintaining photosynthesis during longer-term water stress. The plants kept under 70% FC for four months had stopped growth in height and basal diameter, and significantly increased their sapwood area invested per unit leaf area, yielding higher leaf-specific conductivity. Meanwhile, the plants kept under 70% FC for four months had lower $\delta^{13}\text{C}$, b_2 ,

Ψ_{fV} ', and Ψ_{fJ} ' when compared with plants kept under 100% FC (Fig. 6; Table 2). This combination of trait changes allowed them to increase the intrinsic water use efficiency, decrease g_m , V_{cmax} ', and J_{max} ' slowly to maintain more CO₂ supply to the chloroplasts, and also maintain higher photosynthetic capacity and RuBP regeneration capacity down to lower water potential. Prentice et al. (2014) predicted that Huber value and V_{cmax} ' are necessarily linked, which supported our results on the acclimation of carboxylation capacity and the larger Huber values in plants kept under 70% FC for four months.

It is concluded that the photosynthetic drought responses of plants in the long term can be different from those observed in short-term experiments. For plant physiologists and modellers, this study highlights the importance of considering the acclimation process and its variation with the climatic origin of species when predicting the long-term drought effect. The findings on intra- and inter-species variation of photosynthetic acclimation in long-term drought could also help restoration ecologists on the selection of species for restoration schemes aiming to increase long-term drought resistance and resilience of forest ecosystems.

Acknowledgments

We acknowledge the help of Dr Brian Atwell and Srikanta Dani Kaidala-Ganesha with plant materials and soil preparation, glasshouse maintenance, and watering. We acknowledge Dr Drew Allen for help on R and statistics. Ning Dong provided the global map of Moisture Index. SZ was supported by an international Macquarie University Research Excellence Scholarship.

4.6 References

Adams, HD, Germino MJ, Breshears DD, Barron-Gafford GA, Guardiola-Claramonte M, Zou CB, Huxman TE. 2013. Nonstructural leaf carbohydrate dynamics of *Pinus edulis* during drought-induced tree mortality reveal role for carbon metabolism in mortality mechanism. *New Phytol* 197(4): 1142-1151.

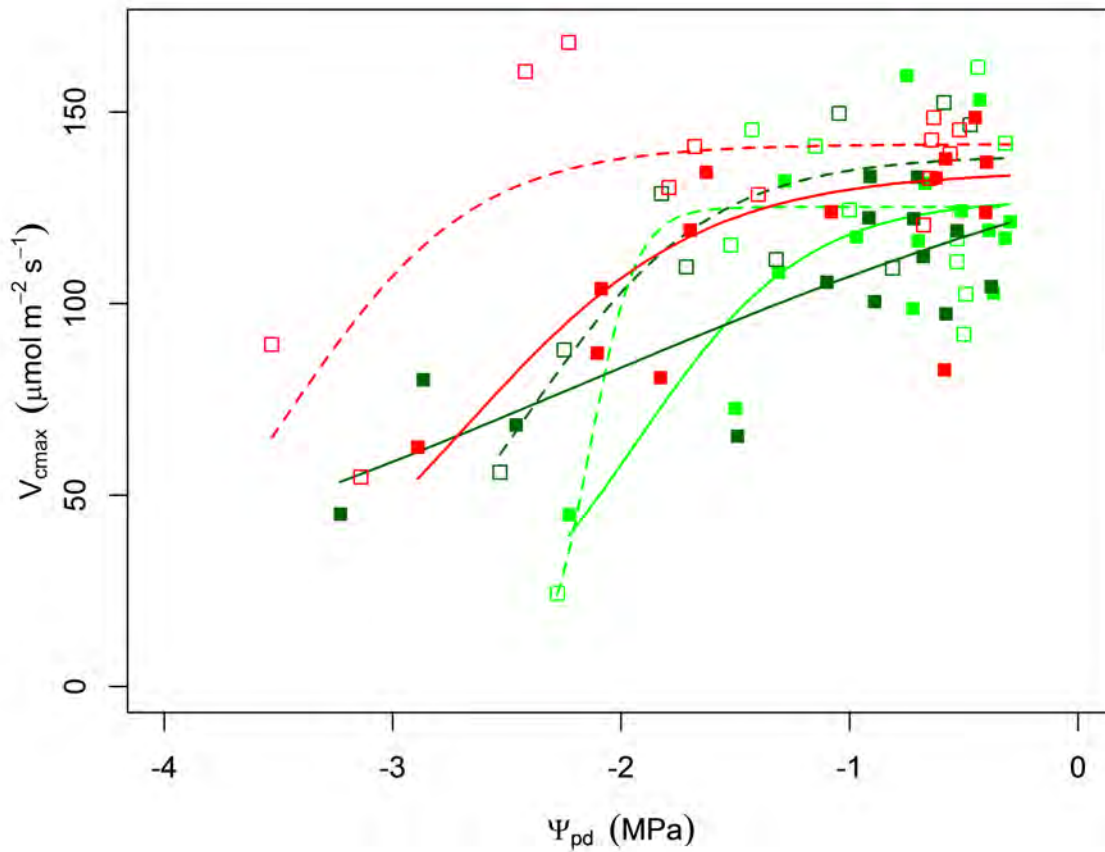
- Arneeth A, Lloyd J, Santruckova H, Bird M, Grigoryev S, Kalaschnikov YN, Gleixner G, Schulze E. 2002. Response of central Siberian Scots pine to soil water deficit and long-term trends in atmospheric CO₂ concentration. *Global Biogeochem Cycles* 16: 5-1-5-13.
- Ball JT, Woodrow IE, Berry JA. 1987. A model predicting stomatal conductance and its contribution to the control of photosynthesis under different environmental conditions. In: Biggins J eds. *Progress in Photosynthesis Research*. Dordrecht, the Netherlands: Martinus-Nijhoff Publishers, 221–224.
- Bernacchi CJ, Portis AR, Nakano H, von Caemmerer S, Long SP. 2002. Temperature response of mesophyll conductance. Implications for the determination of Rubisco enzyme kinetics and for limitations to photosynthesis in vivo. *Plant Physiol* 130: 1992–1998.
- Bota J, Medrano H, Flexas J. 2004. Is photosynthesis limited by decreased Rubisco activity and RuBP content under progressive water stress? *New Phytol* 162: 671–681.
- Cano FJ, López R, Warren CR. 2014. Implications of the mesophyll conductance to CO₂ for photosynthesis and water-use efficiency during long-term water stress and recovery in two contrasting Eucalyptus species. *Plant Cell Environ*. DOI: 10.1111/pce.12325.
- Castrillo M, Fernandez D, Calcagno A. 2001. Responses of ribulose-1, 5-bisphosphate carboxylase, protein content, and stomatal conductance to water deficit in maize, tomato, and bean. *Photosynthetica* 39: 221–226.
- Choat B, Jansen S, Brodribb TJ, *et al.* 2012. Global convergence in the vulnerability of forests to drought. *Nature* 491(7426): 752-755.
- Collatz GJ, Ball JT, Grivet C, Berry JA. 1991. Physiological and environmental regulation of stomatal conductance, photosynthesis and transpiration: a model that includes a laminar boundary layer. *Agric For Meteorol* 54: 107–136.
- Domingues TF, Meir P, Feldpausch TR, *et al.* 2010. Co-limitation of photosynthetic capacity by nitrogen and phosphorus in West Africa woodlands. *Plant Cell Environ* 33: 959–980.
- Egea G, Verhoef A, Vidale PL. 2011. Towards an improved and more flexible representation of water stress in coupled photosynthesis–stomatal conductance models. *Agric For Meteorol* 151: 1370–1384.
- Farquhar GD, von Caemmerer S, Berry JA. 1980. A biochemical model of photosynthetic CO₂ assimilation in leaves of C₃ species. *Planta* 149: 78–90.
- Flexas J, Barbour MM, Brendel O, *et al.* 2012. Mesophyll diffusion conductance to CO₂: an unappreciated central player in photosynthesis. *Plant Sci* 193-194: 70–84.
- Flexas J, Bota J, Loreto F, Cornic G, Sharkey TD. 2004. Diffusive and metabolic limitations to photosynthesis under drought and salinity in C₃ plants. *Plant Biol* 6: 269–279.
- Flexas J, Ribas-Carbó M, Bota J, Galmés J, Henkle M, Martínez-Cañellas S, Medrano H. 2006. Decreased Rubisco activity during water stress is not induced by decreased relative water content but related to conditions of low stomatal conductance and chloroplast CO₂ concentration. *New Phytol* 172: 73–82.

- Galle A, Florez-Sarasa I, Tomas M, Pou A, Medrano H, Ribas-Carbo M, Flexas J. 2009. The role of mesophyll conductance during water stress and recovery in tobacco (*Nicotiana sylvestris*): acclimation or limitation?. *J Exp Bot* 60(8): 2379-2390.
- Gallego-Sala A, Clark J, House J, Orr H, Prentice I, Smith P, Farewell T, Chapman S. 2010. Bioclimatic envelope model of climate change impacts on blanket peatland distribution in Great Britain. *Clim Res* 45: 151–162.
- Galmés J, Aranjuelo I, Medrano H, Flexas J. 2013. Variation in Rubisco content and activity under variable climatic factors. *Photosynth Res* 117: 73–90.
- Grassi G, Magnani F. 2005. Stomatal, mesophyll conductance and biochemical limitations to photosynthesis as affected by drought and leaf ontogeny in ash and oak trees. *Plant Cell Environ* 28: 834–849.
- Grassi G, Vicinelli E, Ponti F, Cantoni L, Magnani F. 2005. Seasonal and interannual variability of photosynthetic capacity in relation to leaf nitrogen in a deciduous forest plantation in northern Italy. *Tree Physiol* 25: 349–360.
- Hanson, AD, Hitz WD. 1982. Metabolic responses of mesophytes to plant water deficits. *Ann Rev Plant Physio* 33(1): 163-203.
- Harley PC, Loreto F, Di Marco G, Sharkey TD. 1992. Theoretical considerations when estimating the mesophyll conductance to CO₂ flux by analysis of the response of photosynthesis to CO₂. *Plant physiol* 98: 1429–1436.
- Hérault A, Lin Y-S, Bourne A, Medlyn BE, Ellsworth DS. 2013. Optimal stomatal conductance in relation to photosynthesis in climatically contrasting *Eucalyptus* species under drought. *Plant Cell Environ* 36: 262–274.
- IPCC. 2014. Stocker TF et al. eds. *Climate Change 2013: The Physical Science Basis. Contribution of Working Group I to the Fifth Assessment Report of the Intergovernmental Panel on Climate Change*. Cambridge: Cambridge University Press.
- Kanechi M, Uchida N, Yasuda T, Yamaguchi T. 1996. Non-stomatal inhibition associated with inactivation of rubisco in dehydrated coffee leaves under unshaded and shaded conditions. *Plant Cell Physiol* 37: 455–460.
- Krau JP, Edwards GE. 1992. Relationship between photosystem II activity and CO₂ fixation in leaves. *Physiol Plant* 86: 180–187.
- Leuning R. 1995. A critical appraisal of a combined stomatal-photosynthesis model for C₃ plants. *Plant Cell Environ* 18: 339–355.
- Lewis AM, Boose ER. 1995. Estimating volume flow rates through xylem conduits. *Am J Bot* 82: 1112-1116.
- Limousin, JM, Longepierre D, Huc R, Rambal S. 2010a. Change in hydraulic traits of Mediterranean *Quercus ilex* subjected to long-term throughfall exclusion. *Tree Physiol* 30(8): 1026-1036.

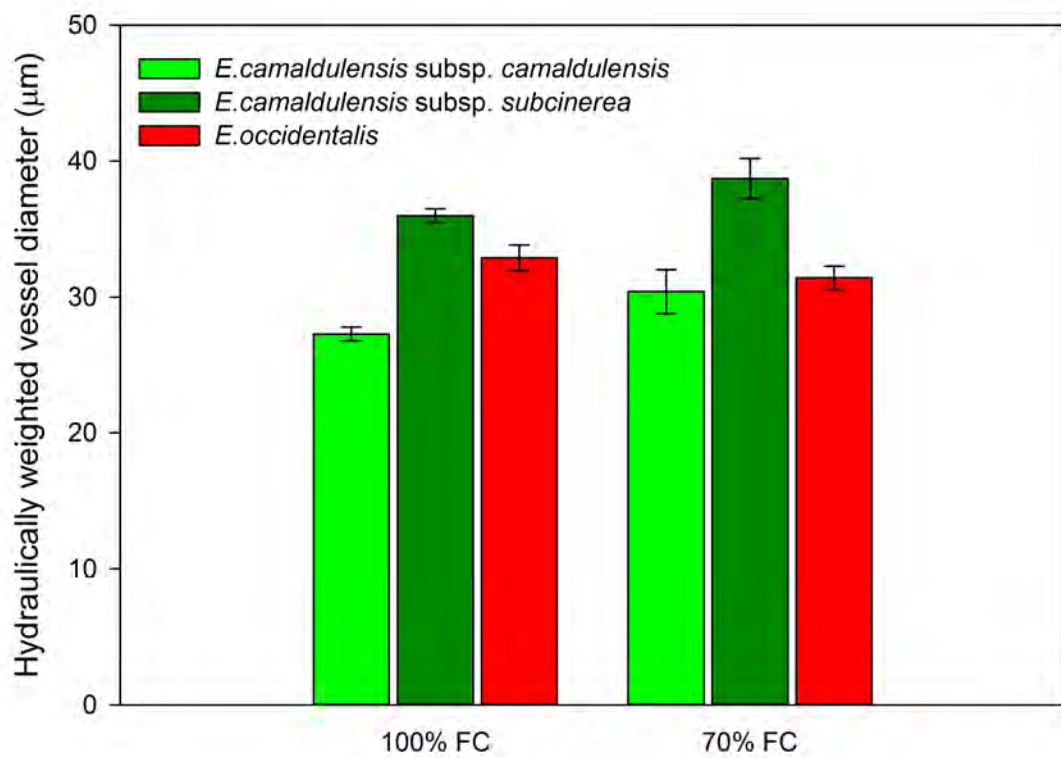
- Limousin, JM, Misson L, Lavoit AV, Martin, NK, Rambal S. 2010b. Do photosynthetic limitations of evergreen *Quercus ilex* leaves change with long-term increased drought severity?. *Plant Cell Environ* 33(5): 863-875.
- Mäkelä A, Berninger F, Hari P. 1996. Optimal control of gas exchange during drought: theoretical analysis. *Ann Bot* 77: 461–467.
- Martin-StPaul NK, Limousin JM, Vogt-Schilb H, Rodríguez-Calcerrada J, Rambal S, Longepierre D, Misson L. 2013. The temporal response to drought in a Mediterranean evergreen tree: comparing a regional precipitation gradient and a throughfall exclusion experiment. *Glob Chang Biol* 19(8): 2413-2426.
- Martin-StPaul NK, Limousin JM, Rodríguez-Calcerrada J, Ruffault J, Rambal S, Letts MG, Misson L. 2012. Photosynthetic sensitivity to drought varies among populations of *Quercus ilex* along a rainfall gradient. *Funct Plant Biol* 39(1): 25-37.
- Maseda PH, Fernández RJ. 2006. Stay wet or else: three ways in which plants can adjust hydraulically to their environment. *J Exp Bot* 57: 3963–3977.
- Medlyn BE, Duursma RA, Eamus D *et al.* 2011. Reconciling the optimal and empirical approaches to modelling stomatal conductance. *Glob Chang Biol* 17: 2134–2144.
- Misson L, Limousin JM, Rodriguez R, Letts MG. 2010. Leaf physiological responses to extreme droughts in Mediterranean *Quercus ilex* forest. *Plant Cell Environ* 33(11): 1898-1910.
- Misson L, Tu KP, Boniello RA, Goldstein AH. 2006. Seasonality of photosynthetic parameters in a multi-specific and vertically complex forest ecosystem in the Sierra Nevada of California. *Tree Physiol* 26: 729–741.
- Mitchell PJ, Veneklaas EJ, Lambers H, Burgess SS. 2008. Using multiple trait associations to define hydraulic functional types in plant communities of south-western Australia. *Oecologia* 158(3): 385-397.
- Niinemets ÜLO, Cescatti A, Rodeghiero M, Tosens T. 2005. Leaf internal diffusion conductance limits photosynthesis more strongly in older leaves of Mediterranean evergreen broad-leaved species. *Plant Cell Environ* 28: 1552–1566.
- Ogaya R, Peñuelas J. 2003. Comparative field study of *Quercus ilex* and *Phillyrea latifolia*: photosynthetic response to experimental drought conditions. *Environ Exp Bot* 50: 137–148.
- Panković, D., Sakač, Z., Kevrešan, S., Plesničar, M. 1999. Acclimation to long-term water deficit in the leaves of two sunflower hybrids: photosynthesis, electron transport and carbon metabolism. *J Exp Bot* 50 (330): 128-138.
- Parry MA, Andralojc PJ, Khan S, LEA PJ, Keys AJ. 2002. Rubisco activity: effects of drought stress. *Ann Bot* 89: 833–839.
- Prentice IC, Dong N, Gleason SM, Maire V, Wright IJ. 2014. Balancing the costs of carbon gain and water transport: testing a new theoretical framework for plant functional ecology. *Ecol Lett* 17: 82–91.

- R Development Core Team. 2010. R: A Language and Environment for Statistical Computing. R Foundation for Statistical Computing, Vienna, Austria, ISBN 3- 900051-07-0, <http://www.R-project.org>
- Sala A, Woodruff, DR, Meinzer FC. 2012. Carbon dynamics in trees: feast or famine?. *Tree Physiol* 32(6): 764-775.
- Schulze ED, Hall AE. 1982. Stomatal responses, water loss and CO₂ assimilation rates of plants in contrasting environments. In: Lange OL, Nobel PS, Osmond CB, Ziegler H, eds. *Physiological Plant Ecology II Water Relations and Carbon Assimilation*. Berlin: Springer-Verlag, 181–230.
- Tezara W. 2002. Effects of water deficit and its interaction with CO₂ supply on the biochemistry and physiology of photosynthesis in sunflower. *J Exp Bot* 53: 1781–1791.
- Tezara W, Lawlor DW. 1995. Effects of water stress on the biochemistry and physiology of photosynthesis in sunflower. *Photosynthesis: from Light to Biosphere* 4: 625-628.
- Tezara W, Mitchell VJ, Driscoll SD, Lawlor DW. 1999. Water stress inhibits plant photosynthesis by decreasing coupling factor and ATP. *Nature* 401: 914–917.
- Thimmanaik S, Kumar SG, Kumari GJ, Suryanarayana N, Sudhakar C. 2002. Photosynthesis and the enzymes of photosynthetic carbon reduction cycle in mulberry during water stress and recovery. *Photosynthetica* 40: 233–236.
- Tuzet A, Perrier A, Leuning R. 2003. A coupled model of stomatal conductance, photosynthesis and transpiration. *Plant Cell Environ* 26: 1097–1116.
- Wilson KB, Baldocchi DD, Hanson PJ. 2000. Quantifying stomatal and non-stomatal limitations to carbon assimilation resulting from leaf aging and drought in mature deciduous tree species. *Tree Physiol* 20: 787–797.
- Xu L, Baldocchi DD. 2003. Seasonal trends in photosynthetic parameters and stomatal conductance of blue oak (*Quercus douglasii*) under prolonged summer drought and high temperature. *Tree Physiol* 23: 865–877.
- Zhou S, Duursma RA, Medlyn BE, Kelly JW, Prentice IC. 2013. How should we model plant responses to drought? An analysis of stomatal and non-stomatal responses to water stress. *Agric For Meteorol* 182: 204-214.
- Zhou S, Medlyn BE, Santiago S, Sperlich D, Prentice IC. 2014. Short-term water stress impacts on stomatal, mesophyll, and biochemical limitations to photosynthesis differ consistently among tree species from contrasting climates. *Tree Physiol*. DOI: 10.1093/treephys/tpu072

4S1. Supplementary Information



Supplementary Figure S1. Rubisco activity V_{max} as a function of pre-dawn leaf water potential during a drying cycle following 4 months of treatment at 100% FC (solid squares for raw data; solid lines for fitted curves) or 70% FC (open squares for raw data; solid lines for fitted curves). Dark green: *E. camaldulensis* subsp. *camaldulensis*; Green: *E. camaldulensis* subsp. *subcinerea*; Red: *E. occidentalis*.



Supplementary Figure S2. Hydraulically weighted vessel diameter of three taxa at 100% and 70% FC treatments after 4 months. Values are means \pm SE ($n = 3$).

Chapter 5

Representing observed plant responses to drought in a land surface model

S. Zhou¹, Martin G. De Kauwe¹, B. E. Medlyn¹, A. J. Pitman², and I. C. Prentice^{1,3}

¹Department of Biological Sciences, Macquarie University, NSW 2109, Australia

²Australian Research Council Centre of Excellence for Climate Systems Science and
Climate Change Research Centre

³AXA Chair of Biosphere and Climate Impacts, Grand Challenges in Ecosystems and the Environment and Grantham Institute – Climate Change and the Environment, Department of Life Sciences, Imperial College London, Silwood Park Campus, Buckhurst Road, Ascot SL5 7PY, UK

This chapter is in preparation for submission to *Ecological Modelling*

5.1 Abstract

Land surface models (LSMs) commonly include generic responses of plant carbon uptake and water loss to soil moisture content. It seems plausible that the performance of LSMs might be improved by including empirically based plant responses to drought, expressed as soil water potential (the key property affecting plant water uptake) and derived from measurements on different plant functional types. The effects of including empirically based representations of responses of stomatal conductance (g_s) and carboxylation capacity (V_{cmax}) to soil water potential were tested in the Community Atmosphere Biosphere Land Exchange (CABLE) LSM, using flux measurements from deciduous and evergreen (needle-leaved and broad-leaved) forests in Europe during the heatwave year of 2003 as a benchmark. We found that the effects were small. However, we also found that the CABLE results diverged markedly from the observations at most sites, particularly during the heatwave period. At the northernmost site (Tharandt), soil moisture limitations were minor and the time course of net ecosystem exchange was well simulated. Elsewhere, modelled ecosystem CO_2 uptake was too large early in the season and then too small during summer. Peaks of modelled latent heat flux were universally too large when soil moisture was abundant, commonly leading to soil moisture depletion and (in the southern European sites) a gross underestimation of evapotranspiration during the heatwave period. These results suggest that structural problems with the model's simulation of evapotranspiration led to an unrealistic seasonal course of soil moisture, which overshadowed the specific responses of plants to drought.

Keywords: CABLE, drought, heatwave, land surface model, Rubisco capacity, stomatal conductance, soil heterogeneity, flux measurements.

5.2 Introduction

Changes in soil moisture availability induced by global climate change could cause widespread tree mortality and forest die-back in regions where drought duration and intensity increase (Allen et al., 2010; McDowell, 2011; IPCC, 2014). Mesic and xeric ecosystems appear to be about equally vulnerable to drought (Choat, et al., 2012), implying that plants from drier or wetter environments possess some degree of adaptation to the soil conditions encountered in their native habitat. Indeed, plants from dry climates are known to operate better down to lower water potential values than plants from wet climates. It is reasonable to assume that this feature of plants from dry climates is adaptive, important for their function under field conditions and shaping their potential geographic ranges (Engelbrecht et al., 2007).

Model predictions of future drought effects on ecosystems, and feedbacks to the atmosphere, should aim to represent drought responses of major plant physiological exchanges (CO_2 and water vapour fluxes between leaf and the atmosphere) realistically. To do so, they must account for the observed differences between the responses of different plant functional types (PFTs) to drought. Models differ in the ways in which they represent drought effects on photosynthesis (De Kauwe et al., 2013). Nonetheless, current state-of-the-art land surface models (LSMs – designed as components of climate models, representing energy, water and CO_2 exchanges between ecosystems and the atmosphere) generally treat PFTs as having similar (stomatal and/or non-stomatal) responses to drought. Experimentally based, plant-specific representations of the drought responses of stomatal conductance (g_s) and carboxylation capacity (V_{cmax}) have not been implemented in current LSMs. Powell et al. (2013) reported apparently unrealistic drought responses in five terrestrial biosphere models, using current water-stress functions to represent soil moisture effects on g_s . Zhou et al. (2013; 2014) reported systematic differences in the effect of decreasing soil water potential on both g_s and V_{cmax} , such that species from dry environments could maintain transpiration and photosynthesis down to lower soil water potentials than species from wetter environments.

Zhou et al. (2013; 2014) also fitted quantitative models for the g_s and V_{cmax} responses to soil water potential, thus providing functions that potentially could represent these responses in process-based models.

Here we use information pertinent to the representation of g_s and V_{cmax} responses in process-based models as provided by Zhou et al. (2013; 2014) to test whether a more realistic representation of plant drought responses would improve the prediction of canopy-atmosphere fluxes during drought in a LSM, the Community Atmosphere Biosphere Land Exchange (CABLE) model (Wang et al., 2011). We obtained CO₂ and latent heat flux measurements at six eddy covariance sites in different forest ecosystem types in Europe through the Protocol for the Analysis of Land Surface models (PALS, <http://pals.unsw.edu.au>; Abramowitz, 2012), and evaluated the results of CABLE with standard and modified parameters against measurements made during the record-breaking “heatwave year” 2003 in Europe. Severe heat and drought occurred during the summer of 2003 in many European regions, especially in central Europe and the Mediterranean region. These conditions caused widespread reductions in gross primary productivity and a strong net source of CO₂ to the atmosphere, reversing the effect of four years of net ecosystem carbon sequestration (Ciais et al., 2005; Fischer et al., 2007; Granier et al., 2007; Reichstein et al., 2007). Thus, we expected that the model would reproduce key features of ecosystems’ responses to the heatwave, and aimed to test whether the inclusion of experimentally based differential drought response functions of g_s and V_{cmax} among different PFTs as reported in Zhou et al. (2013; 2014) would improve the model results.

5.3 Methods

5.3.1 Model description

The CABLE LSM is a complex model of biosphere-atmosphere exchange, including submodels on canopy processes, soil and snow, and vegetation and soil carbon pool dynamics. A complete description of the CABLE LSM can be found in Kowalczyk et al. (2006) and Wang et al. (2011). CABLE represents the canopy with a “two-leaf” submodel that calculates photosynthesis, stomatal conductance and leaf temperature, distinguishing between sunlit and shaded leaves (Leuning et al., 1995; Wang and Leuning, 1998). Aerodynamic properties are a function of canopy height and leaf area index (Raupach, 1994; 1997). The Richards equation for soil moisture, and the heat conduction equation for soil temperature, are numerically integrated with a multilayer soil model, using six soil layers and up to three layers of snow that can accumulate on the soil surface (Kowalczyk et al., 2006). CABLE has been used extensively for both coupled (Cruz et al., 2010; Mao et al., 2011; Lorenz et al., 2014) and offline simulations (Abramowitz et al., 2008; Wang et al., 2011; Kala et al., 2014) at a range of spatial scales. CABLE is the LSM used in the Australian Community Climate Earth System Simulator (ACCESS, see <http://www.accessimulator.org.au>; Kowalczyk et al., 2013), a fully coupled Earth system model that participated in the Coupled Model Intercomparison Project (CMIP5), which provided simulations for the Fifth Assessment Report of the Intergovernmental Panel on Climate Change. In this study we used as our “standard version” CABLEv2.0.1. The source code can be accessed after registration at <https://trac.nci.org.au/trac/cable>.

5.3.2 Implementation of the “optimal” stomatal model

Normally CABLE implements an empirical g_s model following Leuning et al. (1995), with two parameters that vary according to photosynthetic pathway but otherwise are invariant for all PFTs. Following De Kauwe et al. (in review), we implemented the optimal stomatal conductance model introduced by Medlyn et al. (2011) in CABLE. The single parameter g_1 of this model represents plant water use strategy. High values of g_1 denote a “water spending”

strategy, low values represent a “water conserving” strategy:

$$g_s \approx g_0 + 1.6(1 + \frac{g_1 \beta}{\sqrt{D}}) \frac{A}{C_a} \quad (1)$$

where A is the gross carbon assimilation rate ($\mu\text{mol m}^{-2} \text{s}^{-1}$), g_s is the stomatal conductance ($\text{mol H}_2\text{O m}^{-2} \text{s}^{-1}$), g_1 is a fitted parameter ($\text{kPa}^{-0.5}$), C_a is the atmospheric CO_2 concentration at the leaf surface ($\mu\text{mol mol}^{-1}$), D (kPa) is the vapour pressure deficit at the leaf surface, and g_0 represents the residual leaf water vapour conductance when photosynthesis is zero ($\text{mol H}_2\text{O m}^{-2} \text{s}^{-1}$). β is an empirical soil moisture stress factor imposed for down-regulation of stomatal response at decreasing soil moisture, which is assumed to limit A under water stress through the coupled A – g_s model (Egea et al., 2011; Powell et al., 2013; De Kauwe et al., in review). β is implemented in the standard version of CABLE as a function of volumetric water content (θ):

$$\beta = \frac{\theta - \theta_w}{\theta_{fc} - \theta_w}; \beta \in [0, 1] \quad (2)$$

where θ_w is the volumetric water content at wilting point ($\text{m}^3 \text{m}^{-3}$) and θ_{fc} is the volumetric water content at field capacity ($\text{m}^3 \text{m}^{-3}$).

The Medlyn model is consistent with leaves maintaining a value of the $C_i:C_a$ ratio (the ratio of leaf-internal CO_2 concentration, C_i , to C_a), which is conservative with respect to variations in most drivers of A (light intensity, nutrient status and C_a) but declines with increasing D (see Prentice et al., 2014a for an alternative derivation of this model.). Conceptually, g_1 is inversely proportional to the marginal carbon cost of water (Medlyn et al., 2011) and has proved to be a useful measure of stomatal sensitivity across PFTs and climates (H  roult et al., 2013; Zhou et al., 2013; 2014). A soil moisture effect on g_1 is predicted by the theoretical analysis of M  kel   et al. (1996), suggesting that the marginal water cost of carbon gain should decline exponentially with decreasing soil moisture availability, and the decline rate should increase with the probability of rain (Zhou et al., 2013; 2014). Baseline values of g_1 for each

PFT in CABLE were assigned based on De Kauwe et al. (in review) which extracted these baseline values from a global database of stomatal conductance and photosynthesis compiled by Lin et al. (in review).

5.3.3 Implementation of analytical models for the drought responses of g_1 and V_{cmax}

We implemented a new formulation for drought stress on g_1 and V_{cmax} based on information provided by Zhou et al. (2013; 2014). We converted θ into soil water potential (Ψ_{soil}) (the key variable for plant water uptake), using a different equation for each soil type, following Duursma et al. (2008):

$$\Psi_{\text{soil}} = (sucs * 9.81 * 0.001) \left(\frac{\theta}{\theta_{\text{sat}}} \right)^{-bch} \quad (3)$$

where $sucs$ is the soil suction at saturation (m), ($sucs * 9.81 * 0.001$) calculates the soil water potential at saturation (MPa), θ_{sat} is soil volumetric water content at saturation ($\text{m}^3 \text{ m}^{-3}$) (assumed equal to the total pore fraction of the soil), and bch is an empirical coefficient related to the clay content of the soil (Cosby et al., 1984) which is estimated from a typical soil moisture release function (Campbell 1974). Parameter values used in CABLE for different soil types are given in Table 1, based on the summaries in Clapp and Hornberger (1978) and Cosby et al. (1984).

Table 1. Values of soil parameters used in CABLE.

Soil types	θ_{fc}	θ_{w}	θ_{sat}	$sucs$	bch
Coarse sand/Loamy sand	0.143	0.072	0.398	-0.106	4.2
Medium clay loam/silty clay loam/silt loam	0.301	0.216	0.479	-0.591	7.1
Fine clay	0.367	0.286	0.482	-0.405	11.4
Coarse-medium sandy loam/loam	0.218	0.135	0.443	-0.348	5.15
Coarse-fine sandy clay	0.31	0.219	0.426	-0.153	10.4
Medium-fine silty clay	0.37	0.283	0.482	-0.49	10.4
Coarse-medium-fine sandy clay loam	0.255	0.175	0.42	-0.299	7.12

Consistent with experimental findings (Zhou et al., 2013; 2014), we multiplied baseline values of the stomatal sensitivity parameter (g_1) and V_{cmax} by functions of Ψ_{soil} :

$$\beta_{g1} = \exp(b_1 \Psi_{\text{soil}}); \beta_{g1} \in [0, 1] \quad (4)$$

where b_1 is a parameter representing the sensitivity of g_1 to Ψ_{soil} (based on observations of g_1 and pre-dawn leaf water potential, Ψ_{pd}), and:

$$\beta_{V_{\text{cmax}}} = \frac{1 + \exp[S_f \Psi_f]}{1 + \exp[S_f (\Psi_f - \Psi_{\text{soil}})]}; \beta_{V_{\text{cmax}}} \in [0, 1] \quad (5)$$

where S_f is a sensitivity parameter indicating the steepness of the decline of V_{cmax} with increasing soil water deficit, and Ψ_f is a reference value, indicating the water potential at which V_{cmax} decreases approximately to half of its maximum value. We used the g_1 and V_{cmax} values under baseline (well-watered) conditions as in the standard version of CABLE (De Kauwe et al., in review), implementing only the new parameters describing the drought sensitivity of g_1 and V_{cmax} from Zhou et al. (2013; 2014) (b_1 , S_f , Ψ_f , Table 2). b_1 represents the sensitivity of g_1 to Ψ_{pd} , S_f is a sensitivity parameter indicating the steepness of the decline of V_{cmax} to Ψ_{pd} , and Ψ_f is a reference value indicating the water potential at which the V_{cmax} value under well-watered condition decreases to half of its maximum value. In the present study, there are three sets of sensitivity parameter values, as one for each of the three PFTs. The sensitivity values for evergreen broadleaf and deciduous broadleaf plants are refitted from the data of *Quercus ilex* L and *Quercus robur* L. in Zhou et al. (2014), respectively. The sensitivity values for evergreen needleleaf plants are from the values of *Cedrus atlantica* in Zhou et al. (2013). Relative to species from wetter habitats, species from drier habitats showed lower b_1 , S_f and more negative Ψ_f values (Zhou et al., 2013; 2014). Thus we assume that baseline parameter values of V_{cmax} and g_1 obtained from glasshouse-grown plants (Zhou et al., 2013; 2014) are likely to differ from those applying in the field, while the sensitivities of g_1 and V_{cmax} to water stress are assumed to be similar in both contexts. J_{max} is assumed as two times of V_{cmax} in this study.

Table 2. Baseline values of g_1 and V_{cmax} , and values of b_1 , S_f , and Ψ_f applied to three PFTs.

PFT	g_1	b_1	V_{cmax}	S_f	Ψ_f
Deciduous broadleaf	4.45	1.55	60.0	6.0	-0.53
Evergreen broadleaf	4.12	0.82	55.0	1.9	-1.85
Evergreen needleleaf	2.35	0.46	40.0	5.28	-2.31

5.3.4 Site data and model simulations

We ran two sets of baseline simulations. First, we ran CABLE using the Medlyn model of stomatal conductance and the standard equation for the water stress factor β (eqn 2); these runs are denoted CABLE-Standard (Table 3). We also performed model runs in which soil water content was held at field capacity throughout in order to show the effects of soil moisture; these runs are denoted CABLE-No Drought. We finally ran simulation with the new formulation for drought stress on g_1 and V_{cmax} . This set of runs was denoted CABLE-Zhou.

Table 3. A summary of model simulations.

Model Simulation	Description
CABLE-Standard	Control experiment, standard CABLE model with the Medlyn g_s model, with the g_1 parameter calibrated by PFT.
CABLE-No Drought	CABLE simulation without soil moisture stress.
CABLE-Zhou	CABLE simulation with modified parameters, accounting for β_{g1} and $\beta_{V_{\text{cmax}}}$.

Simulations were performed for six flux sites in different forest ecosystems in Europe through the period of the European heatwave in 2003 (Figure 1). We examined the seasonal time course of net ecosystem exchange (NEE; $\text{g C m}^{-2} \text{d}^{-1}$), gross primary production (GPP; $\text{g C m}^{-2} \text{d}^{-1}$), transpiration (E; mm d^{-1}) and latent heat flux (LE; W m^{-2}). Site weather and soil data, in addition to the NEE and LE measurements, were obtained through PALS (<http://pals.unsw.edu.au>; Abramowitz, 2012), a data source that has been pre-processed and quality-controlled specifically for benchmarking use by the LSM community. Two flux tower

sites each were included from deciduous broadleaf forest, evergreen broadleaf forest, and evergreen needleleaf forest (Table 4). All data analyses were performed using the Python language and all plots were generated in the ‘R’ environment (R Development Core Team 2010).

Table 4. The flux tower sites.

Site	CABLE PFT	Latitude	Longitude	Country	Years
Hesse	Deciduous broadleaf	48°40' N	7°05' E	France	1997-2006
Roccarespampani	Deciduous broadleaf	42°24' N	11°55' E	Italy	2000-2006
Castelporziano	Evergreen broadleaf	41°42' N	12°22' E	Italy	1997-2006
Espirra	Evergreen broadleaf	38°38' N	8°36' W	Portugal	2002-2006
El Saler	Evergreen needleleaf	39°20' N	0°19' W	Spain	1996-2006
Tharandt	Evergreen needleleaf	50°58' N	13°34' E	Germany	1996-2006

5.4 Results

5.4.1 CABLE-Standard and CABLE-No Drought *versus* observations

Figures 2-4 show site-scale comparisons between observed and modelled NEE and LE, with modelled GPP and E, for all cases (CABLE-Standard and CABLE-No Drought, CABLE-Zhou) between April and October 2003. The period between June 1st and August 31st 2003, when the most pronounced high temperature anomalies were reported (Fischer et al., 2007; Figure 1), is indicated by grey shading.

At the northernmost site (Tharandt), all model versions showed a good simulation of both the seasonal cycle and the day-to-day variability of NEE. The impact of soil moisture on GPP and NEE in the model was slight, but the inclusion of soil moisture effects improved the realism of simulated LE. However, a problem was noted in the simulation of LE: the height of the peaks of LE were over-estimated by about a factor of two.

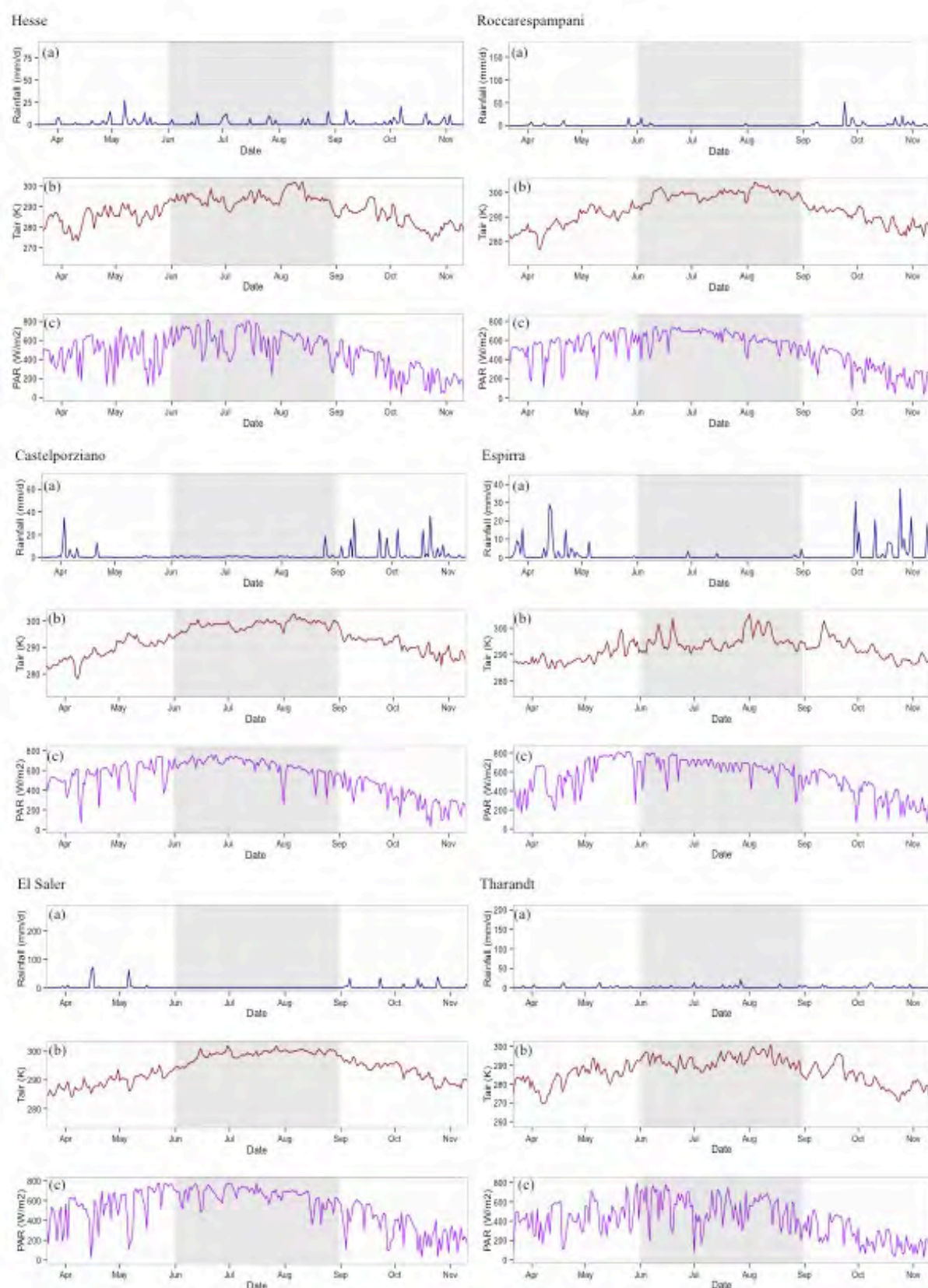


Figure 1. Meteorological data of six sites during the growing season of 2003: (a) day sum of rainfall (Rainf); (b) day mean of air temperature (Tair); (3) day mean of photosynthetically active radiation (PAR, calculated as a product of 2.3 and downward shortwave).

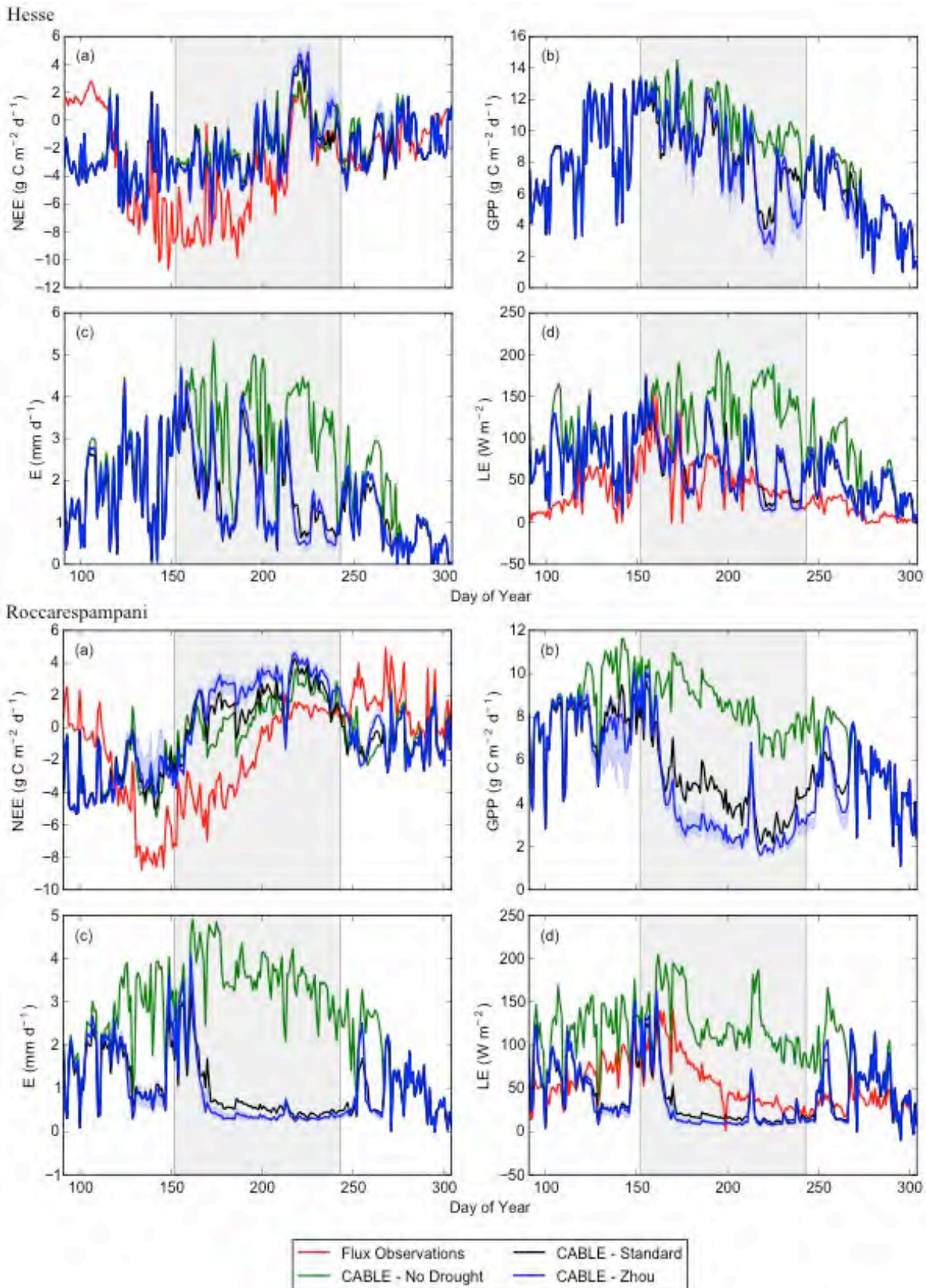


Figure 2. CABLE simulations of (a) net ecosystem exchange (NEE; $\text{g C m}^{-2} \text{d}^{-1}$), (b) gross primary production (GPP; $\text{g C m}^{-2} \text{d}^{-1}$), (c) transpiration (E ; mm d^{-1}) and (d) latent heat flux (LE ; W m^{-2}) at two flux sites (Hesse and Roccarespampani) from deciduous broadleaf forest in 2003, compared to observations of NEE and LE . Blue ribbons: simulations with modified parameters whose values were increased and decreased by 30% of their reference value. The grey bar marks the heatwave period between June 1st and August 31st 2003.

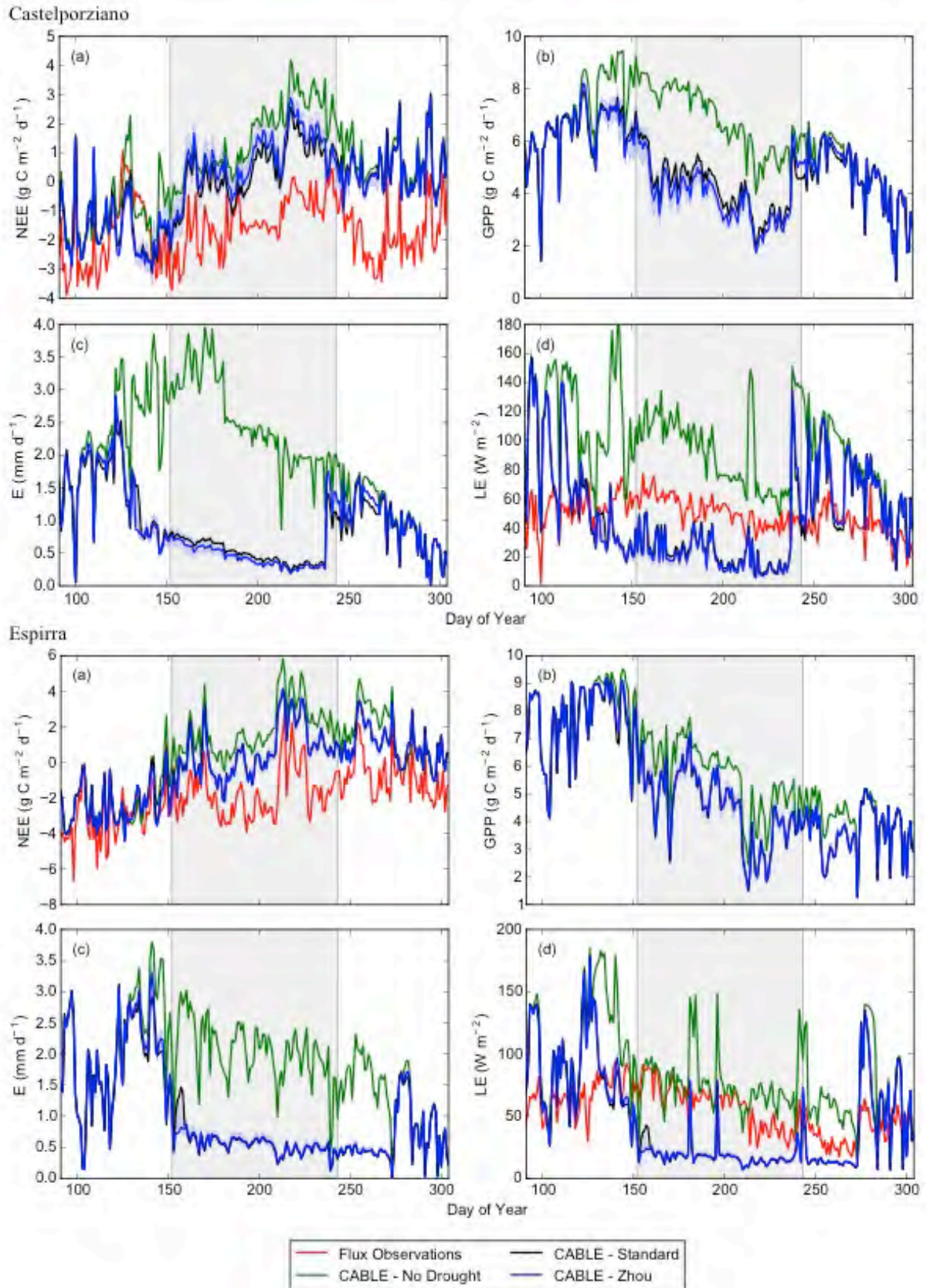


Figure 3. CABLE simulations of (a) net ecosystem exchange (NEE; $\text{g C m}^{-2} \text{d}^{-1}$), (b) gross primary production (GPP; $\text{g C m}^{-2} \text{d}^{-1}$), (c) transpiration (E ; mm d^{-1}) and (d) latent heat flux (LE ; W m^{-2}) at two flux sites (Castelporziano and Espirra) from evergreen broadleaf forest in 2003, compared to observations of NEE and LE . Blue ribbons: simulations with modified parameters whose values were increased and decreased by 30% of their reference value. The grey bar marks the heatwave period between June 1st and August 31st 2003.

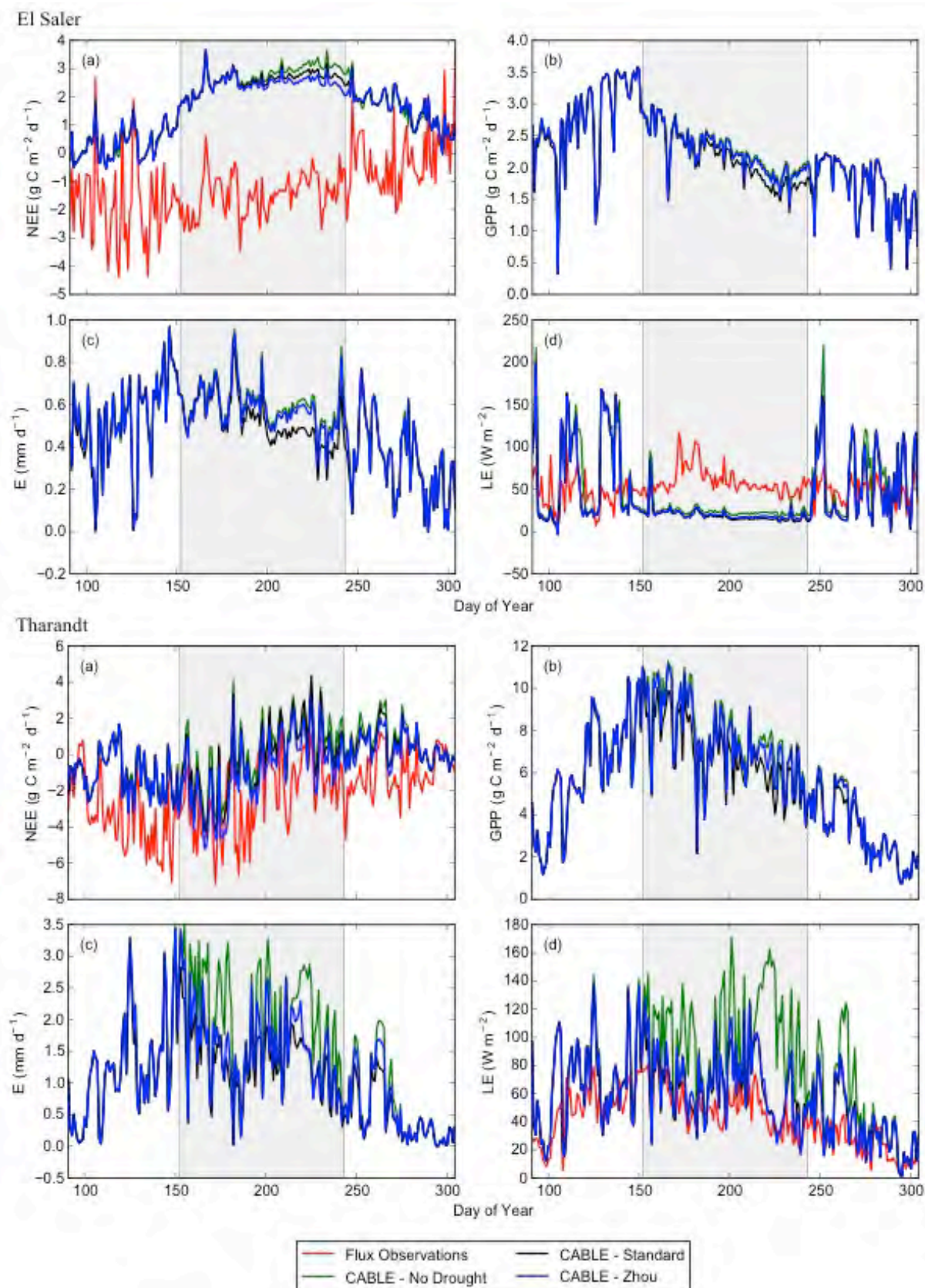


Figure 4. CABLE simulations of (a) net ecosystem exchange (NEE; $\text{g C m}^{-2} \text{ d}^{-1}$), (b) gross primary production (GPP; $\text{g C m}^{-2} \text{ d}^{-1}$), (c) transpiration (E ; mm d^{-1}) and (d) latent heat flux (LE ; W m^{-2}) at two flux sites (El Saler and Tharandt) from evergreen needleleaf forest in 2003, compared to observations of NEE and LE . Blue ribbons: simulations with modified parameters whose values were increased and decreased by 30% of their reference value. The grey bar marks the heatwave period between June 1st and August 31st 2003.

Simulations of NEE at the sites in central and southern Europe suffered from a consistent mismatch with data (albeit more severe at some sites than others). Specifically, the model tended to overestimate ecosystem CO₂ uptake (NEE too negative) during the early part of the growing season, and to underestimate it during summer. At all sites, as at Tharandt, the modelled peaks in LE during times of abundant soil moisture in northern-hemisphere spring and autumn were much too high. At all of the sites further south, over-estimation of LE during the spring was followed by the development of strong soil moisture deficits (as shown by the large difference between the CABLE-Standard and CABLE-No Drought simulations) and a collapse of modelled transpiration and LE to unrealistically low values during the heatwave period. At Hesse, the seasonal cycle LE was reasonably well simulated despite overestimation of the amplitude of the peaks, and the inclusion of soil moisture effects (in CABLE-No Drought) caused a clear improvement. The problem was much more severe at the sites in southern Europe, all of which showed a near-shutdown of plant function (GPP and E), a substantial underestimation of LE, and a substantial underestimation of ecosystem CO₂ uptake during the heatwave.

5.4.2 Standard *versus* modified parameters

The effects of including realistic parameterizations of soil moisture effects in CABLE-Zhou compared to CABLE-Standard as described above (Figures 2-4), were surprisingly small. These effects were most noticeable for the two sites with deciduous broadleaf vegetation (Hesse and Roccarespani), but it was not possible to discern an improvement in model performance as these small effects were overshadowed by the major simulation errors described above.

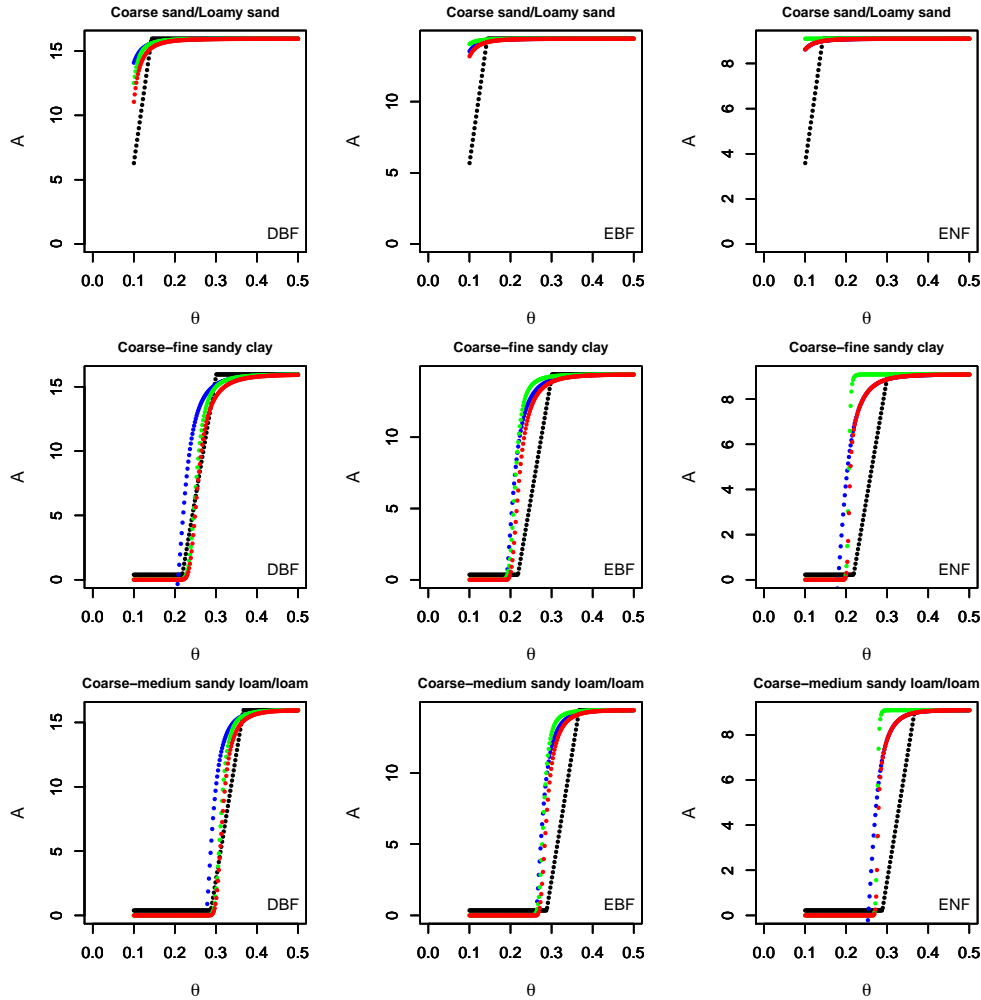
5.4.3 Parameter sensitivity analysis

Figures 2-4 also show the result of two further model simulations in which the individual

sensitivity parameter values (b_1 , S_f , Ψ_f , Table 2) were increased or decreased by 30 % of their reference value, respectively (CABLE-Zhou + 30 %; CABLE-Zhou – 30 %). This analysis showed that the model is relatively insensitive to changes in the drought sensitivity of g_1 and V_{cmax} .

5.4.4 Comparison among soil moisture stress factors

To investigate the mechanisms underlying the poor simulation of soil moisture stress effects and the model's insensitivity to changed parameter values, we compared the θ effect on A in relation to β , β_{g1} , $\beta_{V_{\text{cmax}}}$, or both β_{g1} and $\beta_{V_{\text{cmax}}}$, for three PFTs and seven soil types (Figure 5). A notable feature of all the functions is a rather abrupt transition from near-normal function to nearly complete shutdown, occurring within a narrow range of θ .



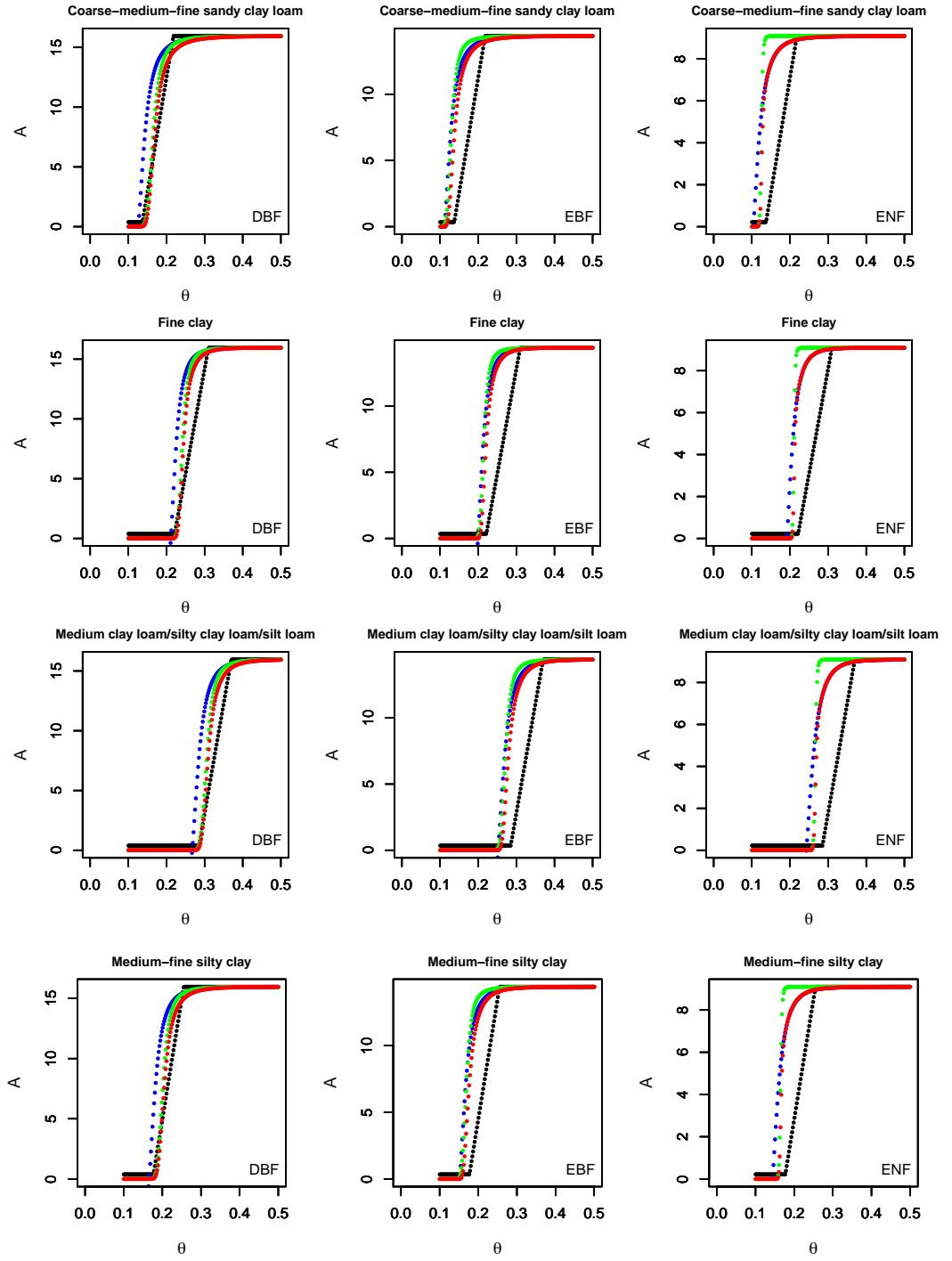


Figure 5. Assimilation rate (A) as a function of volumetric soil moisture content (θ) caused by the reduction of β (Black), β_{g1} (Blue), β_{vmax} (Green), or both β_{g1} and β_{vmax} (Red) during drought, respectively for three PFTs: deciduous broadleaf forest (DBF), evergreen broadleaf forest (EBF), evergreen needleleaf forest (ENF); and seven soil types.

5.5 Discussion

Most other LSMs use similar β formulations to CABLE, allowing an abrupt transition in β to take place within a narrow range of θ (Egea et al., 2011; Powell et al., 2013). Powell et al. (2013) found that four models (Community Land Model version 3.5 (CLM3.5), Integrated Biosphere Simulator version 2.6.4 (IBIS), Joint UK Land Environment Simulator version 2.1 (JULES), and Simple Biosphere model version 3 (SiB3)) implement abrupt transitions of this kind. The alternative response curves illustrated in Figure 5 were derived by combining two presumably reliable sources of information: empirical soil water retention curves, and experimental determinations of plant responses of g_1 and V_{cmax} to soil water potential. The β -function native to CABLE falls quite close to these functions, suggesting that it is not unrealistic.

One possible inference from our results, therefore, might be that the drought responses of plants have little significance for CO_2 and water fluxes. If the fluxes were well simulated in general by CABLE, in all of the alternative versions tested, this might be a natural conclusion. There are at least two problems with this idea, however. One is that if real-world fluxes bore little relation to plant drought responses, this would imply that such responses have minimal adaptive significance. We consider this unlikely. Another is that the simulated fluxes show substantial discrepancies from the observations at most of the sites considered, including excessive modelled evapotranspiration during periods of abundant soil moisture leading (in some cases, notably the southern European sites) to a major underestimate of the soil moisture available to plants during the summer. This problem in the seasonal cycle of soil moisture is presumed also to underlie the relatively poor simulation of the time course of NEE at all but the northernmost site. These discrepancies suggest an underlying problem with the structure of the model, whose effects are so large as to overshadow any effects due to the detailed representation of soil moisture effects on plants.

As one potential contributory explanation, we hypothesize that under field conditions the transition from full vegetation function to drought conditions occurs more gradually than modelled as a consequence of spatial heterogeneity in plant and soil properties (Liang et al., 1994; Prentice et al., 2014b). Soil water storage capacities in CABLE as in most other LSMs are represented by a single value for a grid box, so that any modelled soil subject to drying undergoes an abrupt transition between fully functional and “shut-down” vegetation states. The problem might be alleviated by allowing a statistical distribution of states. This possibility remains to be tested using model experiments considering a range of β functions.

It has been suggested that insufficient attention has been paid to the evaluation of LSMs (Prentice et al., 2014b), in part because their early history of development pre-dates the availability of many relevant measurement data sets. The availability of flux measurements via the FLUXNET “free and fair use” licence offers excellent opportunities for the improvement of LSMs, which deserve to be more widely exploited. We have used flux measurements to identify a particular problem with one LSM, the overestimation of evapotranspiration during periods with abundant soil moisture – leading in some cases to a depletion of soil water and an exaggerated reduction in evapotranspiration during a hot, dry summer. Mueller and Seneviratne (2014) noted that current state-of-the-art climate models (with embedded LSMs) quite generally overestimate evapotranspiration, and specifically that this results in a pattern in northern latitudes whereby the soil moisture store is depleted too rapidly and the bias shifts to underestimation of evapotranspiration during the summer months. Thus, the discrepancies we observed could be a more general feature of current LSMs.

Acknowledgements

This work used eddy covariance data acquired by the FLUXNET community for the La Thuile FLUXNET release, supported by the following networks: AmeriFlux (U.S. Department of Energy, Biological and Environmental Research, Terrestrial Carbon Program

(DE-FG02-04ER63917 and DE-FG02-04ER63911)), AfriFlux, AsiaFlux, CarboAfrica, CarboEuropeIP, CarboItaly, CarboMont, ChinaFlux, Fluxnet-Canada (supported by CFCAS, NSERC, BIOCAP, Environment Canada, and NRCan), GreenGrass, KoFlux, LBA, NECC, OzFlux, TCOS-Siberia, USCCC. We acknowledge the financial support to the eddy covariance data harmonization provided by CarboEuropeIP, FAO-GTOS-TCO, iLEAPS, Max Planck Institute for Biogeochemistry, National Science Foundation, University of Tuscia, Université Laval and Environment Canada and US Department of Energy and the database development and technical support from Berkeley Water Center, Lawrence Berkeley National Laboratory, Microsoft Research eScience, Oak Ridge National Laboratory, University of California - Berkeley, University of Virginia. We thank CSIRO and the Bureau of Meteorology through the Centre for Australian Weather and Climate Research for their support in the use of the CABLE model. S.Z. was supported by an international Macquarie University Research Excellence Scholarship. This paper is a contribution to the AXA Chair Programme in Biosphere and Climate Impacts and the Imperial College initiative on Grand Challenges in Ecosystems and the Environment.

5.6 References

- Abramowitz, G., Leuning, R., Clark, M., Pitman, A., 2008. Evaluating the Performance of Land Surface Models. *J. Clim.* 21, 5468–5481.
- Allen C.D., Macalady, A.K., Chenchouni, H., et al. 2010. A global overview of drought and heat-induced tree mortality reveals emerging climate change risks for forests. *For. Ecol. Manage.* 259(4): 660–684.
- Campbell, G.S., 1974. A simple method for determining unsaturated conductivity from moisture retention data. *Soil Sci.* 117:311–314.
- Choat B., Jansen S., Brodribb T.J., et al. 2012. Global convergence in the vulnerability of forests to drought. *Nature* 491(7426): 752-755.
- Ciais P., Reichstein M., Viovy N., et al. 2005 Europe-wide reduction in primary productivity caused by the heat and drought in 2003. *Nature* 437, 529-533.
- Clapp, R.B. and G.M. Hornberger, 1978. Empirical equations for some soil hydraulic properties. *Water Resour. Res.* 14:601–604.

- Cosby, B.J., G.M. Hornberger, R.B. Clapp and T.R. Ginn, 1984. A statistical exploration of the relationships of soil-moisture characteristics to the physical properties of soils. *Water Resour. Res.* 20:682–690.
- Cruz, F.T., Pitman, A.J., Wang, Y.-P., 2010. Can the stomatal response to higher atmospheric carbon dioxide explain the unusual temperatures during the 2002 Murray-Darling Basin drought? *J. Geophys. Res. Atmospheres* (1984–2012), 115(D2).
- De Kauwe, M.G., Kala J., Lin Y.-S., Pitman A.J., Medlyn, B.E., Duursma R.A., Abramowitz G., Wang Y.-P. and Miralles D.G.. 2014. A test of an optimal stomatal conductance scheme within the CABLE Land Surface Model. In review.
- De Kauwe, M.G., Medlyn, B.E., Zaehle, S., et al. 2013. Forest water use and water use efficiency at elevated CO₂: a model-data intercomparison at two contrasting temperate forest FACE sites. *Glob. Change Biol.* 19, 1759–1779.
- Duursma, R. A., Kolari, P., Perämäki, M., Nikinmaa, E., Hari, P., Delzon, S., Loustau D., Ilvesniemi H., Pumpanen J., Mäkelä, A., 2008. Predicting the decline in daily maximum transpiration rate of two pine stands during drought based on constant minimum leaf water potential and plant hydraulic conductance. *Tree physiol.*, 28(2), 265-276.
- Egea, G., Verhoef, A., Vidale, P.L., 2011. Towards an improved and more flexible representation of water stress in coupled photosynthesis–stomatal conductance models. *Agric. For. Meteorol.* 151, 1370–1384.
- Engelbrecht, B. M., Comita, L. S., Condit, R., Kursar, T. A., Tyree, M. T., Turner, B. L., Hubbell, S. P., 2007. Drought sensitivity shapes species distribution patterns in tropical forests. *Nature*, 447(7140), 80-82.
- Fischer, E. M., Seneviratne, S. I., Lüthi, D., Schär, C., 2007. Contribution of land-atmosphere coupling to recent European summer heat waves. *Geophys. Res. Lett.*, 34(6).
- Granier, A., Reichstein, M., Bréda, N., et al. 2007. Evidence for soil water control on carbon and water dynamics in European forests during the extremely dry year: 2003. *Agric. For. Meteorol.*, 143(1), 123-145.
- Hérault A., Lin Y.-S., Bourne A., Medlyn B.E., Ellsworth D.S., 2013. Optimal stomatal conductance in relation to photosynthesis in climatically contrasting Eucalyptus species under drought. *Plant Cell Environ.* 36: 262–274.
- IPCC. 2014. Stocker TF et al. eds. *Climate Change 2013: The Physical Science Basis. Contribution of Working Group I to the Fifth Assessment Report of the Intergovernmental Panel on Climate Change*. Cambridge: Cambridge University Press.
- Kala, J., Decker, M., Exbrayat, J.-F., Pitman, A.J., Carouge, C., Evans, J.P., Abramowitz, G., Mocko, D., 2014. Influence of Leaf Area Index Prescriptions on Simulations of Heat, Moisture, and Carbon Fluxes. *J. Hydrometeorol.* 15, 489–503.
- Kowalczyk, E.A., Wang, Y.P., Wang, P., Law, R.H., Davies, H.L., 2006. The CSIRO Atmosphere Biosphere Land Exchange (CABLE) model for use in climate models and as an offline model (No. CSIRO Marine and Atmospheric Research paper 013). CSIRO.

Kowalczyk, E. A., Stevens, L., Law, R. M., Dix, M. D., Wang, Y-P., Harman, I. N., Haynes, K., Srbinovsky, J., Pak, B. and Ziehn, T., 2013. The land surface model component of ACCESS: description and impact on the simulated surface climatology. *Australian Meteorological and Oceanographic Journal*, 63, 65-82.

Leuning, R., 1995. A critical appraisal of a combined stomatal-photosynthesis model for C₃ plants. *Plant Cell Environ.* 18, 339–355.

Liang, X., Lettenmaier, D. P., Wood, E. F., and Burges, S. J., 1994. A simple hydrologically based model of land surface water and energy fluxes for general circulation models, *J. Geophys. Res.*, 99, 14415–14428,.

Lin, Y.-S., Medlyn, B. E., Duursma, R. A., Prentice, I. C., Wang, H., Baig, S., Eamus, D., Resco de Dios, V. Mitchell, P., Ellsworth, D. S., Op de Beeck, M., Wallin, G., Uddling, J., Tarvainen, L., Linderson, M-J., Cernusak, L. A., Nippert, J. B., Ocheltree, T. W., Tissue, D. T., Martin-StPaul, N. K., Rogers, A., Warren, J. M., De Angelis, P., Hikosaka, K., Han, Q., Onoda, Y., Gimeno, T. E., Barton, C. V. M., Bennie, J., Bonal, D., Bosc, A., Löw, M., Macinins-Ng, C., Rey, A., Rowland, L., Setterfield, S. A., Tausz-Posch, S., Zaragoza-Castells, J., Broadmeadow, M. S. J., Drake, J. E., Freeman, M., Ghannoum, O., Hutley, L. B., Kelly, J. W., Kikuzawa, K., Kolari, P., Koyama, K., Limousin, J-M., Meir, P., Lola da Costa, A. C., Mikkelsen, T. N., Norma Salinas, Sun, W., 2014. Optimal stomatal behaviour around the world: synthesis of a global stomatal conductance database. In review.

Lorenz, R., Pitman, A., Donat, M., Hirsch, A., Kala, J., Kowalczyk, E., Law, R., Srbinovsky, J., 2014. Representation of climate extreme indices in the ACCESS1. 3b coupled atmosphere-land surface model. *Geosci. Model Dev.* 7, 545–567.

Mäkelä A., Berninger F., Hari P., 1996. Optimal control of gas exchange during drought : theoretical analysis. *Ann. Bot.* 77:461–467.

Mao, J., Pitman, A.J., Phipps, S.J., Abramowitz, G., Wang, Y., 2011. Global and regional coupled climate sensitivity to the parameterization of rainfall interception. *Clim. Dyn.* 37, 171–186.

McDowell, N. G., Beerling, D. J., Breshears, D. D., Fisher, R. A., Raffa, K. F., & Stitt, M., 2011. The interdependence of mechanisms underlying climate-driven vegetation mortality. *Trends in Ecology & Evolution*, 26(10), 523-532.

Medlyn, B.E., Duursma, R.A., Eamus, D. et al. 2011. Reconciling the optimal and empirical approaches to modelling stomatal conductance. *Glob. Chang. Biol.* 17: 2134–2144.

Mueller, B., & Seneviratne, S. I. (2014). Systematic land climate and evapotranspiration biases in CMIP5 simulations. *Geophys. Res. Lett.*, 41(1), 128-134.

Powell, T. L., Galbraith, D. R., Christoffersen, B. O., Harper, A., Imbuzeiro, H., Rowland, L., Samuel Almeida S., Brando P. M., da Costa, A. C. L., Costa M. H., N. M. Levine, Y. Malhi, S. R. Saleska, E. Sotta, M. Williams, P. Meir, and Moorcroft, P. R., 2013. Confronting model predictions of carbon fluxes with measurements of Amazon forests subjected to experimental drought. *New Phytol.*, 200(2), 350-365.

- Prentice I.C., Dong N., Gleason S.M., Maire V., Wright I.J., 2014a. Balancing the costs of carbon gain and water transport: testing a new theoretical framework for plant functional ecology. *Ecol Lett* 17: 82–91.
- Prentice, I. C., Liang, X., Medlyn, B. E., Wang, Y. P., 2014b. Reliable, robust and realistic: the three R's of next-generation land surface modelling. *Atmospheric Chemistry and Physics Discussions*, 14(17), 24811-24861.
- R Development Core Team. 2010. R: A Language and Environment for Statistical Computing. R Foundation for Statistical Computing, Vienna, Austria, ISBN 3- 900051-07-0, <http://www.R-project.org>
- Raupach, M., 1994. Simplified expressions for vegetation roughness length and zero-plane displacement as functions of canopy height and area index. *Bound.-Layer Meteorol.* 71, 211–216.
- Raupach, M., Finkelde, K., Zhang, L., 1997. SCAM (Soil-Canopy-Atmosphere Model): Description and comparison with field data. Aspendale Aust. Csiro Cem Tech. Rep. 81.
- Reichstein M., Tenhunen J.D., Roupsard O., Ourcival J.M., Rambal S., Dore S., Valentini R., 2002. Ecosystem respiration in two Mediterranean evergreen holm oak forests: Drought effects and decomposition dynamics. *Funct. Ecol.* 16, 27-39.
- Reichstein M., Ciais P., Papale D., et al. 2007. Reduction of ecosystem productivity and respiration during the European summer 2003 climate anomaly: A joint flux tower, remote sensing and modelling analysis. *Glob. Change Biol.* 13, 634-651.
- Wang, Y.P., Leuning, R., 1998. A two-leaf model for canopy conductance, photosynthesis and partitioning of available energy I: Model description and comparison with a multi-layered model. *Agric. For. Meteorol.* 91, 89–111.
- Wang, Y.P., Kowalczyk, E., Leuning, R., Abramowitz, G., Raupach, M.R., Pak, B., van Gorsel, E., Luhar, A., 2011. Diagnosing errors in a land surface model (CABLE) in the time and frequency domains. *J. Geophys. Res. Biogeosciences* 2005–2012 116.
- Zhou S., Duursma R.A., Medlyn B.E., Kelly J.W., Prentice I.C., 2013. How should we model plant responses to drought? An analysis of stomatal and non-stomatal responses to water stress. *Agric For Meteorol* 182: 204-214.
- Zhou S., Medlyn B.E., Santiago S., Sperlich D., Prentice I.C., 2014. Short-term water stress impacts on stomatal, mesophyll, and biochemical limitations to photosynthesis differ consistently among tree species from contrasting climates. *Tree Physiol.* DOI: 10.1093/treephys/tpu072

Chapter 6

Conclusion

The research described in this thesis was designed to cast light on the general responses of photosynthesis to short- and long-term soil water deficits, allowing for possible differences among plant functional types (PFTs) and between species from wetter or drier environments. The data synthesis and new experimental work were carried out in a quantitative modelling context, with a view to translating empirical findings into improved process representations for land surface modelling, and testing model results against carbon and water flux measurements at the ecosystem scale.

By analysing a body of published experimental data in this model-oriented framework, I identified systematic response patterns related to species' climatic origin and PFT membership. Both stomatal and non-stomatal responses were shown to be involved. Plants from drier climates were shown to function effectively (maintaining stomata relatively open, and near to full biochemical function) down to lower soil water potentials than plants from wetter climates. These differences are presumed to have adaptive significance for the survival of plants in dry climates (Chapter 2).

By imposing short-term water stress on species originating at different points along a hydro-climatic gradient, I found concurrent limitations on g_1 (the single parameter of the Medlyn et al. optimal model for stomatal behaviour), g_m (mesophyll conductance), V_{cmax} (the maximum rate of carboxylation by Rubisco) and J_{max} (the maximum rate of electron transport) as drought intensified. The drought sensitivities of all four quantities are consistently higher for

species from wetter climates than species from drier climates. The positive correlations among the rates of decline of these parameters as the experimental drought progressed define a spectrum of drought adaptations, from more resistant species thriving in dry environments, to more sensitive species from moist environments. The latter show reduced gas exchange and strong metabolic limitations earlier during the drying-down process (Chapter 3).

By imposing longer-term water stress on *Eucalyptus* species from riparian and xeric habitats, I also found more effective drought *acclimation* in xeric species: after a longer-term drought, the dryland species showed significantly lower V_{cmax} sensitivity than before the drought (Chapter 4).

Finally, the experimentally based and PFT-specific g_1 and V_{cmax} response functions to soil water potential were implemented within the CABLE LSM and the model was run – in its baseline form, in a form with soil moisture stress removed, and with soil moisture represented using the new experimental functions – at six flux measurement sites across Europe, in three vegetation types, during the year 2003 which was characterized by a long summer heatwave and accompanying drought. Surprisingly, the results from the baseline model were only slightly modified by the inclusion of the experimental functions. However, the simulations were somewhat unrealistic for all but the northernmost (50°N) site due to a general tendency to over-estimate evapotranspiration when soils are wet, resulting in excessive drying and near shutdown of vegetation function during the heatwave period. This general problem overshadowed the differences between different representations of soil moisture response, showing that additional work is needed to improve the model and allow realistic representation of ecosystem responses to drought (Chapter 5).

The model-oriented analysis, glasshouse experiments, and modelling described in this thesis amount to a new synthesis of information on the responses of different plant functions to drought. The data-analysis and experimental chapters provide a general methodology for

systematic study of the relationship between plant processes and drought, allowing the derivation of functions that can be used directly in modelling.

One novel aspect of this thesis is the identification of different drought tolerances – both in respect of short-term drought responses (Chapter 3), and acclimation processes by which plants can adapt to longer-term, lower-level drought (Chapter 4) – between species from mesic and xeric habitats. The inherent differences among the three *Eucalyptus* taxa from contrasting climatic origins were shown not only in their contrasting degree of tolerance to short-term drought, but also in their contrasting abilities to compensate for long-term drought. These findings support, and provide a complementary perspective on, the finding by Choat et al. (2012) based on hydraulic traits that trees in mesic habitats – which are not normally considered to be at risk from drought – are actually just as vulnerable to drought as trees in xeric habitats.

Time scale may be of the essence when determining the extent to which climate change is likely to adversely affect forests. Drought acclimation is evidently a real phenomenon in trees adapted to dry climates, and presumably allows such trees to cope with periodic, protracted (but not too severe) droughts. Drought-induced mortality of trees, and carbon loss from forests, could be overestimated if such acclimation is not taken into account. Model projections of drought effects on species distributions and vegetation composition in climate change scenarios should consider the differences in both short-term drought sensitivity and longer-term acclimation potential among species adapted to different climates.

Intra- and inter-species variation in drought tolerance and acclimation also have implications for forest management in water-limited ecosystems, particularly in a long-term perspective that takes future climate change into account. Changes in forest composition related to drought tolerance are already beginning to be observed: for example, the more drought-tolerant *Quercus pubescens* was reported to be replacing *Pinus sylvestris* at low altitudes in

Switzerland, where climate change has brought about recurrent water deficits (Eilmann et al. 2006).

A second novel aspect of this thesis is that chapters 2 and 3 demonstrate a practical and effective approach to gaining information on drought responses in a form directly applicable to modelling. These studies provided evidence for the co-ordinated variation of stomatal regulation, mesophyll conductance, and photosynthetic capacity (Rubisco and electron transport) in response to soil water deficits, and used non-linear statistical fitting methods to quantify these variations in a ‘model-friendly’ form. Such quantitative information, gathered on a wider range of species, could allow testing for the existence of a spectrum of drought-response traits, and ultimately a deeper understanding of drought-response strategies (Wright et al., 2004; Prentice et al., 2014a; Reich et al., 2014) and a more comprehensive approach to both trait data analysis and vegetation modelling (Prentice et al., 2014a).

An explicit theoretical framework is needed to incorporate the variation, interrelationships and environmental dependencies of plant traits into models. Current large-scale vegetation models treat plant ecophysiological properties simplistically (Prentice & Cowling 2013), disregarding known aspects of trait correlation and trait-environment relationships (Wright et al. 2004; Maire et al. 2012). Covariation of different plant traits is expected to be an expression of optimality principles (Wright et al., 2004; Prentice et al., 2014a; Reich et al., 2014) and should simplify the parameterizations of fundamental eco-physiological responses to environmental drivers, including drought. By providing process-based analytical models for both g_s and V_{cmax} responses to drought, values of key parameters that define these responses for contrasting species, and experimental evidence for important differences in drought sensitivity between xeric and mesic species, this study offers potentially robust solutions to the problem of representing adaptive differences among PFTs into land surface models.

Many research efforts have been devoted to improving models through the use of new representations of specific processes based on new data syntheses or experimental findings (e.g. Medlyn et al., 2011; Bonan et al., 2011; 2012; Prentice et al., 2014a). The realistic representation of g_s and V_{cmax} responses to drought in models will be fundamental to the prediction of drought-induced mortality at plant scale (due to hydraulic failure, carbon starvation, and/or other mechanisms), or carbon loss at the ecosystem scale. Thus, a third novel aspect of this thesis is the incorporation of experimentally based, PFT-specific stomatal and non-stomatal drought responses functions in the CABLE land surface model (Chapter 5). The observed large and co-ordinated variations in the drought sensitivity of g_1 and V_{cmax} were modelled as continuous parameter variation within the CABLE PFTs. However, it emerged that the inclusion of experimentally based g_s and V_{cmax} response functions did not substantially improve the simulation of drought impacts on fluxes at most of the sites considered. The key problem encountered was a persistent positive bias in the model's simulation of evapotranspiration during periods with high soil moisture, which led to excessive summer drying, whose adverse effects on data-model agreement overshadowed the differences between model versions with different drought response functions. This problem (the overestimation of evapotranspiration) appears to be a common feature of current land surface models, and needs to be corrected in order to make it useful to represent plant drought adaptations more realistically.

Investigating the general trends of trait variation with key environmental factors, and translating this variation into improved process representation in vegetation models, are important developments for the improvement of land surface models and dynamic global vegetation models. The model-oriented data analyses and experiments described in this thesis can be seen as part of a wider movement towards the observationally driven parameterization of fundamental vegetation processes (Prentice et al., 2014a; 2014b). Such work can also contribute to climate-change adaptation, through facilitating more accurate predictions of how

(for example) forestry systems are likely to respond to projected changes in drought intensity and duration in a rapidly changing world.

6.1 Reference

Bonan, G. B., Lawrence, P. J., Oleson, et al. (2011) Improving canopy processes in the Community Land Model version 4 (CLM4) using global flux fields empirically inferred from FLUXNET data. *J. Geophys. Res.: Biogeosciences* (2005–2012), 116(G2).

Bonan, G. B., Oleson, K. W., Fisher, R. A., Lasslop, G., Reichstein, M. (2012) Reconciling leaf physiological traits and canopy flux data: Use of the TRY and FLUXNET databases in the Community Land Model version 4. *J. Geophys. Res.: Biogeosciences* (2005–2012), 117(G2).

Choat, B., Jansen, S., Brodribb, T.J., et al. (2012) Global convergence in the vulnerability of forests to drought. *Nature* 491(7426): 752–755.

Eilmann, B., Weber, P., Rigling, A., Eckstein, D. (2006). Growth reactions of *Pinus sylvestris* L. and *Quercus pubescens* Willd. to drought years at a xeric site in Valais, Switzerland. *Dendrochronologia*, 23(3), 121–132.

Maire, V., Gross, N., Hill, D., Martin, R., Wirth, C., Wright, I.J., Soussana, J.F. (2013) Disentangling coordination among functional traits using an individual-centred model: impact on plant performance at intra- and inter-specific levels. *Plos One*. 8

Medlyn B.E., Duursma R.A., Eamus D. et al. 2011. Reconciling the optimal and empirical approaches to modelling stomatal conductance. *Glob. Chang. Biol.* 17: 2134–2144.

Prentice, I. C., Cowling, S. A. (2013) Dynamic global vegetation models, in: *Encyclopedia of Biodiversity*, 2nd edition, edited by: Levin, S. A., Academic Press, 607–689.

Prentice, I.C., N. Dong, S.M. Gleason, V. Maire and I.J. Wright (2014a) Balancing the costs of carbon gain and water loss: testing a new quantitative framework for plant functional ecology. *Ecol. Let.* 17: 82–91.

Prentice, I.C., X. Liang, B. Medlyn and Y. Wang (2014b) Reliable, robust and realistic: the three R's of next-generation land-surface modelling. *Atmospheric Chemistry and Physics Discussions* 14: 24811–24861.

Reich, P.B. (2014) The world-wide 'fast-slow' plant economics spectrum: a traits manifesto. *Journal of Ecology*. 102:275–301.

Wright, I.J., Reich, P.B., Westoby, M., et al. (2004) The worldwide leaf economics spectrum. *Nature*. 428: 821–827.